学位論文

Synthesis and properties of group 8 metal dithiolene complexes

(8 族金属ジチオレン錯体の合成とその性質に関する研究)

平成 30 年 3 月

佐川　拓矢

Chapter 1

General Introduction

1-1 Coordinatively unsaturated complexes

1-1-1 Introduction

Carbon atoms in organic compounds, have the electron configuration of noble gas, applied as an 8-electrons rule. Orbitals of the carbon are filled to 8-electrons with 2*s* and three 2*p* orbitals to form four bonding orbitals. On the other hand, the 18-electron rule is known as a tendency which decides the stability of *d*-block transition metal complexes. This rule is applied to the stable and diamagnetic mononuclear transition metal complexes, and these complexes almost always contain 18-electrons. This rule follows a similar line of reasoning in 8-electrons rule. The metal has one *s*, three *p*, and five *d* orbitals.[1, 2]

For example, first-row carbonyl complexes are followed by the 18-electron rule (Figure 1-1). These metals contribute the same number of electrons as their group number, and the CO ligand contributes two electrons from its lone pair. However, the odd number of electrons on the metal can't reach an even number, by adding two electrons ligands such as CO. This problem was resolved by a way as follows: in $V(CO)_6$, this complex is 17-electrons, but this complex is easily reduced and 18-electrons anion $V(CO)_6^-$ is obtained. $Mn(CO)_5$ fragment and $Co(CO)_4$ fragment are also 17-electrons, these fragments form a dimer, respectively. On the other hand, the even-electron metals can achieve 18-electron carbonyl complexes when the appropriate number of CO ligands bind on the metal centered.

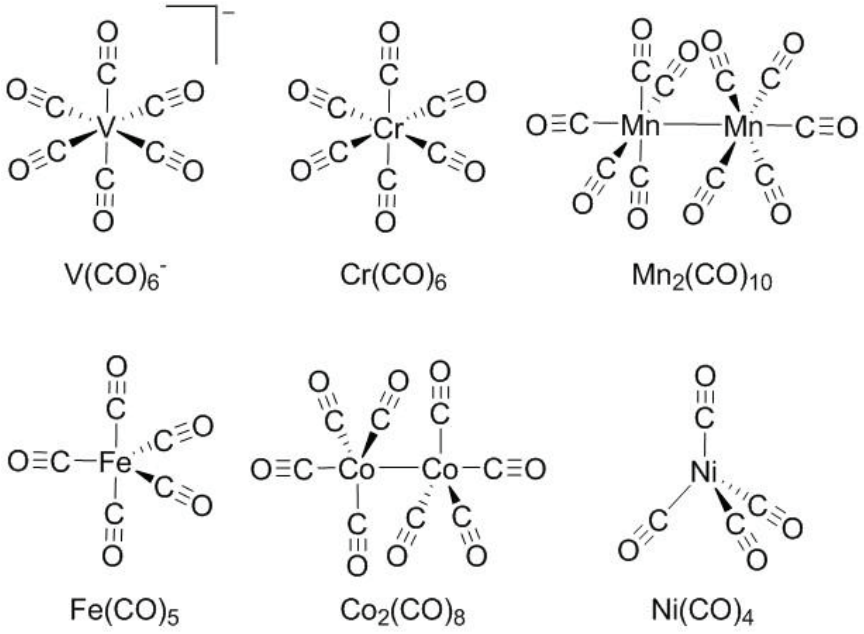

Figure 1-1. First-row carbonyl complexes

There are many cases that the electron count of a stable complex is not 18. For example, sandwich compounds such as Cp_2M (Cp = cyclopentadienyl anion, M = Ti, V, Cr, Mn, Fe, Co, Ni) are almost unable to apply 18-electron rule (Figure 1-2).[1, 2] These complexes have a reactivity which they attain an 18-electorn configuration, for instance, the 19-electrons Cp_2Co is one electron reductant and the 17-electrons $[Cp_2Fe][PF_6]$ is an one electron oxidant (Scheme 1-1).[3, 4]

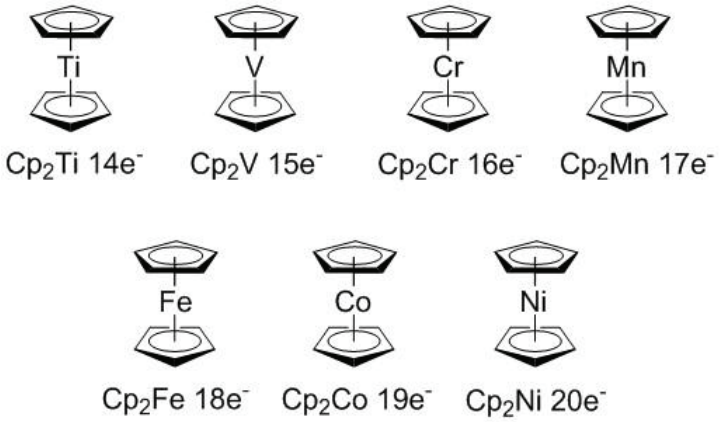

Figure 1-2. First-row sandwich compounds

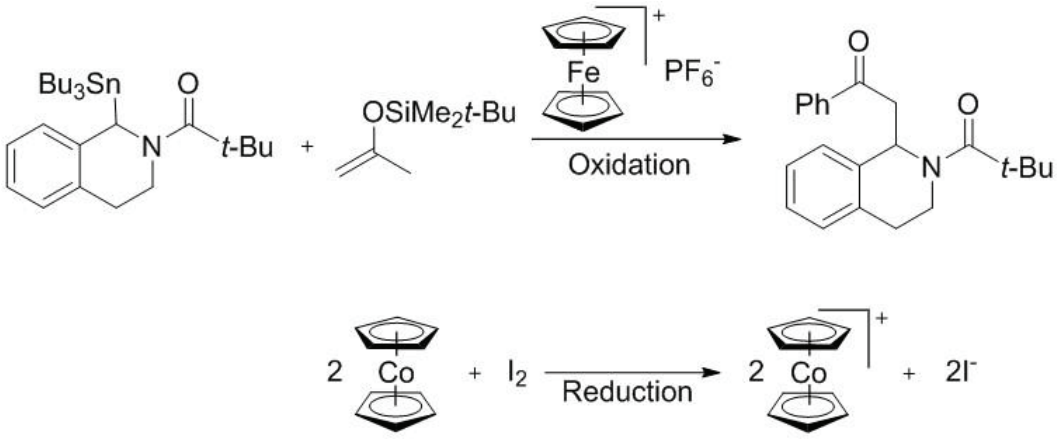

Scheme 1-1 The examples of sandwich complexes with redox agents

1-1-2 Synthesis method of coordinatively unsaturated complexes

Main factors have been reported to generate coordination unsaturated transition metal complexes as follows:

1. the d^0 metals for early transition metal complexes
2. the d^8 metals for groups 8–11 elements complexes
3. steric hindrance
4. reductive elimination reaction

In the d^0 metals for early transition metal complexes, these complexes have electrons less than 18 (e.g., $TiMe_4$, Cp^*WOCl_3, $W(OMe)_6$) (Figure 1-3).[5–7] These complexes undergoes π donation from the ligand which have π-type lone pairs into metal d_π orbitals. For example, $W(OMe)_6$ is apparently 12-electrons complex, but these oxygens have each two lone pairs and a total of 24 additional electrons are donated to the central metal.[2]

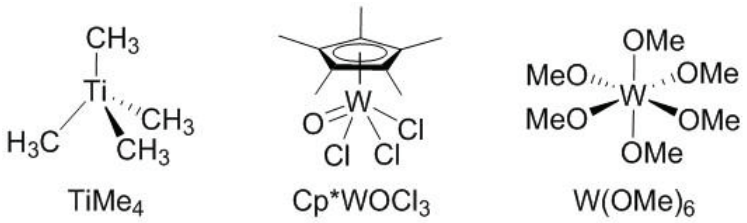

Figure 1-3. The d^0 metals of early transition metal complexes

An important class of the d^8 metals of group 8-11 complexes follows 16-electrons, rather than 18-electron rule because one of the nine orbitals lies very high and is usually empty (Table 1-1). This potential is minimum for group 8 and shows maximum for group 11 because 16-electron is established. These complexes usually form square and planer geometry, but large distortion occurs.[8] Some examples of 16-electrons complexes are $RhCl(PPh_3)_3$, $IrCl(CO)(PPh_3)_2$, $PdCl_2(PPh_3)_2$, $[PtCl_4]^{2-}$ and $[AuMe_4]^-$ (Figure 1-4).[9–13]

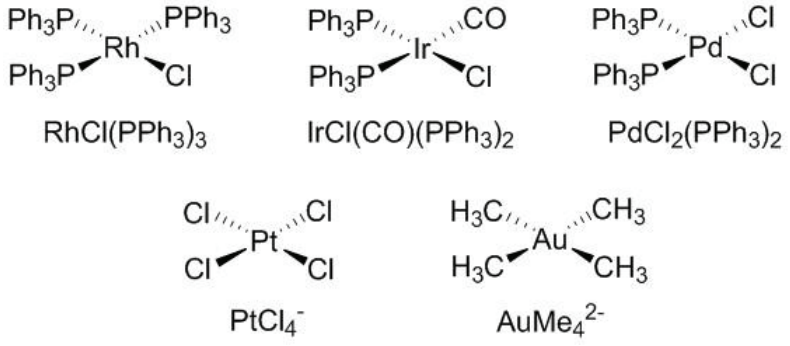

Figure 1-4. The d^8 metals in group 8-11 complexes

Table 1-1. The d^8 metals that can adopt a 16-electrons square and planer configuration

Group of elements			
8	9	10	11
Fe(0)[a]	Co(I)[b]	Ni(II)	Cu(III)[c]
Ru(0)[a]	Rh(I)[b]	Pd(II)	-
Os(0)[b]	Ir(I)[b]	Pt(II)	Au(III)

[a] 18-electrons is preferred than 16-electrons.

[b] The 16-electrons configuration is often found, but 18-electrons complexes are common.

[c] A rare oxidation state.

The coordinative unsaturation compound is obtained when having large steric hindrance of ligands such as the ligands having large substituent groups, the polydentate ligands, and so on. These complexes are generally stable because the central metal is surrounded with the large substituent, and a nucleophilic attack to central metal with various chemical species is rarely occurred. On the other hand, a complex of electronic unsaturation is obtained when the early transition metal as central metal is used. For example, the metal center of sandwich complexes Cp_2MCl_2 (M = Ti or Zr) is coordinated unsaturation (16-electrons), and $V(CO)_6$ is a 17-electrons complex (Figure 1-5).[14, 15] These complexes are almost coordinatively saturated.

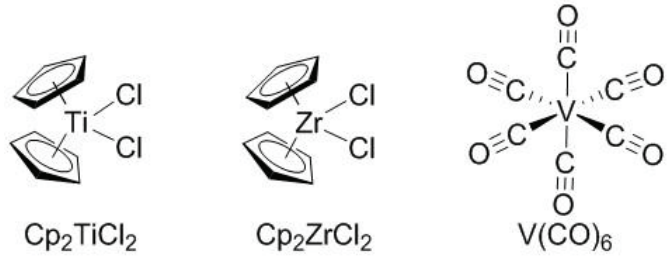

Figure 1-5. The coordinatively unsaturated compound with early transition metal

Scheme 1-2 shows a general method of oxidative addition and reductive elimination for simultaneously introducing pairs of anionic ligands, A and B. Reductive elimination leads to the extrusion of A–B molecule such as H_2 or CH_3I from 18-electrons complex, and a 16-electrons coordinative unsaturated complex is generated.[1, 2] This reaction can be stimulated by oxidation or photolysis. For instance, octahedral complexes of Pt(IV), Pd(IV), Ir(III), and Rh(III) undergo reductive elimination with initial loss of a ligand to generate penta-coordinated complex. An example of the complex *mer*-[RhH(Me)Cl(PMe_3)$_3$], with H and Me *cis*, give reductive elimination even at 30 °C (Scheme 1-3).[16] The penta-coordinated intermediate distorts to reach the transition state for reductive elimination, and the two groups, R and H, eliminated very close

together. After reductive elimination, a tri-coordinated species are formed, and the ligand is added to the metal center. Additionally, the photochemically reductive elimination of one hydrogen from metal–dihydride complexes generates intermediate by the addition of alkanes as shown in Scheme 1-4.[17–19] In these complexes, the photochemical irradiation is provided induce the reductive elimination process.

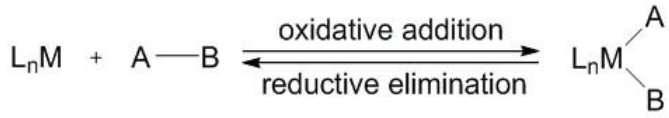

Scheme 1-2. A general method of oxidative addition and reductive elimination

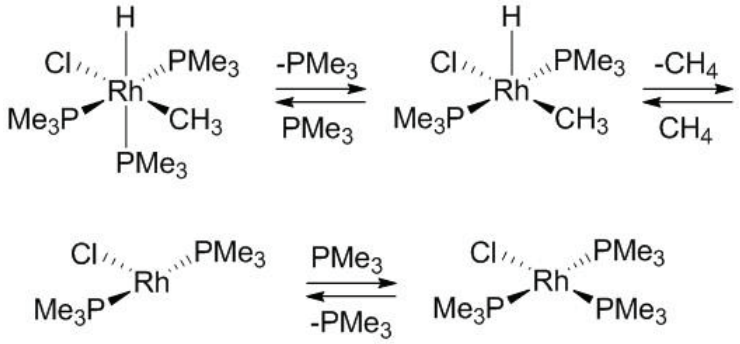

Scheme 1-3. Reductive elimination of *mer*-[RhH(Me)Cl(PMe_3)$_3$], with H and Me.

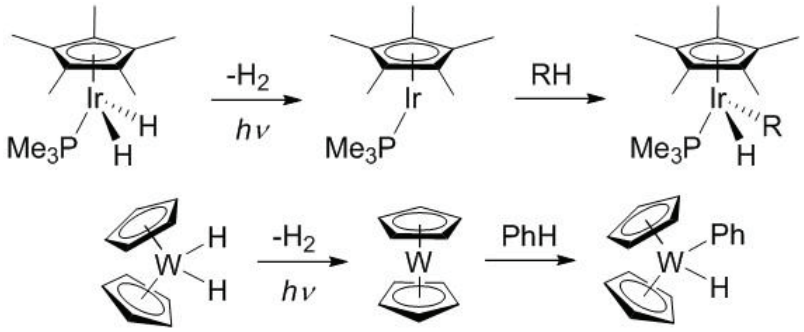

Scheme 1-4. The photochemical reductive elimination of one hydrogen and formation of the intermediate by addition of an alkane.

A binuclear reductive elimination reaction was also reported when an intermolecular path ought to be available as in Nortons's *cis*-$Os(CO)_4RH$ (R = Me or Et) complexes.[20] Alkyl hydride usually gives alkane by elimination reaction, but this reaction doesn't proceed because $Os(CO)_4$ specie is highly unstable (Scheme 1-5). Nevertheless, Norton's mechanism provides a biomolecular way to eliminate alkane that doesn't involve tetra-

coordinated Os(0) (Scheme 1-6). The first step is the migratory insertion reaction to form a coordinatively unsaturated 16-electorons acyl complex. Next, the vacant site of this complex is filled by an Os–H bond from a second molecular. As a result, R group of the acyl eliminates with the hydride from the metal to give a binuclear complex including an Os–Os bond. On the other hand, the similar complex *cis*-$Os(CO)_4Me_2$, lacking a hydride, not proceed an elimination, binuclear, or otherwise reactions.

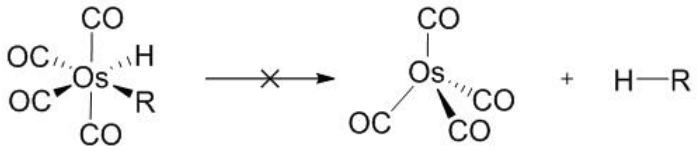

Scheme 1-5. The elimination reaction of an alkane for Os complex.

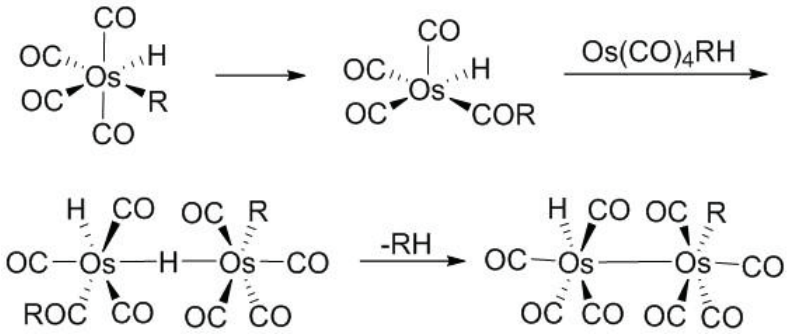

Scheme 1-6. The migratory insertion reaction and eliminative reduction.

1-1-3 Application of coordinative unsaturated complexes

Coordinative unsaturated compounds are known to have high reactivities. Therefore, they are utilized in various catalysts and initiation of building block. For example, Wilkinson's catalyst [$RhCl(PPh_3)_3$] and its relevant complexes are available as hydrogenation catalyst of alkene and alkyne with approximately 1 atm of hydrogen gas.[9, 21, 22] The cycle of this catalyst is as follows (Figure 1-8):

1. 16-electrons complex [$RhCl(PPh_3)_3$] is oxidatively added by H_2 to form dihydride complex [$RhH_2Cl(PPh_3)_3$].
2. PPh_3 ligand in [$RhH_2Cl(PPh_3)_3$] eliminates to give alkene complex [RhH_2Cl (alkene)$(PPh_3)_2$].
3. 16-electrons intermediate complex is generated followed by addition of PPh_3 ligand.
4. Reductive elimination is occurred to regenerate [$RhCl(PPh_3)_3$] with and elimination of alkane.

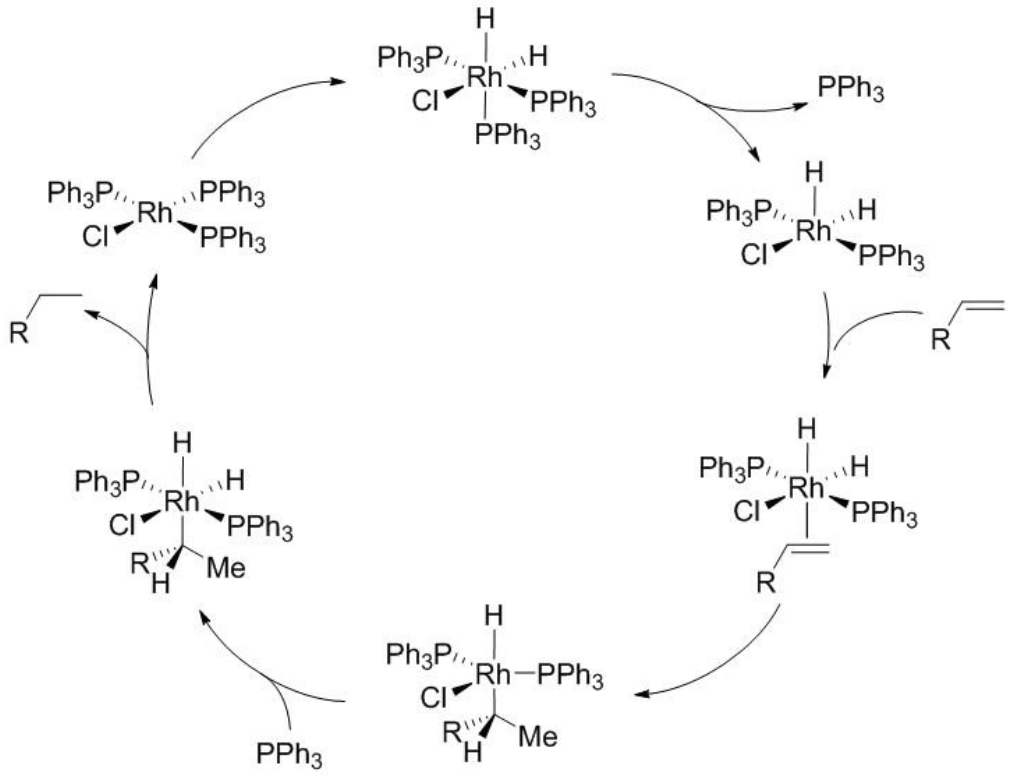

Figure 1-6. The reaction cycle using Wilkinson's catalyst

Additionally, this complex also catalyzes other hydrofunctionalization reactions such as hydroacylation, hydroboration, and hydrosilylation of alkenes.[23–25]

The reduction of N_2 to NH_3 is difficult because of its high stability of the N≡N triple bond. Peters and coworkers reported that the catalytic conversion of N_2 to NH_3 by coordinative unsaturated specie P_3BFe^+ (P_3B = tris(*σ*-diisopropylphosphinophenyl)-borane) can be achieved with a low driving force by coupling Cp^*_2Co with $[Ph_2NH_2]^+$ or $[PhNH_3]^+$ (Scheme 1-8).[26]

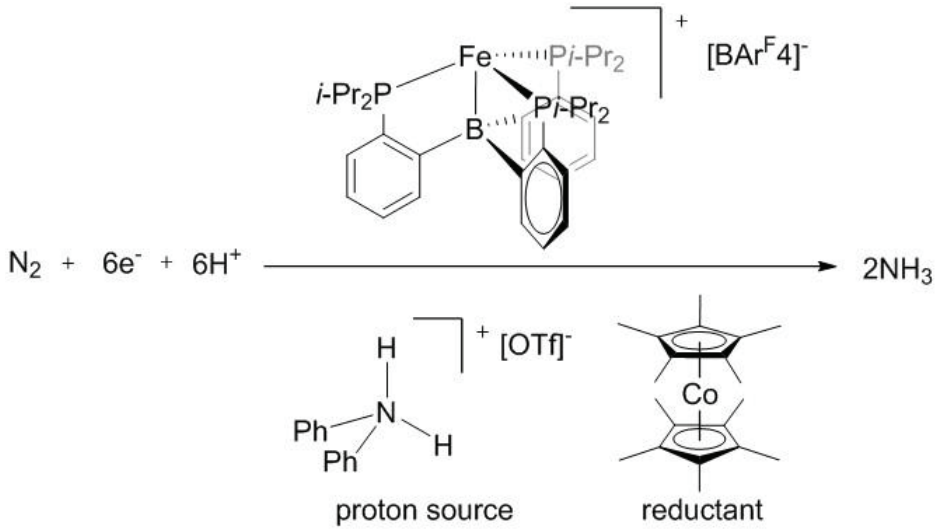

Scheme 1-7. the catalytic conversion of N_2 to NH_3 using coordinative unsaturated species P_3BFe^+

On the other hand, coordinative unsaturated compounds are also utilized as building block of metal cluster complexes. Using bridging ligands derived from elements of the main group such as P or S, cluster complexes can be synthesized. The generated bridging ligands will play important role on the stabilization of metal-metal bond. For example, 16-electrons complex $[PtHCl(PR_3)_2]$ (R = PEt_3, PMe_2Ph) reacts with lithium salt $[M(CO)_5PPh_2]Li$ (M = Cr, Mo, W), and dinuclear complex $[M(CO)_4(PPh_2)HPt(PEt_3)_2]$.[27] Scheme 1-8 displays an example of the method to use polydentate phosphine ligand. A $PPh_2CH_2PPh_2$ (dppm) ligand and OMe group bridge two transition metals to generate $[Fe(CO)_3\{\mu\text{-}Si(OMe)_2OMe\}(dppm)PdCl]$.[28] Besides, sulfur bridged complex $[Mo_2S_2(\mu\text{-}S)_2(S_2CNEt_2)_2]$ was reacted with an equimolar amount of $[RhCl(PPh_3)_3]$, and a unique triangular cluster $[Rh(PPh_3)(m\text{-}S)_2\{Mo(S_2\text{-}CNEt_2)_2\}(\mu^2\text{-}S)_2]$ was obtained. In addition, a cubane-type tetranuclear cluster $[\{Rh(PPh_3)\}_2\{Mo(S_2\text{-}CNEt_2)_2\}(\mu^2\text{-}S)_2]$ was obtained when 2 equivalent $[RhCl(PPh_3)_3]$ was reacted (Scheme 1-9).[29] Another synthetic method is shown in Scheme 1-10: a complex of the general formula $W(SNS)_2M(dppe)$ (M = Pd, Pt; $(SNS)H_3$ = bis(2-mercapt-*p*-tolyl)amine; dppe = $PPh_2CH_2CH_2PPh_2$) was synthesized by combining the $(dppe)MCl_2$ synthon with tungsten complex under reduced condition.

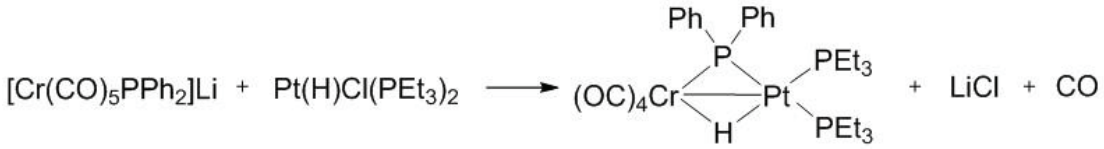

Scheme 1-8. The addition of metal fragment to ligand to a second metal complex.

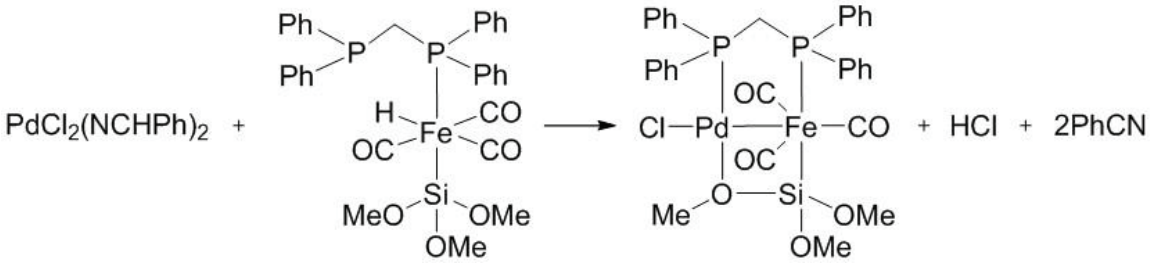

Scheme 1-9. An example using polydentate ligands.

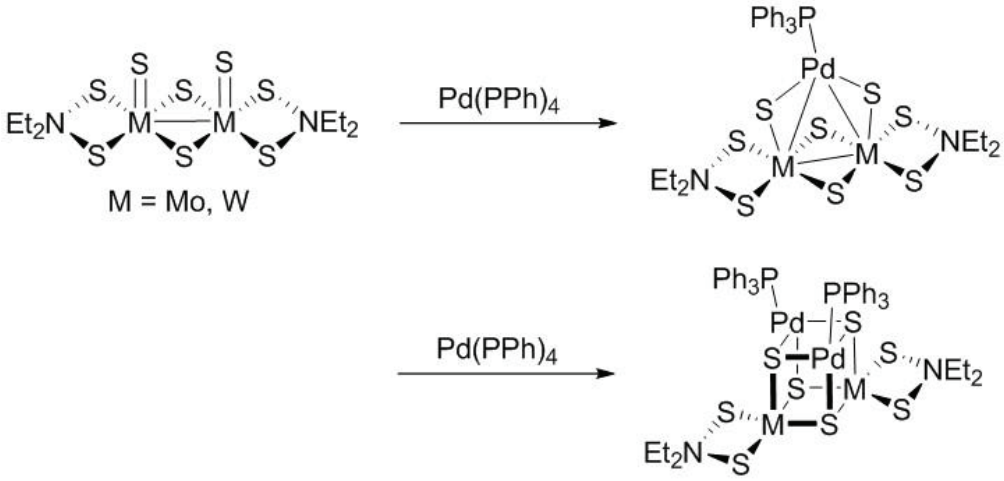

Scheme 1-10. Mixed metal sulfide clusters containing incomplete cubane type core.

1-2 Metalladithiolene complexes

1-2-1 Introducition

Researches on metalladitholene complexes have remained active since the beginning in the early 1960s.[30] At first, the complexes of redox and structural properties were studied.[31–33] After a few decades, dithiolene compound was attracted by relating to the science in photonics and electronic conductors.[34–36] In the 1990s, researches on Mo^{-} and W^{-} containing enzymes ligated dithiolate were attracted which are incorporated into the heterocyclic pyranopterins.[37–40] Therefore, dithiolene complexes are known as a functionalized molecule and have been studied continuously.

Metalladithiolene complexes have a five-membered ring composed of two sulfurs, two unsaturated carbons and a central metal. These complexes have following several valuable features.

・The ring of metalladithiolene complexes have planarity and quasi-aromaticity caused by strong dπ-pπ interaction (Figure 1-7).

・The central metal of metalladitholene complex can be stabilized in coordination unsaturated 16-electron form for group 8–10 metals.

The combination of these features enables us an additional reaction with various chemical species on the metalladithiolene ring.[41] Additionally, these complexes utilized as building blocks of metal cluster complexes by the reaction with metal species.[42] On the other hand, metalladithiolene complexes have redox active properties of metal-centered and dithiolene-centered. These properties are essential for the expression and study of electrochemical properties.

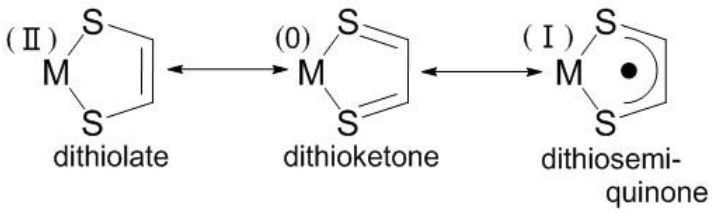

Figure 1-7. Dithiolene five-membered ring.

1-2-2 Arene-1,2-dithiol and its derivatives

Arene-1,2-dithiol are remarkably stable and are various precursors for dithiolene compounds. In particular, benzenedithiol and its derivatives, toluene-3,4-dithiol, 3,6-dimethylbenzenedithiol, 3,4,5,6-tetramethylbenzenedithiol, 3,6-dichlorobenzenedithiol, 3,4,6-trichlorobenzenedithiol, 3,4,5,6-tetrachlorobenzenedithiol, 2,3-naphtalenedithiol, quinoxalinedithiol, and so on (Figure 1-8), are the most common members of this class of ligands.

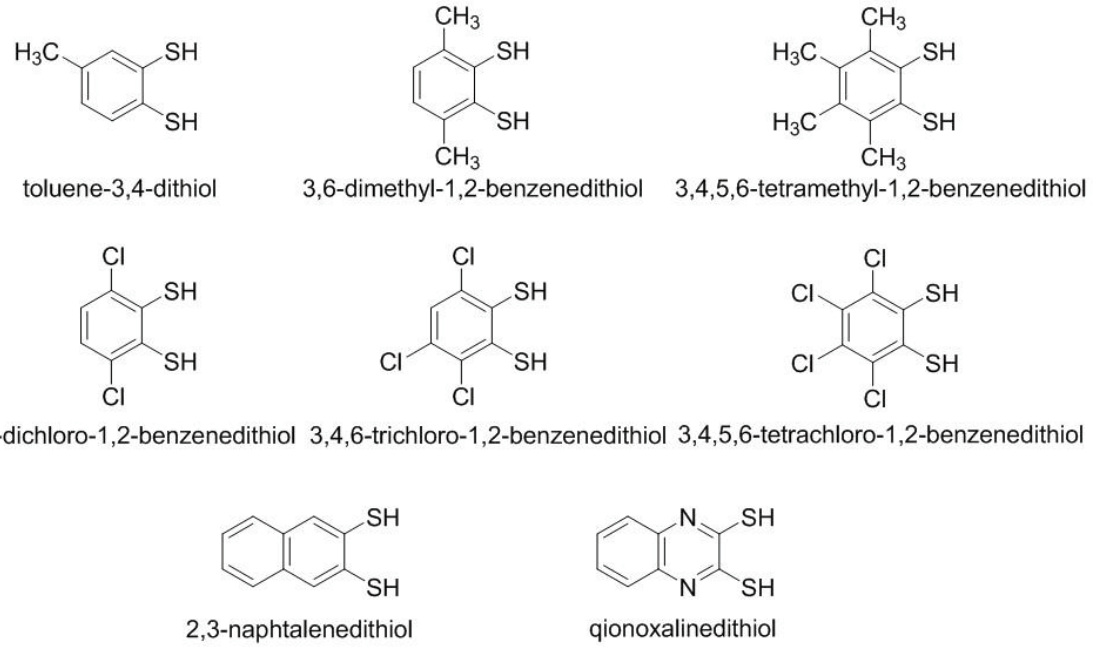

Figure 1-8. Benzenedithiol derivatives.

Metalladithiolene complexes ligated by various arene-1,2-dithiolate are reported to change their properties such as catalytic,[43, 44] magnetic,[45] and electrochemical properties.[42, 46] For example, Felton and coworkers synthesized di-iron dithiolene complexes ligated by toluene-3,4-dithiolate and various number of chlorobenzenedithiolate (Figure 1-9).[47] These complexes were carried out for proton reduction in the presence of acetic acid and their reduction potentials were different. The reduction potential of toluene-3,4-ditiolate complex was lower than that of chlorobenzenedithiolate complexes. Additionally, the more number of chloro group on the benzene ring was ligated, the higher reduction potential was shown. Hoveyda and coworkers reported the olefin metathesis catalysts ligated by dithiolate ligand substituted by halogen or methyl group on the benzene ring (Figure 1-10).[48, 49] These catalysts were carried for *Z*-selective olefin metathesis reactions with high efficiency including products that contain hindered groups such as a phenol or carboxylic acid.

Wieghardt and coworkers studied the electron paramagnetic resonance (EPR) spectra broadband array of monoanionic molybdenum and tungsten tris dithiolene complexes (Figure 1-11).[50, 51] These complexes was characterized by the two different electronic structures for the monoanion by the spin-Hamiltonian parameters. Kajitani and coworkers reported the structures and electrochemical properties of monomeric and dimeric cobalt dithiolene complexes substituted by benzenedithiolate ligands (Figure 1-12).[41] The monomers undergo dimerization by electrochemical oxidation by based on the EC reaction (E: electron transfer, C: Chemical reaction) in solution and the oxidized dimers was reduced to form the monomer.

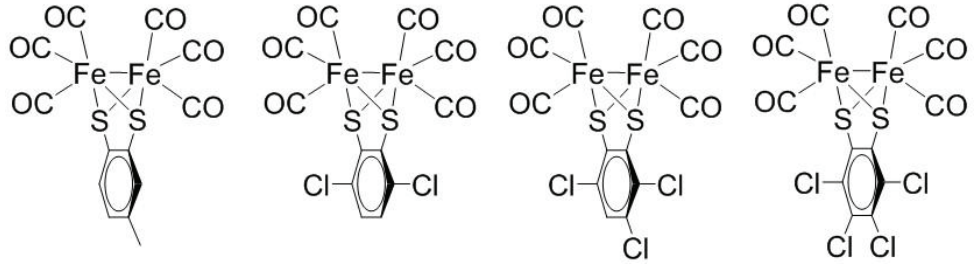

Figure 1-9. Benzenedithiol derivatives.

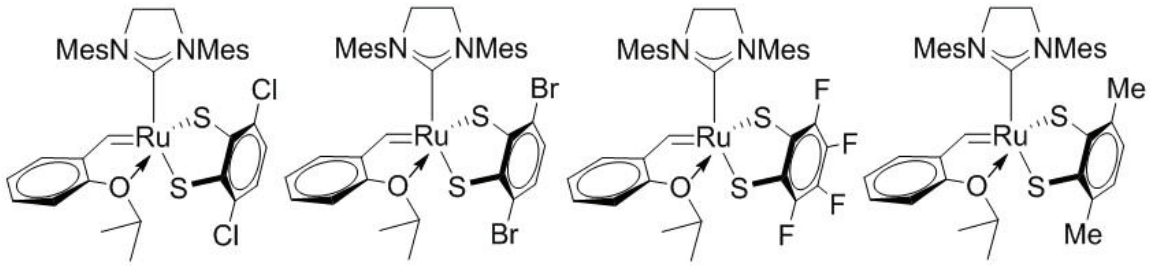

Figure 1-10. Olefin metathesis catalysts ligated by various dithiolate ligand.

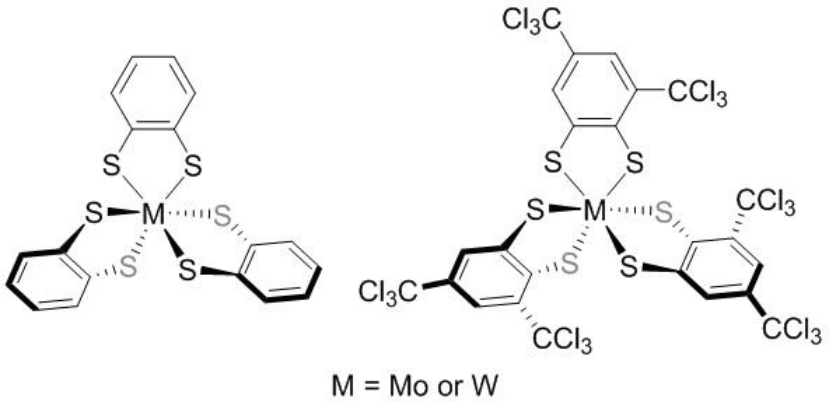

Figure 1-11. Monoanionic molybdenum and tungsten tris(dithiolene) complexes

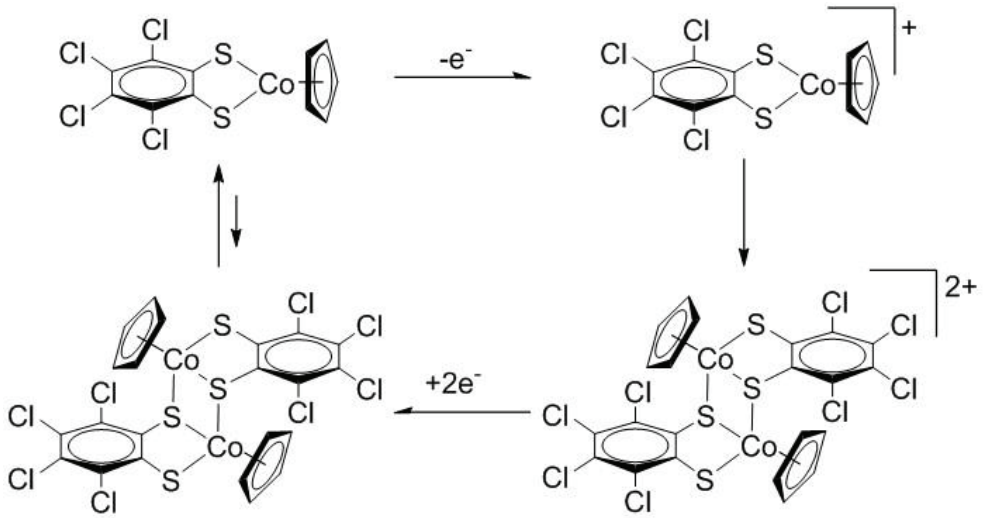

Figure 1-12. The ECEC mechanism (E: electron transfer, C: Chemical reaction) of [CpCo(Cl_4bdt)]

Benzenedithiols are generally synthesized by the reductive dealkylation of 1,2-$C_6R_4(SR')_2$ which are obtained by the reaction of dibromobenzene with alkali metal or cuprous thiolates (Scheme 1-11).[52] Additionally, a new process of the synthesis of 1,2-benzenedithiol and its derivatives has been reported[53, 54] by the *o*-lithiation of benzenethiol derivatives with alkyl lithium to give 2-LiC_6H_4(SLi) (Scheme1-12).

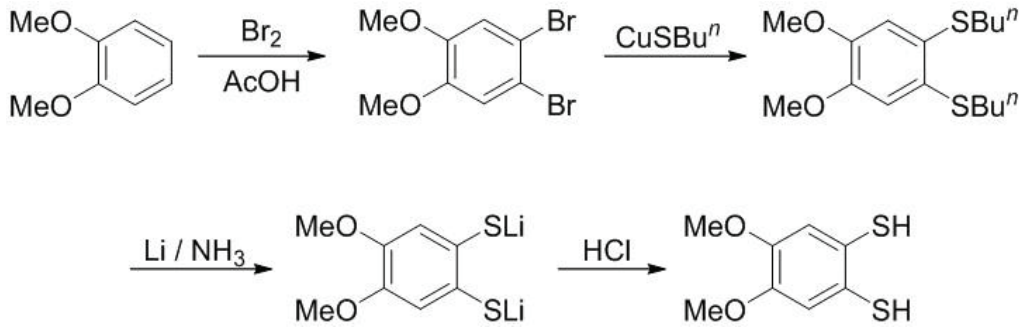

Scheme 1-11. Reaction of dibromobenzene with alkali metal or cuprous thiolate.

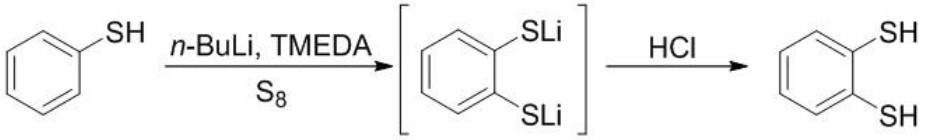

Scheme 1-12. Synthesis of 1,2-benzenedithiol

1-2-3 Reactivity of metalladithiolene complexes

The dithiolene complexes including η^5-cyclopentadienyl (Cp) or η^6-arene (C_6R_6) are main target compounds on the research. Among them, the half-sandwich complexes, Cp or C_6R_6/dithiolene ratio is 1:1, have been investigated.[41] These complexes have both aromaticity and unsaturation in the five-membered dithiolene ring. Thus, 16-electron metalladithiolene complexes undergo addition reaction with various chemical species and these derivatives take place the elimination reaction.

For example, the cobalt dithiolene complex [(η^5-C_5H_5)Co(bdt)] (bdt = 1,2-benzenedihtiolate) reacts with diazo compounds such as diazomethane or ethyl diazoacetate (Scheme 1-13).[55] The adducts are isolated as air-stable microcrystalline solids and were spectroscopically characterized. This complex also reacts with quadricyclane, and the cobalt dithiolene complex ligated norbornadiene is obtained (Scheme 1-13).[56] The rearrangement of the strained molecule was confirmed by ^{1}H NMR and single crystal X-ray diffraction. Adduct has a piano-stool geometry and is coordinatively unsaturated. Additionally, [(η^5-C_5H_5)Co(bdt)] was reported to catalyze the isomerization of quadricyclane to norbornadiene up to 176 equivalent based on the catalyst at 120 °C (Figure 1-13).[57] When the adduct was used instead of [(η^5-C_5H_5)Co(bdt)], the isomerization took place. However, the activity of adduct was lower than that of [(η^5-C_5H_5)Co(bdt)] under the same condition (58 equivalent based on the catalyst).

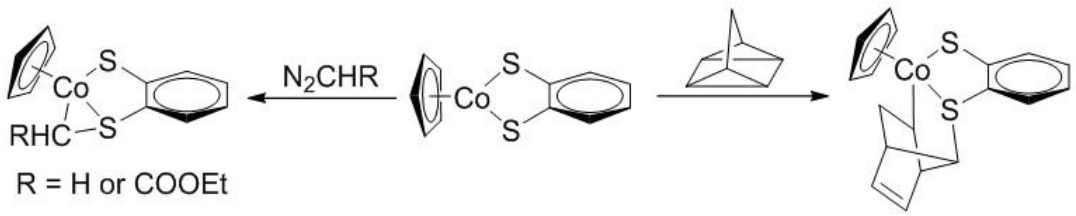

Scheme 1-13. Addition reaction of [(η^5-C_5H_5)Co(bdt)]

The ruthenium dithiolene complex coordinated by hexamethylbenzene [(η^6-C_6Me_6)Ru(bdt)] was reacted with *tert*-butyl isocyanide in THF and [(η^6-C_6Me_6)Ru(*t*-BuCN)(bdt)] was obtained in 74% yield (Scheme 1-14).[58] In the crystal structure, the length between Ru center and the centroid of the aromatic ring of the hexamethylbenzene ligand is longer by 0.072 Å than that of non-coordinating one. On the other hand, the ruthenium complex [(η^6-C_6Me_6)Ru(bdt)] was reacted with hydrazine and the hydrazine complex [(η^6-C_6Me_6)Ru(bdt)]$_2$(μ-NH_2NH_2) was obtained in 71% yield (Scheme 1-14).[59] In the complex, the hydrazine was reported to act as a bridged ligand

through the NH-S hydrogen bond. In addition, [(η^6-C_6Me_6)Ru(bdt)] was reported to react with other ligands such as PEt_3.[58]

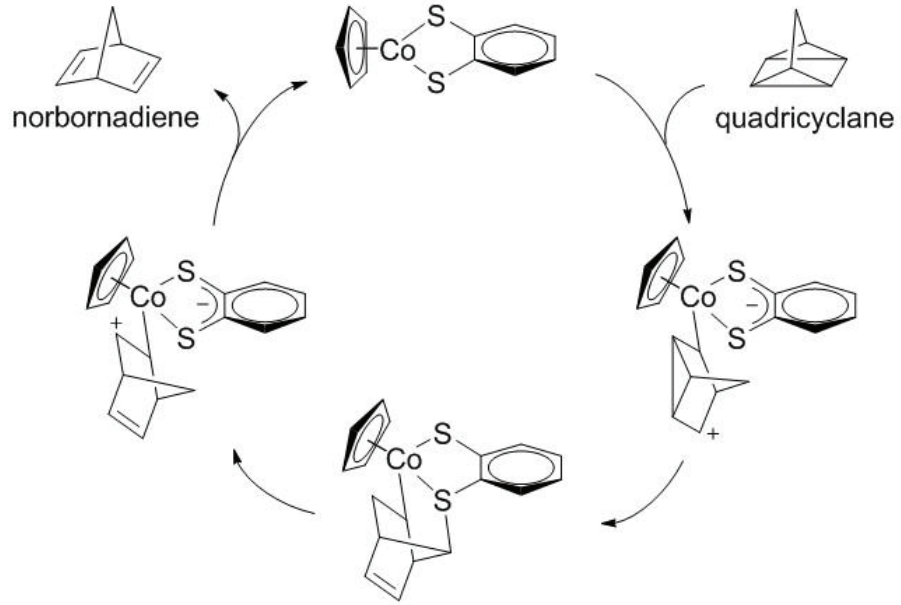

Figure 1-13. A possible mechanism for catalytic isomerization of quadricyclane to norbornadiene.

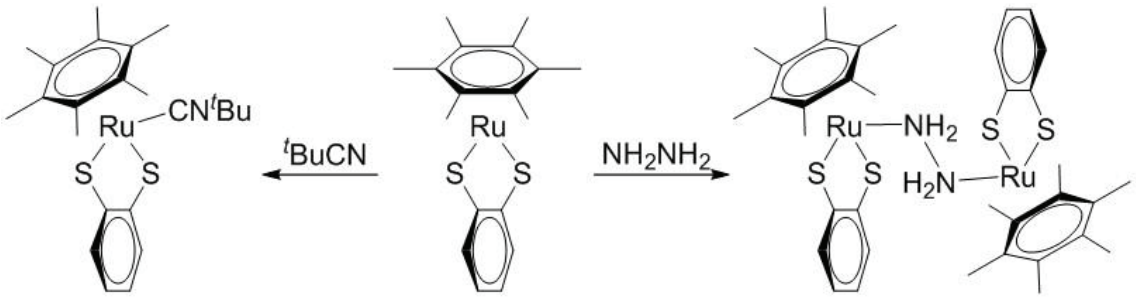

Scheme 1-14. Addition reaction for [(η^6-C_6Me_6)Ru(bdt)]

1-2-4 Synthesis of dithiolene cluster complexes

Metalladithiolene complexes is known to oligomerize in π-conjugated fashion, and several π-conjugated metalladithiolene multinuclear complexes have been synthesized. Nishihara and coworkers attempt to polymerize the mononuclear cobalt dithiolene complex. However, polymeric compounds were not observed because of steric hindrance on the S atom of neighboring dithiolene unit. Instead, dinuclear metaladithiolene complexes and trinuclear metalladithiolenes were obtained (Scheme 1-15).[60] These complexes were reported as a modified method for hexamercaptobenzene (Scheme 1-16).[61–63]

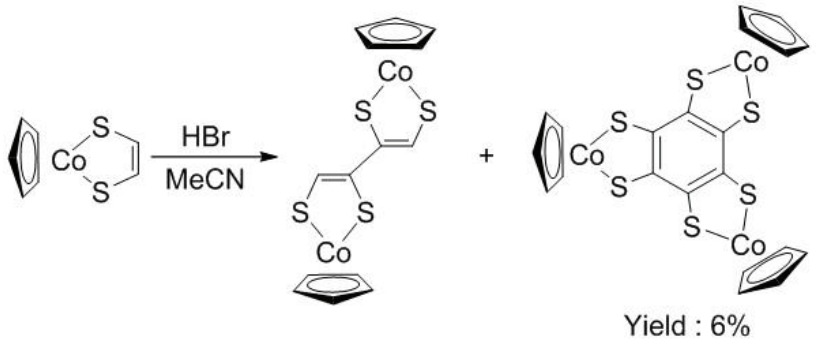

Scheme 1-15. Oxidative trimerization of cobalt dithiolene complex.

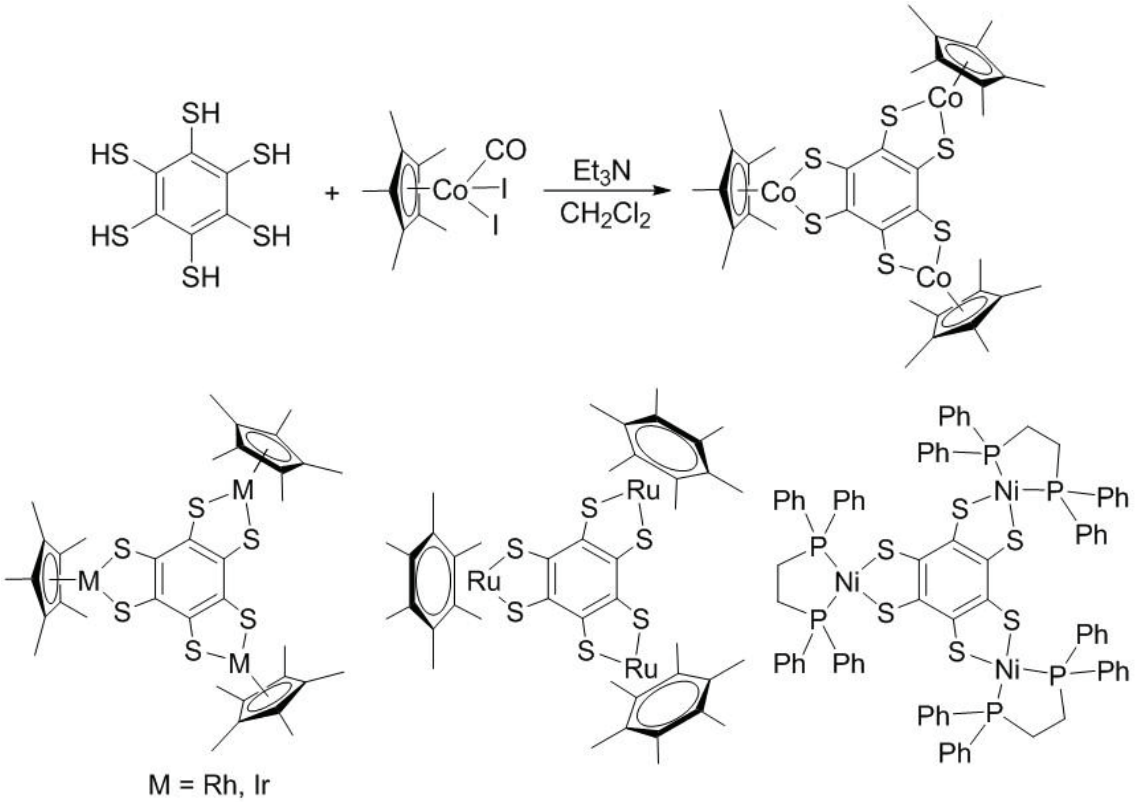

Scheme 1-16. Hexamercaptobenzene derivatives.

On the other hand, Metalladitholene complexes containing 8-10 metal undergo a variety of addition reactions. In particular, these complexes built metal-metal bonds and metalladithiolene cluster was formed when these are reacted with metal species. The first metal–metal bond formation reaction of metalladitholene was the reaction of cobalt dithiolene complex [CpCo(bdt)] with $M(CO)_3(pyridine)_3$ (M = Mo, W) in the presence of $BF_3{\cdot}Et_2O$ and the group 9–6–9 trinuclear complex [{CpCo(bdt)}$_2$-$M(CO)_2$] (M = Mo, W) was obtained (Scheme 1-17).[64] This complex is used to the reaction with electron-rich zero-valent metals onto the metalladithiolene ring. Additionally, activation of group 8 zero-valent metal sources is also carried out in the presence of Me_3NO instead of BF_3Et_2O. The cobalt dithiolene complex [CpCo(bdt)] was reacted with $Fe(CO)_5$ or $Ru(CO)_3(P^tBu_3)_2$ in the presence of Me_3NO and dinuclear complex [CpCo(bdt)Fe(CO)$_3$] or [CpCo(bdt)Ru(CO)$_2$P^{t}Bu$_3$] was obtained, respectively (Scheme 1-18).[64] In these reactions, the orbital of sulfur in the metalladihtiolene rings become sp^3 from sp^2. Consequently, the planarity of metalladihtiolene ring is lost and the quasi-aromaticity of the metalladithiolene ring is also lost.

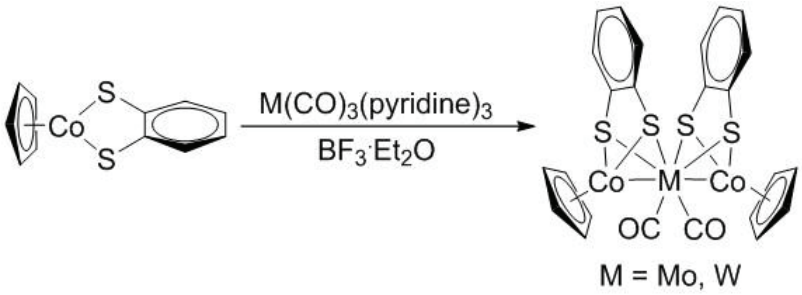

Scheme 1-17. Synthesis of trinuclear dithiolene complex [{CpCo(bdt)}$_2$-$M(CO)_2$] (M = Mo, W)

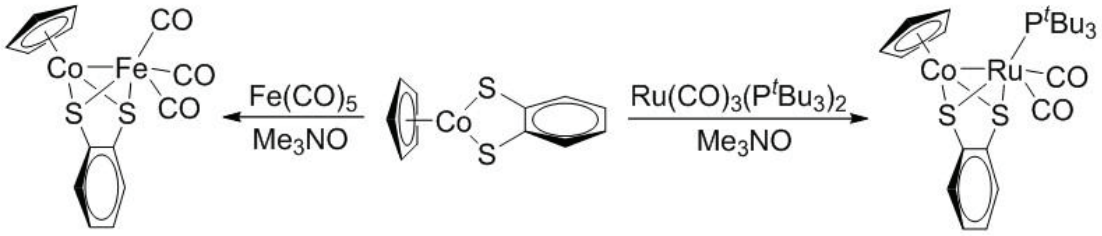

Scheme 1-18. Synthesis of dinuclear dithiolene complexes [CpCo(bdt)Fe(CO)$_3$] and [CpCo(bdt)Ru(CO)$_2$P^{t}Bu$_3$]

Furthermore, metalladihtiolene complexes, [(η^5-C_5Me_5)M(bdt)] (M = Rh or Ir) and [(η^6-C_6Me_6)Ru(bdt)], were reacted with $Co_2(CO)_8$ in the presence of Me_3NO, and trinuclear cluster complexes [(η^5-C_5Me_5)M(bdt)$Co_2(CO)_5$] (M = Rh or Ir) and [(η^6-

C_6Me_6)Ru(bdt)$Co_2(CO)_5$] were obtained (Scheme 1-19).[65] In these complexes, the planarity of the metalladithiolene ring is maintained. Surprisingly, the cluster complex [(η^6-C_6Me_6)Ru(bdt)$Co_2(CO)_5$] underwent the reaction with [(η^5-C_5Me_5)M(bdt)] (M = Rh or Ir), and the trinuclear cluster complexes [(η^5-C_5Me_5)M(bdt)$Ru_2(CO)_4$(bdt)] (M = Rh or Ir) and [(η^6-C_6Me_6)Ru(bdt)$Ru_2(CO)_4$(bdt)] were obtained (Scheme 1-20).[66] This reaction is the first time to reconstruct a metal-metal bond by scission and formation reaction.

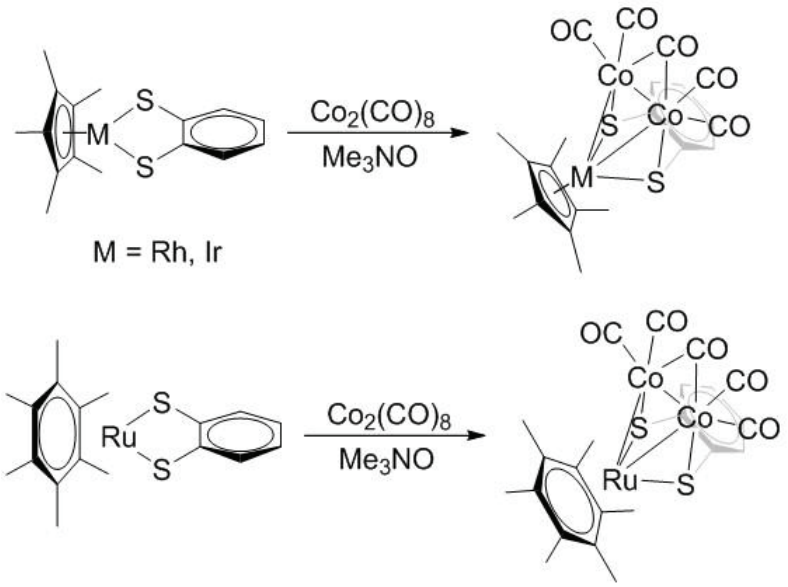

Scheme 1-19. Synthesis of trinuclear dithiolene complexes [(η^5-C_5Me_5)M(bdt)] (M = Rh or Ir) and [(η^6-C_6Me_6)Ru(bdt)]

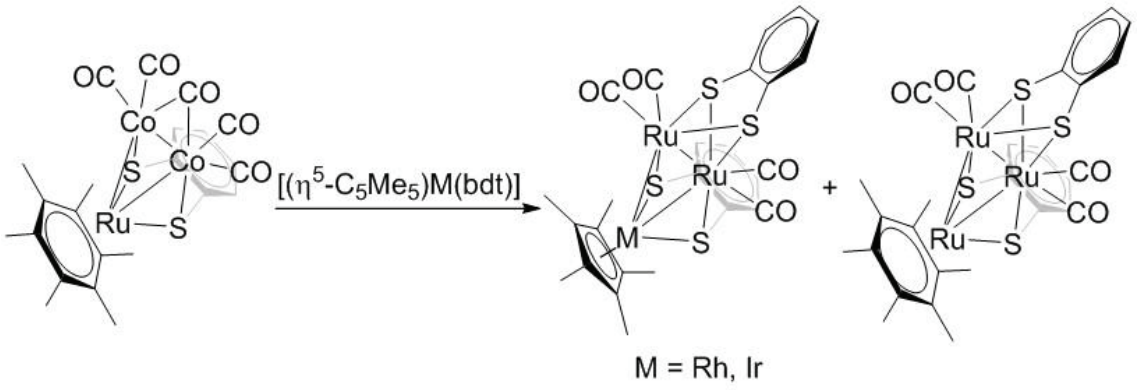

Scheme 1-20. The reconstruction of a metal-metal bond by scission and formation reaction.

1-3 The model complexes of active site in various enzymes

Metal sulfide cluster complexes in enzymes have fundamental roles in the control of biological electron-transfer and biological redox reactions. For example, the protein-bound iron and molybdenum sulfide complex (FeMoco) in nitrogenase enzyme, that binds and reduces N_2 more efficiency than any nonbiological process, has been a driving force for an amount of research on metal sulfide cluster complexes. The presence of an interstitial light atom in the FeMoco was established in 2002,[67] and structural, spectroscopic, and biochemical data have recently established its identity as a C-atom (Figure 1-14).[68, 69] However, the mechanism of catalytic N_2 reduction has been unclear yet. In order to elucidate this mechanism, the model complexes of FeMoco have been studied (Figure 1-14). Qu and coworkers used a thiolate-bridged diiron system that binds *cis*-diazene, and this complex can be protonated to give N_2H_3 species (Scheme 1-21).[70] Furthermore, treatment with 2 equivalent of reducing reagent and protonation, N_2H_3 specie was transformed into the bridged amide complex (Scheme 1-21). In other words, these reactions are relevant because transformation of dinitrogen to ammonia might be mediated by two neighboring Fe atom in FeMoco. In addition, this diiron complex is reported as a model complex of active site of [FeFe]-hydrogenase which is the enzyme to have a redox ability of H_2.[71] This complex was reacted with 1 equivalent of $HBF_4{\cdot}Et_2O$ and hydride bridged iron dinuclear complex was obtained. The redox property of the diiron complex was studied by cyclic voltammetry and displayed a reversible one-electron reduction. Moreover, the proton reduction occurred in the presence of $HBF_4{\cdot}Et_2O$.

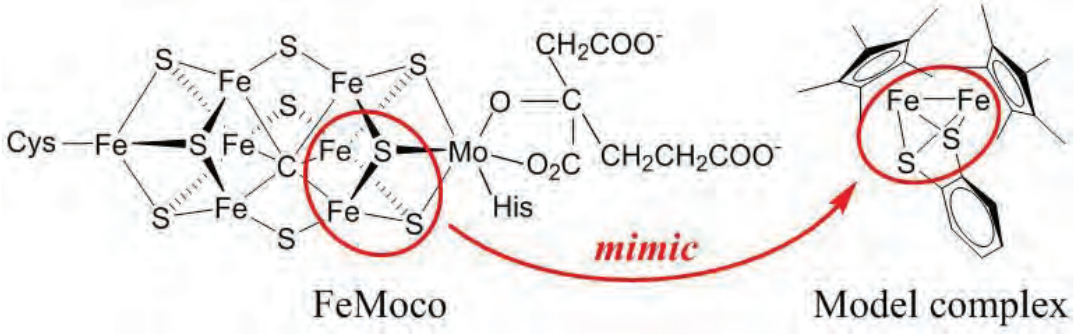

Figure 1-14. The structure of FeMoco and the model complex.

On the other hand, the central metals of these model complexes can be utilized ruthenium instead of iron. Qu and coworkers synthesized thiolate bridged diruthenium complex as a mimic of the active site of [FeFe]-hydrogenase.[71] This complex was reacted with 1 equivalent of $HBF_4{\cdot}Et_2O$ and hydride bridged iron dinuclear complex was

obtained, and the proton reduction occurred in the presence of $HBF_4{\cdot}Et_2O$ (Scheme 1-22). Additionally, this complex was reported to activate C–H of pentamethylcyclopentadienyl (Cp*) ligand coordinated to ruthenium center.[72] The coordinated Cp* ligand in this complex converted to fulvene-like Cp* ligand in complex salt by the C–H activation in the presence of weak base and one-electron oxidant (Scheme 1-23). Surprisingly, the diruthenium complex ligated fulvene-like Cp* can react with I_2, S_8, and carbon monoxide.

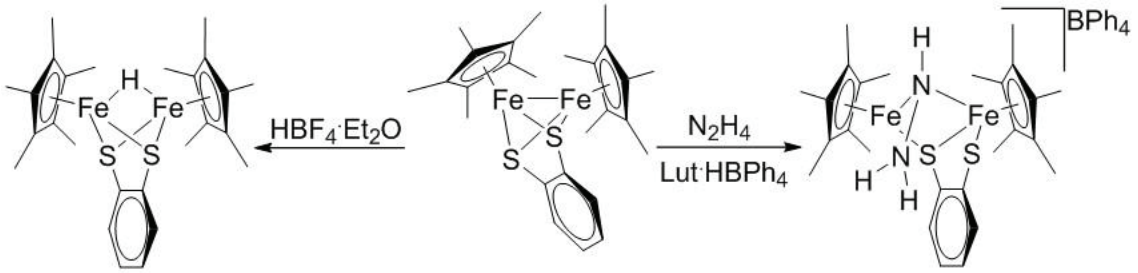

Scheme 1-21. Reaction of thiolate-bridged diiron complex with N_2H_4 and HBF_4.

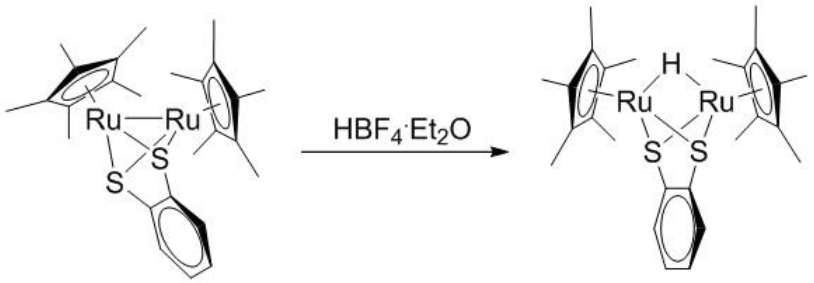

Scheme 1-22. Reaction of thiolate-bridged diruthenium complex with $HBF_4{\cdot}Et_2O$.

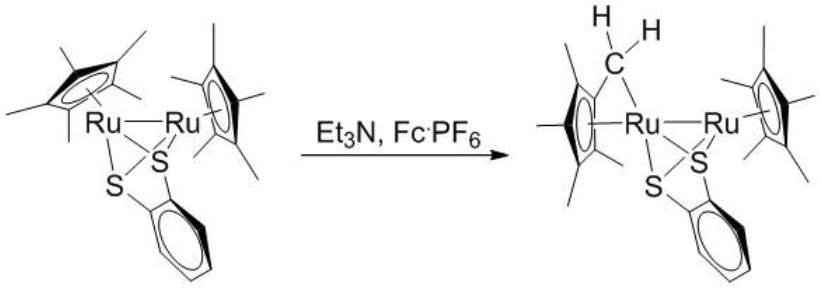

Scheme 1-23. C–H activation of pentamethylcyclopentadienyl (Cp*) ligand coordinated to a ruthenium center.

1-4 The aim of this research

The model complexes containing ruthenium center were reported to have unique reactivity such as addition reaction and C–H activation. However, there have been few reports on the synthesis and application of these complexes.

In this thesis, therefore, synthesis and application of tri-, di-, and mono-nuclear ruthenium dithiolene complexes will be investigated. These compounds are important as key molecules to mimic the active site of enzymes.

This aim would be completed by studying the synthesis of iron-ruthenium trinuclear complex and hydride bridged ruthenium dinuclear complexes and the appliation to catalytic proton reduction and the reaction with carbon dioxide. Additionally, reactivity of mononuclear ruthenium ditholene complex with carbon monoxide and polymer nanocomposite film will be investigated.

In chapter 2, structural and electrochemical properties of ruthenium-diiron trinuclear complex are discussed.

In chapter 3, synthesis and reactivity of ruthenium dithiolene complexes including bridged hydride are discussed.

In chapter 4, synthesis of mononuclear ruthenium dithiolene complexes and its reactivity with carbon monoxide are discussed.

References

[1] J. F. Hartwig, *Organotransition Metal Chemistry From Bonding to Catalysis*, Universal Science Books, **2010**.

[2] R. H. Crabtree, *The Organometallic Chemistry of the Transition Metals*, A John Willy and Sons, Inc., **2005**.

[3] K. Narasaka, Y. Kohno, S. Shimada, *Chem. Lett.* **1993**, 125–128.

[4] E. Diana, M. R. Chierotti, E. M. C. Marchese, G. Croce, M. Milanesio, P. L. Stanghellini, *New J. Chem.* **2012**, *36*, 1099–1107.

[5] S. Berger, W. Bock, G. Frenking, V. Jonas, F. Müller, *J. Am. Chem. Soc.* **1995**, *117*, 3820–3829.

[6] J. W. Faller, Y. Ma, *J. Organomet. Chem.* **1989**, *368*, 45–56.

[7] L. B. Handy, K. G. Sharp, F. E. Brinckman, *Inorg. Chem.* **1972**, *11*, 523–531.

[8] M. Ogasawara, S. A. Macgregor, W. E. Streib, K. Folting, O. Eisenstein, K. G. Caulton, *J. Am. Chem. Soc.* **1995**, *117*, 8869–8870.

[9] J. A. Osborn, F. H. Jardine, J. F. Young, G. Wilkinson, *J. Chem. Soc. A* 1966, 1711–1732.

[10] L. Vaska, J. W. Diluzio, *J. Am. Chem. Soc.* **1961**, *83*, 2784–2785.

[11] F. G. Mann, A. F. Wells, *J. Chem. Soc.* **1938**. 702–710.

[12] G. T. Kerr, A. E. Schweizer, *Inorg. Synth.* **1980**, *20*, 48–49.

[13] G. W. Rice, R. S. Tobias, *Inorg. Chem.* **1976**, *15*, 489–490.

[14] B. P. D. Bartlett, B. Seidel, *J. Am. Chem. Soc.* **1961**, *83*, 581–584.

[15] A. F. Reid, P. W. Wailes, *Aust. J. Chem.* **1966**, *19*, 309–312.

[16] D. Milstein, *Acc. Chem. Res.* **1984**, *17*, 221–226.

[17] A. H. Janowicz, R. G. Bergman, *J. Am. Chem. Soc.* **1982**, *104*, 352–354.

[18] A. H. Janowicz, R. G. Bergman, *J. Am. Chem. Soc.* **1983**, *105*, 3929–3939.

[19] M. V. Baker, L. D. Field, *J. Am. Chem. Soc.* **1987**, *109*, 2825–2826.

[20] J. R. Norton, *Acc. Chem. Res.* **1979**, *12*, 139–145.

[21] P. Meakin, J. P. Jesson, C. A. Tolman, *J. Am. Chem. Soc.* **1972**, *94*, 2825–2826.

[22] R. A. Sanchez-Delgado, M. Rosales, *Coord. Chem. Rev.* **2000**, *196*, 249–280.

[23] E.-A. Jo, C.-H. Jun, *Tetrahedron Lett.* **2009**, *50*, 3338–3340.

[24] G. Xu, P. Renaud, *Angew. Chem.* **2016**, *128*, 3721–3725.

[25] L. Nielsen, T. Skrydstrup, *J. Am. Chem. Soc.* **2008**, *130*, 13145–13151.

[26] M. J. Chalkley, T. J. D. Castillo, B. D. Maston, J. P. Robby, J. C. Peters, *ACS Cent. Sci.* **2017**, *3*, 217−223.

[27] J. Powell, M. R. Gregg, J. F. Sawyer, *Inorg. Chem.* **1989**, *28*, 4451–4460.

[28] R. Schwesinger, C. Hasenfratz, H. Schlemper, L. Walz, E.-M. Peters, K. Peters, H.

G. Schnering, *Angew. Chem. Int. Ed. Engl.* **1989**, *28*, 1361–1363.
[29] T. Ikada, S. Kuwata, Y. Mizobe, M. Hidai, *Inorg. Chem.* **1999**, *38*, 64–69.
[30] G. N. Schrauzer, V. P. Meyweg, *J. Am. Chem. Soc.* **1962**, *84,* 3221.
[31] R. Eisenberg, *Prog. Inorg. Chem.* **1970**, *12*, 295–369.
[32] J. A. McCleverty, *Prog. Inorg. Chem.* 1968, *10*, 49–221.
[33] G. N. Schrauzer, *Acc. Chem.Res.* **1969**, *2*, 72–80.
[34] *Dithiolene Chemistry: Synthesis, Properties, and Applications; Progress in Inorganic Chemistry, Vol. 52* (Ed.: E. I. Stiefel), Wiley, Hoboken, **2004**.
[35] A. E. Pullen and R.-M. Olk, *Coord. Chem. Rev.* **1999**, *188*, 211–262.
[36] N. Robertson, L. Cronin, *Coord. Chem. Rev.* **2002**, *227*, 93–127.
[37] H. R. Holm, *Coord. Chem. Rev.* **1990**, *100*, 183–221.
[38] D. C. Rees, Y. L. Hu, C. Kisker, and H. Schindelin, *J. Chem. Soc., Dalton Trans.* **1997**, 3909–3914.
[39] C. Kisker, H. Schindelin, D. C. Rees, *Ann. Rev. Biochem.* **1997**, *66*, 233–267.
[40] M. J. Rudolph, M. M. Wuebbens, K. V. Rajagopalan, H. Schindelin, *Nat. Struct. Biol.* **2001**, *8*, 42–46.
[41] M. Nomura, *Dalton Trans.* **2012**, *40,* 2112–2140.
[42] R. Sakamoto, S. Tsukada, H. Nishihara, *Dalton Trans.* **2012**, *41,* 10123–10135.
[43] P. E. M. Siegbahn, J. W. Tye, M. B. Hall, *Chem. Rev.* **2007**, *107*, 4414–4435.
[44] J. A. Denny, M. Y. Darensbourg, *Chem. Rev.* **2015**, *115*, 5248−5273.
[45] R. Kato, *Bull. Chem. Soc. Jpn.* **2014**, *87*, 355–374.
[46] F. Hartl, P. Rosa, L, Licard, P. L. Floch, S. Zalis, *Coord. Chem. Rev.* **2007**, *251*, 557–576.
[47] E. S. Donovan, J. J. McCromick, G. S. Nichol, G. A. N. Felton, *Organometallics* **2012**, *31*, 8067−8070.
[48] R. K. M. Khan, S. Torker, A. H. Hoveyda, *J. Am. Chem. Soc.* **2013**, *135*, 10258–10261.
[49] M. J. Koh, R. K. M. Khan, S. Torker, M. Yu, M. S. Mikus, A. H. Hoveyda, *Nature* **2015**, *517*, 181–186.
[50] R. R. Kapre, E. Bothe, T. Weyhermüller, S. D. George, K. Wieghardt, *Inorg. Chem.* **2007**, *46*, 5642−5650.
[51] S. Sproules, P. Banerjee, T. Weyhermüller, Y. Yan, J. P. Donahue, K. Wieghardt, *Inorg. Chem.* **2011**, *50*, 7106–7122.
[52] N. D. Lowe, C. D. Garner, *J. Chem. Soc. Dalton Trans.* **1993**, 2197–2207.
[53] G. D. Figuly, C. K. Loop, J. C. Martin, *J. Am. Chem. Soc.* **1989**, *111*, 654–658.
[54] D. M. Giolando, K. Kirschbaum, *Synthesis* **1992**, 451–452.
[55] M. Sakurada, M. Kajitani, K. Dohki, T. Akiyama, A. Sugimori, *J. Organomet. Chem.*

1992, *423*, 141–161.
[56] M. Kajitani, H. Hatano, T. Fujita, T. Okumachi, H. Nagao, T. Akiyama, A. Sugimori, *J. Organomet. Chem.* **1992**, *430*, C64–C67.
[57] M. Kajitani, T. Fujita, T. Okumachi, M. Yokoyama, H. Hatano, H, Ushijama, T. Akiyama, A. Sugimori, *J. Mol. Catal.* **1992**, *77*, L1–L5.
[58] K. Mashima, H. Kaneyoshi, S. Kaneko, A. Mikami, K. Tani, A. Nakamura, *Organometallics* **1997**, *16*, 1016–1025.
[59] K. Mashima, S. Kaneko, K. Tani, H. Kaneyoshi, A. Nakamura, *J. Organomet. Chem.* **1997**, *545–546*, 345–356.
[60] H, Nishihara, M. Okuno, N. Akimoto, N. Kogawa, K. Aramaki, *J. Chem. Soc., Dalton Trans.* **1998**, 2651–2656.
[61] J. A. Harnisch, R. J. Angelici, *Inorg. Chim. Acta* **2000**, *300–302*, 273–279.
[62] Y. Shibata, B. Zhu, S. Kume, H. Nishihara, *Dalton Trans.* **2009**, *11*, 6856–6858.
[63] T. Kambe, S. Tsukada, R. Sakamoto, H. Nishihara, *Inorg. Chem.* **2011**, *50*, 6856–6858.
[64] M. Murata, S. Habe, S. Araki, K. Namiki, T. Yamada, N. Nakagawa, T. Nankawa, M. Nihei, J. Mizutani, M. Kurihara, H. Nishihara, *Inorg. Chem.* **2006**, *45*, 1108–1116.
[65] N. Nakagawa, T. Yamada, M. Murata, M. Sugimoto, H. Nishihara, *Inorg. Chem.* **2006**, *45*, 14–16.
[66] N. Nakagawa, M. Murata, M. Sugimoto, H. Nishihara, *Eur. J. Inorg. Chem.* **2006**, *11*, 2129–2131.
[67] O. Einsle, F. A. Tezcan, S. L. A. Andrade, B. Schmid, M. Yoshida, J. B. Howard, D. C. Rees, *Science* **2002**, *297*, 1696–1700.
[68] T. Spatzal, M. Aksoyoglu, L. Zhang, S. L. A. Andrade, E. Schleicher, S. Weber, D. C. Rees, O. Einsle, *Science* **2011**, *334*, 940.
[69] K. M. Lancaster, Y. Hu, U. Bergmann, M. W. Ribbe, S. DeBeer, *J. Am. Chem. Soc.* **2013**, *135*, 610–612.
[70] Y. Li, Y. Li, B. Wang, Y. Luo, D. Yang, P. Tong, J. Zhao, L. Luo, Y. Zhou, S. Chen, F. Cheng, J. Qu, *Nat. Chem.* **2013**, *5*, 320–326.
[71] D. Yang, Y. Li, B. Wang, X. Zhao, L. Su, S. Chen, P. Tong, Y. Luo, J. Qu, *Inorg. Chem.* **2015**, *54*, 10243–10249.
[72] X. Ji, D. Yang, P. Tong, J. Li, B. Wang, J. Qu, *Organometallics* **2017**, *36*, 1515−1521.

Chapter 2

Structural and electrochemical properties of ruthenium-diiron trinuclear complex

2-1 Introduction

The past decade has witnessed growing interest in multinuclear complexes including dithiolate ligands because they have unique structures, properties, and reactivity.[1–4] Multinuclear dithiolate complexes having group 8 metals such as iron and ruthenium have been studied as model complexes of hydrogenase, the enzyme responsible of catalyzing the reductive generation and oxidative decomposition of molecular hydrogen.[5–7] These complexes coordinate various thiolate ligands like alkanethiolate, 1,2-ethanedithiolate (edt^{2-}) or 1,2-benzenedithiolate (bdt^{2-}), and their structures, electrochemical properties, electrocatalytic proton reduction, and ability to generate dihydrogen have been examined.[8–10] The bdt^{2-} ligated catalysts, peculiarity, were observed lower potential at catalytic proton reduction than the other thiolate ligated catalyst because of an interaction among the metal orbitals, sulfur p_π orbitals and the benzene p_π orbitals.[8] For example, the diiron complex, $[Fe_2(CO)_6(\mu\text{-bdt})]$, ligated with bdt^{2-} is reported to proton reduction in acetonitrile in the presence of acetic acid at approximately –2.1 V, with the reaction mechanism investigated by both experimentally and theoretically.[8]

Hogarth and coworkers reported the use of a bio-inspired mixed-valence triiron complex including edt^{2-}, $[Fe_3(CO)_7(\mu\text{-edt})]$, as a proton reduction catalyst in the presence of HBF_4.[9, 10] This complex reduced proton at a relatively low over-potential compared with that of related diiron complexes ligated with edt^{2-}. Adams and Yamamoto synthesized a triruthenium complex including edt^{2-} $[Ru_3(CO)_7(\mu\text{-edt})]$ and investigated the isomerization between *syn*- and the *anti*-isomers.[11] Despite these advancements, there is no report to our knowledge on the synthesis of a bdt-bridged trinuclear complex including iron and ruthenium in conjunction with a structural and electrochemical investigation.

At present, we are interested in examining the synthesis of a heteronuclear complex containing a dithiolate diiron unit for application to the synthesis of heteronuclear dithiolene complexes. Metalladitholene complexes of late-transition metals are known to be unsaturated on the metal center.[12–17] Some metalladithiolene complexes thus add easily to the metal center.[18–20] This reactivity has enabled us to synthesize a trinuclear dithiolene complex containing iron and ruthenium. Herein, we describe the synthesis and characterization of the ruthenium-diiron dithiolate complex $[(\eta^6\text{-}C_6Me_6)Ru(CO)(\mu\text{-}CO)_2Fe_2(\mu\text{-bdt})(CO)_4]$. This complex showed two crystallographic isomers when the recrystallization temperature was controlled. Additionally, this complex was shown to be an electrocatalyst for proton reduction in the presence of acetic acid.

2-2 Results and discussion

2-2-1 Synthesis and characterization

The starting material [Ru(η^6-C_6Me_6)($S_2C_6H_4$)] (labeled **1** in Scheme 2-1) was prepared using a slightly modified method reported previously.[21] A reaction of **1** with $Fe(CO)_5$ in the presence of Me_3NO in toluene gave a ruthenium-diiron dithiolate complex [(η^6-C_6Me_6)Ru(CO)(μ-CO)$_2$Fe$_2$(μ-bdt)(CO)$_4$] (labeled **2** in Scheme 2-1) as a reddish-purple solid. This reaction also gave a carbonyl complex [Ru(η^6-C_6Me_6)(CO)($S_2C_6H_4$)] **3**[22] as an orange solid. In the ^{1}H NMR spectrum of **2**, the doublet of doublets at 6.54 and 7.00 ppm are assigned to the benzenedithiolate ligand. These signals were shifted to lower field than that of **1** (7.03 and 7.81 ppm), suggesting deformation of the metalladithiolene ring in **2**. Although **2** had a carbonyl ligand, no signals due to carbonyl ligands in **2** were observed in the ^{13}C NMR spectrum. On the other hand, the IR spectrum (in KBr) showed strong absorption bands at 2039, 1983, 1970, and 1963 cm^{-1} and a strong absorption band at 1766 cm^{-1}, which we attribute to the terminal carbonyl ligands and bridged carbonyl ligand, respectively. Complex **2** was unstable in air and also decomposed in toluene over the course of one day to give a yellow ocher precipitate.

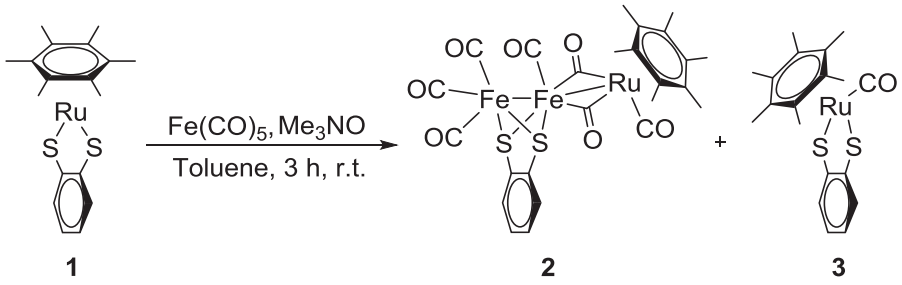

Scheme 2-1. Synthesis of ruthenium-diiron dithiolate complex [(η^6-C_6Me_6)Ru(CO)(μ-CO)$_2$Fe$_2$(μ-bdt)(CO)$_4$] **2**

2-2-2 Isomerization at crystal state

The molecular structure of **2** was successfully characterized by single crystal X-ray diffraction analysis (Figure 2-1). A single crystal of **2** was obtained by recrystallization in a mixed solvent of dichloromethane and hexane. Complex **2** has a diiron unit and a ruthenium unit: the former structural unit has two irons, a benzenedithiolate ligand, and six carbonyl ligands, resembling the $[Fe_2(CO)_6(S_2C_6H_4)]$ structure labeled **4** in Figure 1. The latter structural unit contains a ruthenium atom, a terminal carbonyl ligand, and a hexamethylbenzene ligand. The Fe(1)–Fe(2) bond in **2** is bridged by a dithiolate ligand and the Fe(2)–Ru bond in **2** is bridged by two CO ligands.

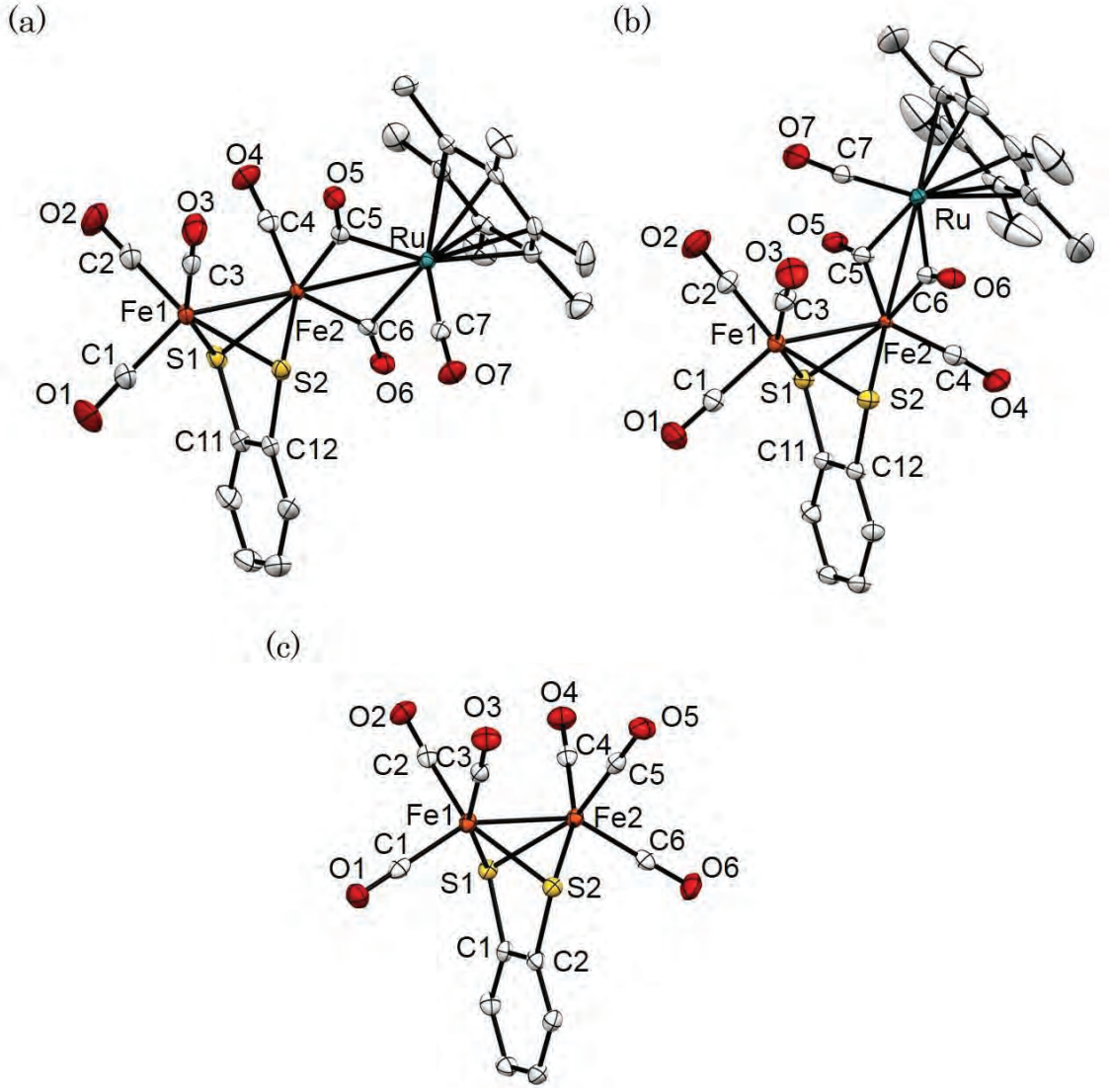

Figure 2-1. ORTEP drawing of (a) **2**, (b) **2'** and (c) $[Fe_2(CO)_6(S_2C_6H_4)]$ **4** with thermal ellipsoids shown at 50 % probably level. Hydrogen atoms are omitted for clarity.

Two isomers of **2** were observed in the crystal state, which depend on the recrystallization temperature: **2** and **2'** were obtained at –30 ºC and room temperature, respectively. These crystals were insoluble in pentane, hexane, and other paraffins. As indicated in Scheme 2-2, a single crystal of **2** was converted to **2'** by leaving it in hexane at room temperature for one week. However, a single crystal of **2'** did not convert to **2** in hexane at –30 ºC. Instead, **2** could only be obtained by the recrystallization of **2'** from a mixed solvent of dichloromethane and hexane, as was necessary during the initial recrystallization step of **2**. Overall, these results suggest that **2** is the most stable isomeric form in solvent. The isomerization of **2** to **2'** can be understood in terms of a rotation of the carbonyl ligands coordinating Fe(2), as shown in the Newman projection viewed from the Fe(1)–Fe(2) axis of **2** and **2'** (Figure 2-2). The three carbonyl ligands coordinated to Fe(2) in **2** rotate anticlockwise by approximately 120° to convert **2** to **2'**.

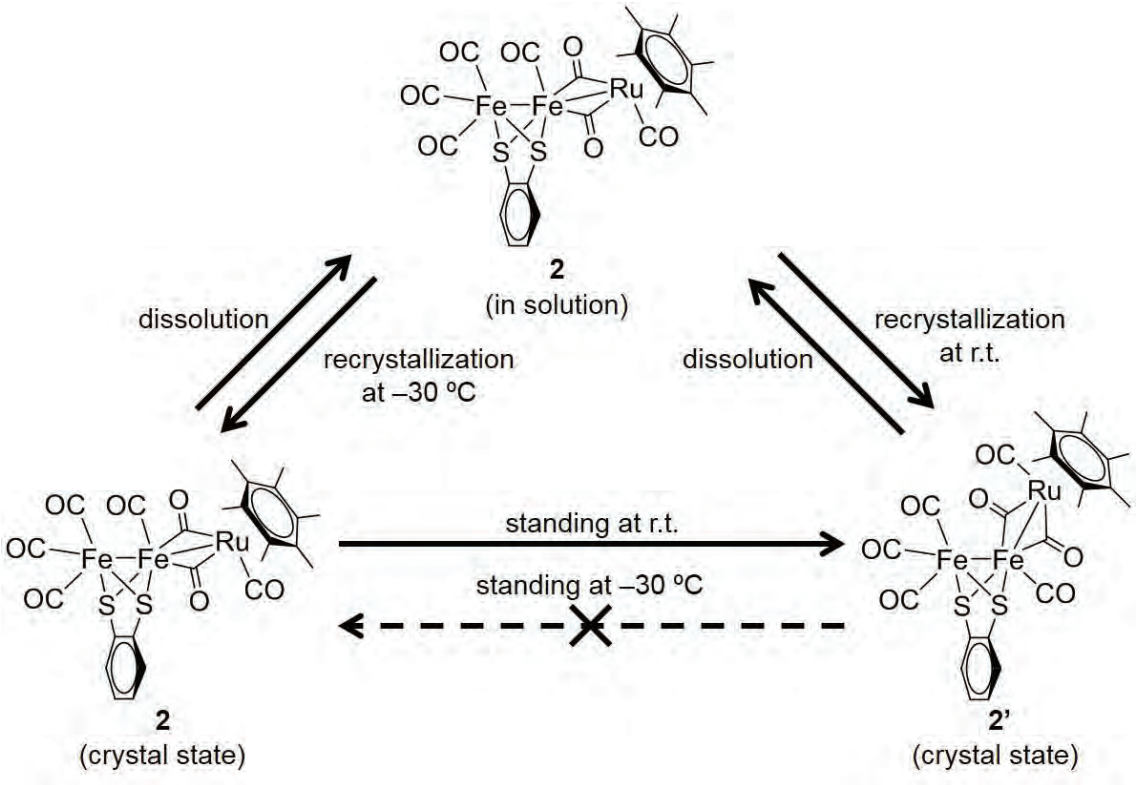

Scheme 2-2. The isomerization between **2** and **2'**

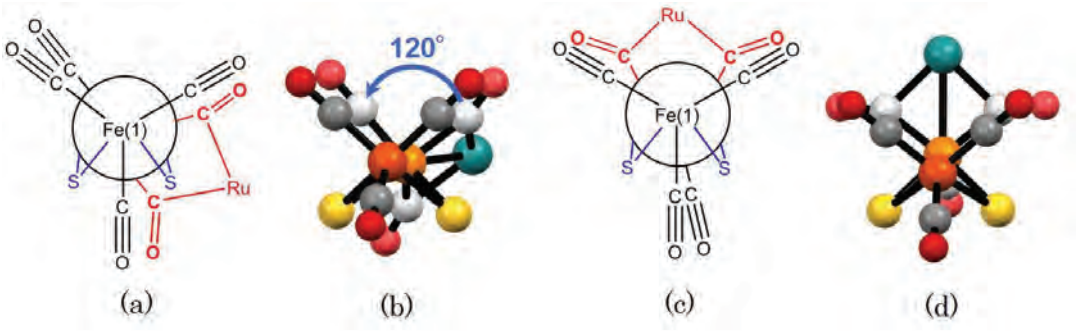

Figure 2-2. (a) Newman projection along the Fe(1)–Fe(2) axis of **2**. (b) Molecular structure of the central skeleton of **2**. (c) Newman projection along the Fe(1)–Fe(2) axis of **2'**. (d) Molecular structure of the central skeleton of **2'**.

2-2-3 Molecular structure

Selected bond lengths, angles, and torsion angles of complexes **2**, **2'**, and **4** are shown in Table 2-1. Complex **2** has an approximately linear metal linkage (i.e., Fe(1)–Fe(2)–Ru), with an angle of 152.00(1)°. This angle is similar to those of the triiron complex $[Fe_3(CO)_7(\mu\text{-edt})]$ and the triruthenium complex *anti*-$[Ru_3(CO)_7(\mu\text{-edt})]$ reported by Yamamoto and Hogarth, respectively.[10, 11] The bond angles of Fe–Fe–Fe in $[Fe_3(CO)_7(\mu\text{-edt})]$ and of Ru–Ru–Ru in *anti*-$[Ru_3(CO)_7(\mu\text{-edt})]$ are reported to be 151.74(3)° and 151.52(3)°, respectively.[10, 11] For comparison, the bond angles of Fe(1)–Fe(2)–Ru in **2'** and Ru–Ru–Ru in *syn*-$[Ru_3(CO)_7(\mu\text{-edt})]$ are 112.11(5)° and 73.55(2)°, respectively[10, 11]. The isomerization of *anti*-$[Ru_3(CO)_7(\mu\text{-edt})]$ to generate the *syn*-compound can occur via an approximate 180° rotation of the ligands coordinating to central Ru, which differs from the case of **2**.[11]

Table 2-1. Selective bond length (Å), angles (deg) and torsion angles (deg) for **2**, **2'** and **4**

	2	**2'**	**4**
Fe1-Fe2	2.4924(4)	2.5530(16)	2.4776(5)
Fe2-Ru	2.6613(3)	2.6705(12)	-
C1-O1	1.136(3)	1.135(11)	1.132(3)
C2-O2	1.141(3)	1.154(9)	1.138(2)
C3-O3	1.143(3)	1.154(9)	1.137(3)
C4-O4	1.146(3)	1.146(11)	1.140(3)
C5-O5	1.173(3)	1.178(8)	1.136(4)
C6-O6	1.164(3)	1.178(8)	1.138(2)
C7-O7	1.141(3)	1.162(11)	-
Fe1-Fe2-Ru	152.00(1)	112.11(5)	-
S1-Fe1-S2-C12	-43.31(7)	-43.8(2)	-40.03(6)
S2-Fe1-S1-C11	43.04(8)	43.8(2)	40.25(7)
S1-Fe2-S2-C12	38.01(7)	40.2(2)	42.10(6)
S2-Fe2-S1-C11	-38.60(8)	-40.2(2)	-42.07(6)

Thus, the difference of bond angles between the two isomers of **2** (39.89°) is smaller than that of $[Ru_3(CO)_7(\mu\text{-edt})]$ (77.97°). The Fe1–Fe2 bond distance in **2** is 2.4924(4) Å, which is essentially identical to that in **4** (2.4776(5) Å). However, the bond distance of Fe1–Fe2 in **2'** is longer than those of **2** and **4** (2.5530(16) Å), which is caused by steric hindrance between the terminal carbonyl ligands on Ru and Fe1 of **2'**. Additionally, the C–O bond lengths of seven carbonyl ligands in **2'** are longer than those of **2**, as evidenced by the corresponding IR spectra in which their corresponding absorption bands are shifted to slightly shorter wavenumbers. The IR spectrum of **2'** (in KBr) shows strong absorption bands at 2036, 1980, 1969, and 1940 cm^{-1} and a strong absorption band at 1764 cm^{-1}, which are attributed to the terminal carbonyl ligands and bridged carbonyl ligand, respectively. The bond lengths of the Ru1-hexamethylbenzene ligands in **2** and **2'** are 1.863 Å and 1.855 Å, respectively, which are longer than that in **1** (1.684 Å).[21] These elongations are attributed to the steric barrier between the hexamethylbenzene ligand and three carbonyl ligands coordinated to ruthenium. Additionally, we note that the planarity of the dithiolate ring in **2** and **2'** is lost as same as **4**, which has also been reported.[23]

Table 2-2 Crystallographic Data and Structure Refinement Detail for **2**, **2'** and **4**

	2	**2'**	**4**
Emprical formula	$C_{25}H_{22}Fe_2O_7RuS_2$	$C_{25}H_{22}Fe_2O_7RuS_2$	$C_{12}H_4Fe_2O_6S_2$
Formula weight	711.32	711.32	419.97
T (K)	100	103	103
Wavelength (Å)	1.54178	0.71073	0.71073
Crystal system	Monoclinic	Orthorhombic	Monoclinic
Space group	*P*2(1)/*c*	*Pnma*	*P*2(1)/*c*
a (Å)	12.0283(5)	14.628(3)	8.2231(18)
b (Å)	11.5811(5)	12.049(3)	14.801(3)
c (Å)	19.3208(9)	14.628	12.489(3)
α (deg)	90	90	90
β (deg)	94.645(2)	90	107.525(4)
γ (deg)	90	90	90
V ($Å^3$)	2682.6(2)	2578.2(9)	1449.5(6)
Z	4	4	4
D_{calc} (g m^{-3})	1.761	1.833	1.924
F (000)	1424	1424	832
Reflection collected	42710	12573	7571
Independent refrections (R_{int})	5312 (0.0377)	2522 (0.0343)	2643 (0.0210)
R_1 ($I > 2\sigma(I)$)	0.0214	0.0503	0.0217
w*R*2 (all data)	0.0547	0.1183	0.0540
Goodness of fit (GOF) on F^2	1.038	1.207	1.071

2-2-4 DFT calculation

In order to obtain further insight into the molecular structure, frontier orbitals, and energy difference of these complexes, density functional theory (DFT) calculations were performed for **2** and **2'**. In particular, the B3LYP exchange-correlation functional was used with the LANL2DZ (for Fe and Ru) and 6-31G(d,p) (for H, C, O, and S) basis sets. The highest occupied molecular orbital (HOMO) and the lowest unoccupied molecular orbital (LUMO) of **2** and **2'** are shown in Figure 2-3. The HOMO of **2** is highly delocalized. In contrast, the HOMO of **2'** is mainly localized on the Fe–Fe bond, which is a similar finding to those of the iron dinuclear complex **4** and the iron trinuclear complex $[Fe_3(CO)_7(\mu\text{-edt})]$.[9, 10] The LUMOs of **2** and **2'** are highly delocalized, resulting from a combination of the antibonding orbitals of the Fe–Fe bond, the Fe–Ru bond, and the bridged carbonyl ligands. Therefore, it is expected that the Fe–Fe and Fe–Ru bonds in **2** and **2'** are cleaved with concomitant elimination of the bridged carbonyl ligands following electron reduction, in an identical manner as occurs with $[Fe_3(CO)_7(\mu\text{-edt})]$.[10]

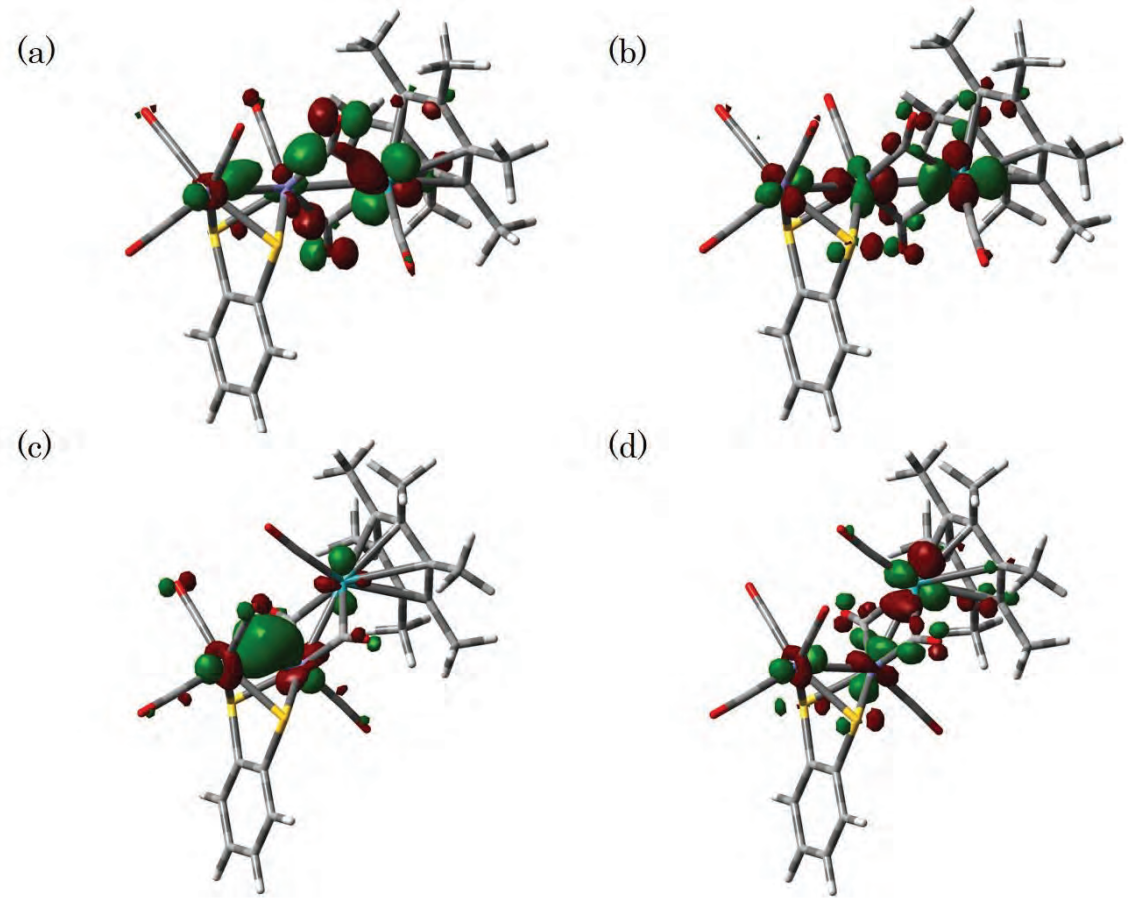

Figure 2-3. (a) HOMO and (b) LUMO of **2**. (c) HOMO and (d) LUMO of **2'**. The contour plots are shown with an isovalue of 0.055.

2-2-5 Packing structure

Adams and Yamamoto have previously shown that *anti*-[$Ru_3(CO)_7(\mu$-edt)] converts into the thermodynamically favored *syn*-[$Ru_3(CO)_7(\mu$-edt)] upon heating (Scheme 2-4).[11] Compared with the *anti* isomer, the *syn* isomer is lower in enthalpy by 2.9 kcal mol^{-1}.[10] Analogously, it is reasonable that the enthalpy of **2'**, which is converted from **2** at room temperature, is smaller than that of **2**. However, the enthalpy of **2'** was actually calculated to be 2.85 kcal mol^{-1} higher than that of **2** (Figure 2–4), the reason of which is unclear. Further, the packing structure of **2'** shows interactions involving three terminal CO ligands coordinated to Fe(1) (labeled C2–O2 and C3–O3), Ru (labeled C7–O7), the hexamethylbenzene ligand of another molecule, and another complex interacting to another molecule (Figure 2–5). The distances between O2, O3, and O7 and the hexamethylbenzene ring of a neighbouring molecule are 3.452 Å, 3.452 Å, and 2.909 Å, respectively. These results suggest stronger π-orbital back donation of the three CO ligands of **2'** than that of **2**.[24, 25] It follows that the bond lengths of C2–O2, C3–O3 and C7–O7 of **2'** are longer relative to those of **2** (Table 2–1). However, the packing structure of **2** didn't show an interaction between the hexamethylbenzene ligand and a CO ligand of an adjacent complex (Figure 2–6). Therefore, it is suggested that the packing structure of **2'** is thermodynamically more stable than that of **2**.

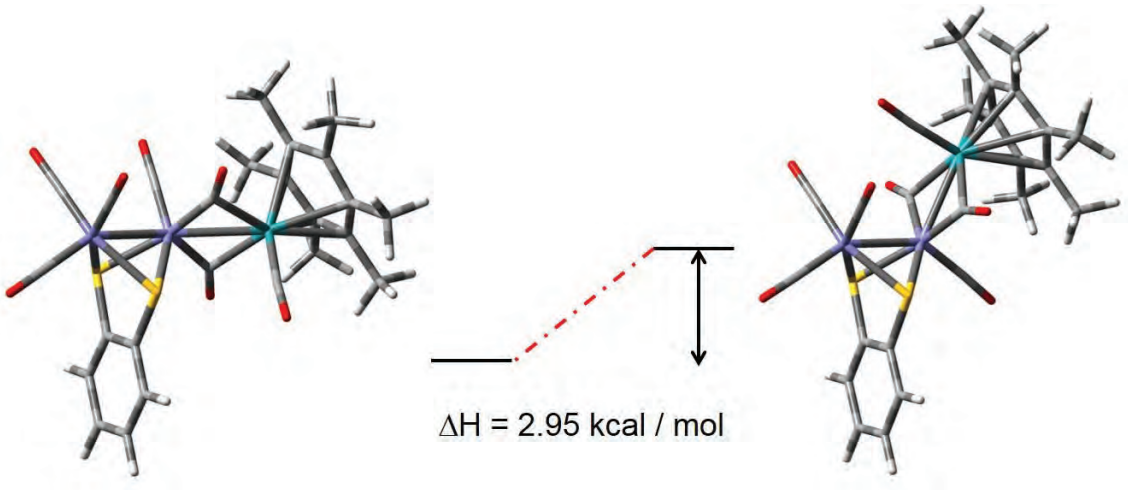

Figure 2-4. Geometry-optimized B3LYP structures of the **2** (left) and **2'** (right) isomers and the gorund-state enthalpy difference in the isomeric **2** and **2'**.

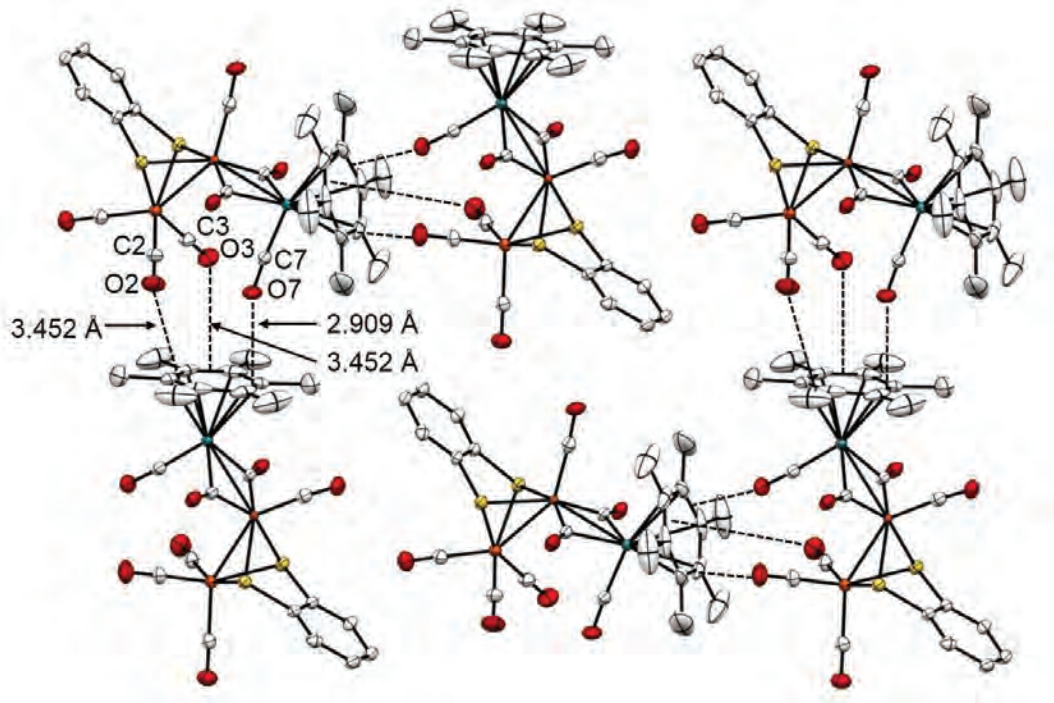

Figure 2-5 Packing structure of **2'**

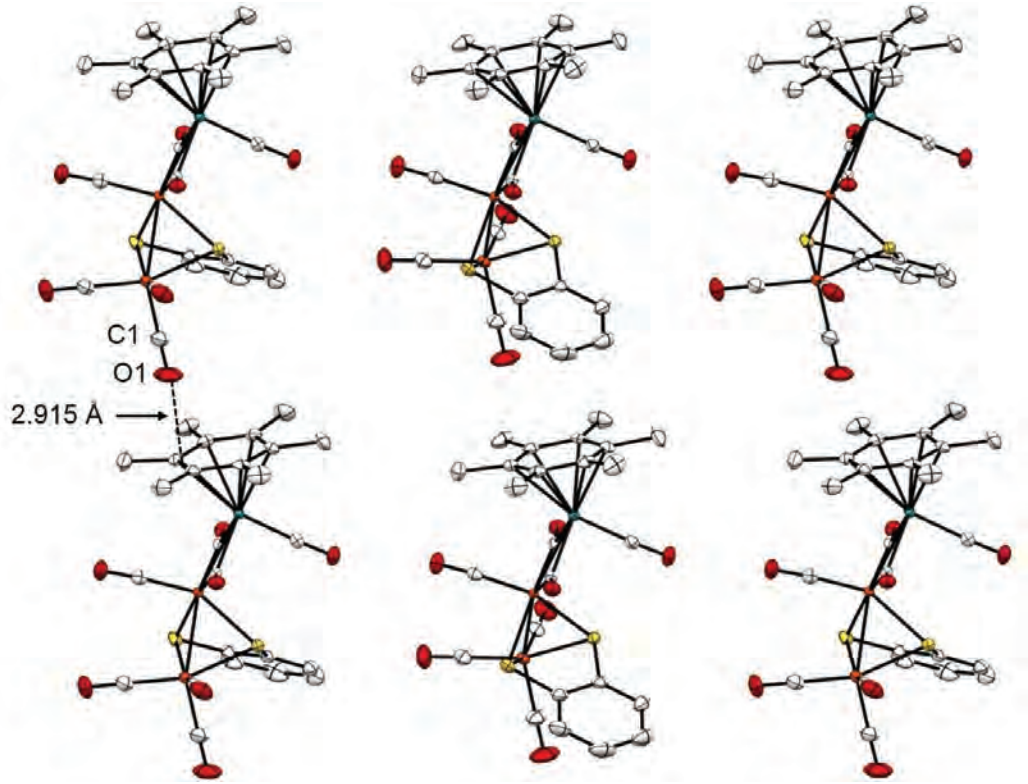

Figure 2-6 Packing structure of **2**

2-2-6 Electrochemical properties

Figure 2-7 shows the cyclic voltammograms (CVs) of **2** that was analyzed in acetonitrile under an argon atmosphere at room temperature. As seen, **2** presents two irreversible reduction peaks at –1.59 V and –2.03 V. The electron density distribution of the LUMO of **2** suggests cleavage of the bridged CO ligands and decomposition during the reduction phase. In addition, **2** doesn't show paired oxidation peaks but a single peak on reduction, which supports an irreversible oxidation and reduction process.

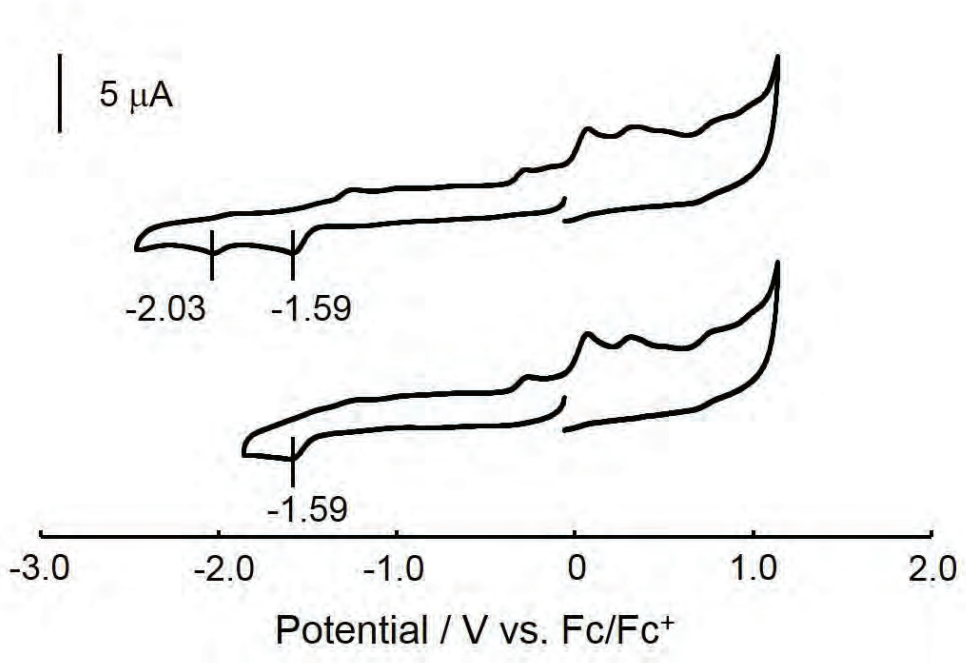

Figure 2-7. CVs of **2** (0.5 mM) in 0.1 M TBAP in acetonitrile under Ar atmosphere at a scan rate of 0.1 V s^{-1} (vs. Fc/Fc^+).

We also studied the reduction behaviour of **2** in the presence of acetic acid (pK_a = 22.3 in acetonitrile[8]) as a weak acid. Generally, the proton reduction is less effective for catalysts in the presence of weaker acid. However, as the acid become weaker, the standard reduction potential of the acid moves in the negative direction.[25, 26] In other words, the overpotential for the catalytic reduction with weaker acid becomes smaller than that with stronger acid.[8] To this end, the CVs of **2** in the presence of acetic acid were measured and shown in Figure 2-8. Catalytic proton reduction occurs at a potential of –2.1 V and 250 μA in 50 equivalents of acetic acid. Therefore, **2** can reduce proton catalytically at a lower potential than **4**, which reduces proton at a potential of –2.2 V.[10] In addition, **2** showed a second catalytic proton reduction peak at a potential of approximately –2.5 V.

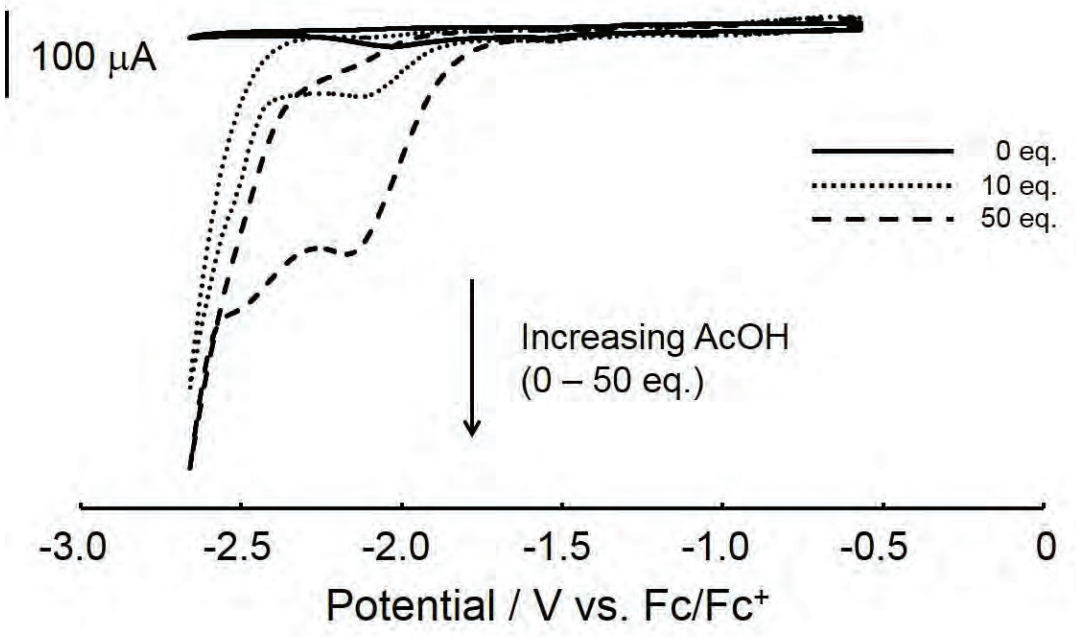

Figure 2-8. CVs of **2** (0.5 mM) in 0.1 M TBAP in acetonitrile under an Ar atmosphere at a scan rate of 0.1 V s^{-1} with increments of AcOH (0, 10, 50 equiv) per amount of molar **2** (vs. Fc/Fc^+).

2-3 Experimental Section

2-3-1 General

Toluene, dichloromethane, and hexane were purchased from Kanto Chemical, Tokyo, Japan. Toluene was distilled from Na, dried over 4 Å molecular sieves, and degassed with nitrogen before use. Other solvents were distilled from calcium hydride, dried over 4 Å molecular sieves, and degassed with nitrogen before use. Pentacarbonyliron was purchased from Kanto Chemical, Tokyo, Japan and trimethylamine *N*-oxide was purchased from Tokyo Chemical Industry, Tokyo, Japan.

$[(\eta^6\text{-}C_6Me_6)Ru(S_2C_6H_4)]$ (**1**)[21] and $[Fe_2(CO)_6(S_2C_6H_4)]$ (**4**)[23] were prepared according to previously reported literature methods.

All NMR spectra were recorded on an ECP-500 (500 MHz) spectrometer. ^1H NMR (500 MHz) and $^{13}C\{^1H\}$ NMR (126 MHz) spectra were measured using tetramethylsilane as an internal standard. IR spectra were recorded using a JASCO FT-IR 6100 spectrometer. Melting points were measured using a Bibby Stuart Scientific SMP3 instrument. All melting points are uncorrected. HR-ESI MS were recorded on a JEOL JMS-T100CS "AccuTOF CS" spectrometer.

For structural determination, crystal data were collected using a Bruker AXS SMART APEX CCD X-ray diffractometer equipped with a rotating-anode X-ray generator emitting graphite-monochromatic Mo-Kα radiation (0.7107 Å) and Cu-Kα radiation (1.5418 Å). Empirical absorption corrections using equivalent reflections and Lorentzian polarization correction were performed using the SADABS program.[27] All data were collected with the SMART and Bruker SAINTPLUS (Version 6.45) software packages. The structures were solved using the SHELXS-97[28] program and refined against F^2 using SHELEXL-97.[29] CCDC No. 1554925 (**2**), 1554926 (**2'**) and 1557709 (**4**) contain supplementary crystallographic data for this paper. These data can be obtained free of charge from The Cambridge Crystallographic Data Centre *via* www.ccdc.cam.ac.uk/conts/retrieving.html. The crystal structure of **4** was previously reported in reference 9; however, it has not been registered with the Cambridge Crystallographic Data Center. Therefore, we deposited the structure of **4**.

The three-parameter Becke-Lee-Yang-Parr (B3LYP) hybrid exchange-correlation functional was employed for the theoretical calculations. The Lanl2DZ basis set was used for Fe and Ru, whereas the 6-31G(d,p) basis set was used for H, C, O, and S.[30-32] Initial structures were taken from the relevant single-crystal X-ray structures. All calculations were performed using the Gaussian 09W (Revision-A.02) software program.[33]

Electrochemical data were recorded with an ALS 650E electrochemical analyzer. Bu_4NClO_4 used as a supporting electrolyte, which was recrystallized from EtOH and

dried under vacuum for 24 h. A series of measurements were performed under an argon atmosphere in a three-electrode cell (BAS Inc.) using 3 mm-diameter glassy carbon as the working electrode (BAS Inc.), platinum wire as the counter electrode, and $Ag/AgClO_4$ as the reference electrode (0.01 M $AgClO_4$ in 0.1 M Bu_4NClO_4/acetonitrile, BAS Inc.). After each measurement, ferrocene was added as an internal standard. Note that Bu_4NClO_4 is a potentially explosive chemical. Catalytic studies were performed by adding equivalents of CH_3COOH purchased from Kanto Chemical Co., Inc.

2-3-2 Synthesis of $[(\eta^6\text{-}C_6Me_6)Ru(CO)(\mu\text{-}CO)_2Fe_2(\mu\text{-}bdt)(CO)_4]$ **2**

All chemical syntheses were performed under an argon atmosphere. To a stirred solution of $[(\eta^6\text{-}C_6Me_6)Ru(S_2C_6H_4)]$ (**1**) (162 mg, 0.40 mmol) and Me_3NO (60 mg, 0.80 mmol) in toluene (20 mL) was added $Fe(CO)_5$ (78.2 mg, 0.40 mmol). After the mixture was stirred at room temperature for 3 h, the volatiles were removed under reduced pressure. The resulting residual was developed by silica gel column chromatography with toluene as the eluent. The third red-purple colored fraction was collected, which gave 36 mg (0.051 mmol, 13 %) of a reddish-purple solid of **2**. Recrystallization of the reddish-purple material using dichloromethane and hexane at –30 °C gave a reddish-purple needle crystal of **2**. Additionally, the first orange-colored fraction was collected, which gave 60 mg (0.14 mmol, 35 %) of an orange solid of **3**. Recrystallization of this orange material using toluene and dichloromethane at room temperature afforded an orange needle crystal of **3**. Although **2** had a carbonyl ligand, no signals due to carbonyl ligands in **2** were observed in the ^{13}C NMR spectrum.

2: ^1H NMR (500 MHz, CD_2Cl_2) δ (ppm): 2.28 (s, 18H, $C_6(CH_3)_6$), 6.54 (dd, 2H, J = 3.0, 5.5 Hz, $S_2C_6H_4$), 7.00 (dd, 2H, J = 3.0, 5.5 Hz, $S_2C_6H_4$). ^{13}C NMR (126 MHz, CD_2Cl_2) δ (ppm): 16.6, 115.0, 125.8, 127.9, 150.0. IR(KBr): ($\nu_{C\equiv O}$) 2039, 1983, 1970, 1963 cm^{-1}; ($\nu_{C=O}$) 1766 cm^{-1}. HRMS (HR-ESI-TOF) *m/z*: Calcd. for $C_{19}H_{22}Fe_2O_7RuS_2Na$: 734.84470 $[M+Na]^+$, Found: 734.84218 $[M+Na]^+$

3: ^1H NMR (500 MHz, CD_2Cl_2) δ (ppm): 2.14 (s, 18H, $C_6(CH_3)_6$), 6.63 (dd, 2H, J = 3.2, 5.6 Hz, $S_2C_6H_4$), 7.12 (dd, 2H, J = 3.2, 5.6 Hz, $S_2C_6H_4$). ^{13}C NMR (126 MHz, CD_2Cl_2) δ (ppm): 16.1, 110.2, 121.8, 127.3, 144.3, 197.6. IR(ATR): ($\nu_{C\equiv O}$) 1951 cm^{-1}. HRMS (HR-ESI-TOF) *m/z*: Calcd. for $C_{25}H_{22}ORuS_2Na$: 455.00532 $[M+Na]^+$, Found: 455.00584.

2-3-3 Preparation of single crystal of **2'**

The reddish-purple material of **2** was recrystallized in dichloromethane-hexane solvent

at room temperature to give a red-purple needle crystal of **2'**, which was subsequently characterized by single crystal X-ray diffraction.

2-3-4 Isomerization of single crystal of **2**

The single crystal of **2** (5.0 mg) was left in hexane for one week at room temperature, after which time the single crystal of **2'** was obtained (2.7 mg, 54 %). This crystal was characterized by single crystal X-ray diffraction.

2-3-5 Isomerization of single crystal of **2'**

The single crystal of **2'** (5.0 mg) was left in hexane for one week at –30 ºC, after which time the single crystal of **2'** did not change. This crystal was characterized by single crystal X-ray diffraction.

2-3-6 Recrystallization of single crystal of **2'** at –30 °C

The single crystal of **2'** (5.0 mg) was dissolved in dichloromethane and recrystallized in dichloromethane-hexane solvent at –30 ºC. After this time, the single crystal of **2** was obtained (0.9 mg, 18 %) and then characterized by single crystal X-ray diffraction.

2-4 References

[1] C. Tard, C. J. Pickett *Chem. Rev.* **2009**, *109*, 2245–2274.

[2] F. Gloaguen, T. B. Rauchfuss *Chem. Soc. Rev.* **2009**, *38*, 100–108.

[3] J. Capon, F. Gloaguen, F. Y. Pétillon, P. Schollhammer, J. Talarmin *Coord. Chem. Rev.* **2009**, *253*, 1476–1494.

[4] Y. Li, T. B. Rauchfuss *Chem. Rev.* **2016**, *116*, 7043–7077.

[5] Frey, M. *ChemBioChem* **2002**, *3*, 153–160.

[6] J. W. Peters, W. N. Lanzilotta, B. J. Lemon, L. C. Seefeldt *Science* **1998**, *282*, 1853–1858.

[7] Y. Nicolet, C. Piras, P. Legrand, C. E. Hatchikian, J. C. Fontecilla-Camps *Structure* **1999**, *7*, 13–23.

[8] G. A. N. Felton, A. K. Vannucci, J. Chen, L. T. Lockett, N. Okumura, B. J. Petro, U. I. Zakai, D. H. Evans, R. S. Glass, D. L. Lichtenberger *J. Am. Chem. Soc.* **2007**, *129*, 12521–12530.

[9] S. Ghosh, G. Hogarth, K. B. Holt, S. E. Kabir, A. Rahaman, D. G. Unwin *Chem. Commun.* **2011**, *47*, 11222–11224.

[10] A. Rahaman, S. Ghosh, D. G. Unwin, S. Basak- Modi, K. B. Holt, S. E. Kabir, E. Nordlander, M. G. Richmond, G. Hogarth *Organometallics* **2014**, *33*, 1356–1366.

[11] R. D. Adams, J. H. Yamamoto *J. Cluster Sci.* **1996**, 7, 643–654.

[12] *Dithiolene Chemistry: Synthesis, Properties, and Applications; Progress in Inorganic Chemistry, Vol. 52* (Ed.: E. I. Stiefel), Wiley, Hoboken, **2004**.

[13] R. Eisenberg, *Prog. Inorg. Chem.* **1970**, *12*, 295–369.

[14] R. P. Burns, C. A. McAuliffe, *Adv. Inorg. Chem. Radiochem.* **1979**, *22*, 303–348.

[15] M. Fourmigue, *Coord. Chem. Rev.* **1998**, *178–180*, 823–864.

[16] A. Sugimori, T. Akiyama, M. Kajitani, T. Sugiyama, *Bull. Chem. Soc. Jpn.* **1999**, *72,* 879–908.

[17] R. Sakamoto, S. Tsukada, H. Nishihara, *Dalton Trans.* **2012**, *41*, 10123–10135.

[18] M. Sakurada, M. Kajitani, K. Dohki, T. Akiyama A. Sugimori *J. Organomet. Chem.* **1992**, *423*, 141–161.

[19] M. Nomura, M. Fujii, K. Fukuda, T. Sugiyama, Y. Yokoyama, M. Kajitani *J. Organomet. Chem.* **2005**, *690*, 1627–1637.

[20] M. Murata, S. Habe, S. Araki, K. Namiki, T. Yamada, N. Nakagawa, T. Nankawa, M. Nihei, J. Mizutani, M. Kurihara, H. Nishihara *Inorg. Chem.* **2006,** *45*, 1108–1116.

[21] K. Mashima, H. Kaneyoshi, S. Kaneko, A. Mikami, K. Tani, A. Nakamura, *Organometallics* **1997**, *16*, 1016–1025.

[22] S. Tsukada, T. Sagawa, T. Gunji *Chem. Asian J.* **2015**, *10*, 1881–1883.

[23] J. A. Cabeza, M. A. Martinez-Garcia, V. Riera *Organometallics* **1998**, *17*, 1471–1477.
[24] A. Gambaro, P. Ganis, F. Manoli, A. Polimeno, S. Santi, A. Vanzo *J. Organomet. Chem.* **1999**, *583*, 126–130.
[25] H. Paramahamsan, A. J. Pearson, A. A. Pinkerton, E. A. Zhurova *Organometallics*, **2008**, *27*, 900–907.
[26] G. A. N. Felton, R. S. Glass, D. L. Lichatenberger, D. H. Evans, *Inorg. Chem.* **2006**, *45*, 9181-9184.
[27] G. M. Sheldrick, *SADABS*, *Program for area detector absorption correction*, University of Göttingen, Germany, 1996.
[28] G. M. Sheldrick, *SHELXS–97*, *Program for crystal structure solution*, University of Göttingen, Germany, 1997.
[29] G. M. Sheldrick, *SHELXL–97*, *Program for crystal structure refinement*, University of Göttingen, Germany, 1997.
[30] A. D. Becke, *Phys. Rev. A* **1988**, *38*, 3098-3100.
[31] A. D. Becke, *J. Chem. Phys.* **1993**, *98*, 5648-5652.
[32] J. P. Perdew, Y. Wang, *Phys. Rev. B* **1992**, *45*, 13244-13249.
[33] M. J. Frisch, G. W. Trucks, H. B. Schlegel, G. E. Scuseria, M. A. Robb, J. R. Cheeseman, G. Scalmani, V. Barone, B. Mennucci, G. A. Petersson, H. Nakatsuji, M. Caricato, X. Li, H. P. Hratchian, A. F. Izmaylov, J. Bloino, G. Zheng, J. L. Sonnenberg, M. Hada, M. Ehara, K. Toyota, R. Fukuda, J. Hasegawa, M. Ishida, T. Nakajima, Y. Honda, O. Kitao, H. Nakai, T. Vreven, J. A. Montgomery, Jr., J. E. Peralta, F. Ogliaro, M. Bearpark, J. J. Heyd, E. Brothers, K. N. Kudin, V. N. Staroverov, R. Kobayashi, J. Normand, K. Raghavachari, A. Rendell, J. C. Burant, S. S. Iyengar, J. Tomasi, M. Cossi, N. Rega, J. M. Millam, M. Klene, J. E. Knox, J. B. Cross, V. Bakken, C. Adamo, J. Jaramillo, R. Gomperts, R. E. Stratmann, O. Yazyev, A. J. Austin, R. Cammi, C. Pomelli, J. W. Ochterski, R. L. Martin, K. Morokuma, V. G. Zakrzewski, G. A. Voth, P. Salvador, J. J. Dannenberg, S. Dapprich, A. D. Daniels, O. Farkas, J. B. Foresman, J. V. Ortiz, J. Cioslowski, D. J. Fox, *Gaussian 09, Revision A.02*, Gaussian, Inc.; Wallingford CT, 2009.

Chapter 3

Synthesis and reactivity of ruthenium dithiolene complexes including bridged hydride

3-1 Introduction

Transition metal hydride complexes were interested in for long time because these complexes have unique reactivity such as insertion reactions and metathesis reactions.[1–5] In particular, sulfur bridged bimetallic complexes of group 8 metals including hydride ligand are reported to have catalytic reactivity and to react with various chemical species.[6–8] For example, Wilson and coworkers reported the synthesis of bridged hydride and propanedithiolate ruthenium complex $[Ru_2(S_2C_3H_6)(\mu\text{-}H)(H)(CO)_3(PCy_3)_2]$ and studied the crystal structures to be useful as model for the investigation of the active site in hydrogenase.[7] Holland and coworkers reported the synthesis of iron sulfide complex with a bridging hydride [NaCrypt-222][$L^{Me}Fe(\mu\text{-}H)(\mu\text{-}S)FeL^{Me}$] where L^{Me} is a bulky β-diketiminate ligand. This complex reacted with carbon dioxide and a formate sulfide complex [NaCrypt-222][$L^{Me}Fe(\mu\text{-}CHOO)(\mu\text{-}S)FeL^{Me}$].[8]

Metalladithiolene complexes of late-transition metals are known to be unsaturated compounds on the metal center[9–14] to which metalladithiolene complexes are easily added[15, 16]. For example, Nomura and coworkers reported the synthesis of bridged hydride rhodium-ruthenium heteronuclear complex $[Rh(\eta^5\text{-}C_5Me_5)(S_2C_6H_4)RuClH(PPh_3)_2]$ by the reaction of $[Rh(\eta^5\text{-}C_5Me_5)(S_2C_6H_4)]$ with $[RuClH(PPh_3)_3]$ and dihydride rhodium-ruthenium heteronuclear complex by the reaction of $[Rh(\eta^5\text{-}C_5Me_5)(S_2C_6H_4)RuH_2(PPh_3)_2]$ with potassium hydroxide in isopropyl alcohol. This dihydride compound is thermally stable up to 110 ºC in toluene. On the other hand, this compound reacts smoothly with carbon monoxide or ethynyl derivatives.[17] In other words, this compound has thermally stability and high reactivity at the same time. Accordingly, ruthenium dinuclear complex including bridged hydride is expected to have thermal stability and different reactivity from heteronuclear complex such as the reaction with carbon monoxide or carbon dioxide. We focus on the synthesis of dithiolate bridged ruthenium bimetallic complexes including hydride ligand to apply to the synthesis of heteronuclear dithiolene complex $[Rh(\eta^5\text{-}C_5Me_5)(S_2C_6H_4)RuClH(PPh_3)_2]$.

In this work, we describe the synthesis and characterization of hydride bridged ruthenium dinuclear complex $[Ru(\eta^6\text{-}C_6Me_6)(S_2C_6H_4)RuClH(PPh_3)_2]$ (**6**) and the dihydride ruthenium dinuclear complex $[Ru(\eta^6\text{-}C_6Me_6)(S_2C_6H_4)RuH_2(PPh_3)_2]$ (**7**). Compound **7** exhibited the reaction with carbon monoxide, which was obtained as dicarbonyl complex $[Ru(\eta^6\text{-}C_6Me_6)(S_2C_6H_4)Ru(CO)_2(PPh_3)]$ (**8**) and tetracarbonyl complex $[Ru_2(CO)_4(PPh_3)_2(S_2C_6H_4)]$ (**9**). Additionally, the reaction of **7** with carbon dioxide under ambient condition and generation of formic acid are also described.

3-2 Results and discussion

3-2-1 Synthesis of [Ru(η^6-C_6Me_6)($S_2C_6H_4$)RuClH(PPh_3)$_2$] (**6**)

The starting material [Ru(η^6-C_6Me_6)($S_2C_6H_4$)] (**1**) and [RuClH(PPh_3)$_3$] (**5**) were prepared using literature methods as reported previously.[18, 19] The molecular structure of **5** was successfully determined by single crystal X-ray diffraction analysis for the first time (Figure 3-1, Table 1).[9] Single crystal of **5** was obtained by recrystallization in toluene. **5** was added to the THF solution of **1** at room temperature. After washing with Et_2O, hydride bridged ruthenium dinuclear complex [Ru(η^6-C_6Me_6)($S_2C_6H_4$)RuClH(PPh_3)$_2$] (**6**) was obtained as green solid with 72% yield (Scheme 3-1). In the ^{1}H NMR spectrum (Figure 3-2 (a)), the triplet signal at −17.47 ppm (J_{P-H} = 12 Hz) was assigned to the bridged hydride. A singlet at 1.65 ppm was assigned to methyl proton in the hexamethylbenzene ligand. Double doublets at 6.60 ppm and 7.36 ppm were assigned to protons in the benzenedithiolate ligand which were shifted to the lower-field than those of **1** (7.03 and 7.81 ppm)[20] to show the deformation of metalladithiolene ring in **6**. A singlet at 51 ppm in ^{31}P NMR spectrum (Figure 3-2 (b)) confirms that both the PPh_3 ligands in **6** are chemically equivalent. The molecular structure of **3** was successfully determined by single crystal X-ray diffraction analysis (Figure 3-3 (a), Table 3-1). Single crystal of **6** was obtained by recrystallization in a mixed solvent of chloroform and hexane. The conformation of **6** is found to resemble a three-legged piano-stool structure around Ru1 (Figure 3-3 (b)) and a distorted-octahedral geometry around Ru2 (Figure 3-3 (c)). The terminal chloride ligand is positioned *trans* to the bridged hydride in the crystal structure. The average length of Ru2–S (2.3611 Å) is shorter than that of Ru1–S (2.4226 Å) due to the steric hindrance between benzenedithiolate and chloride ligands.

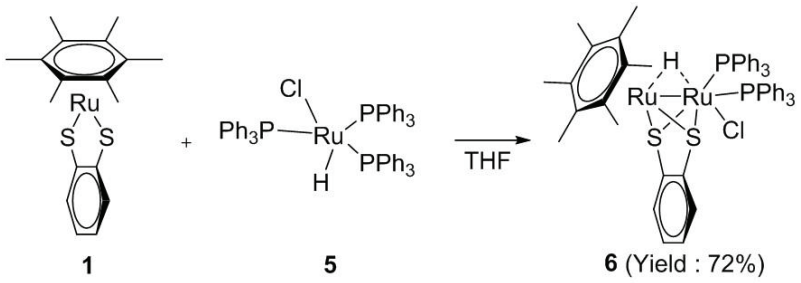

1 **5** **6** (Yield : 72%)

Scheme 3-1 Synthesis of hydride bridged ruthenium dinuclear complex [Ru(η^6-C_6Me_6)($S_2C_6H_4$)RuClH(PPh_3)$_2$] (**6**).

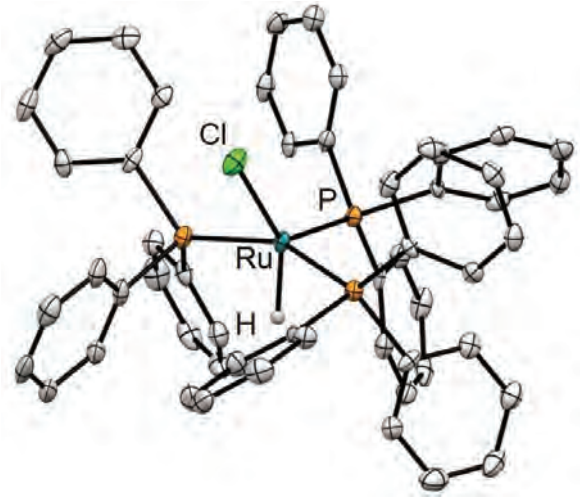

Figure 3-1. ORTEP drawing of **5** with thermal ellipsoids shown at 50 % probably level. Hydrogen atoms, excluding the bridging and terminal hydrides, are omitted for clarity.

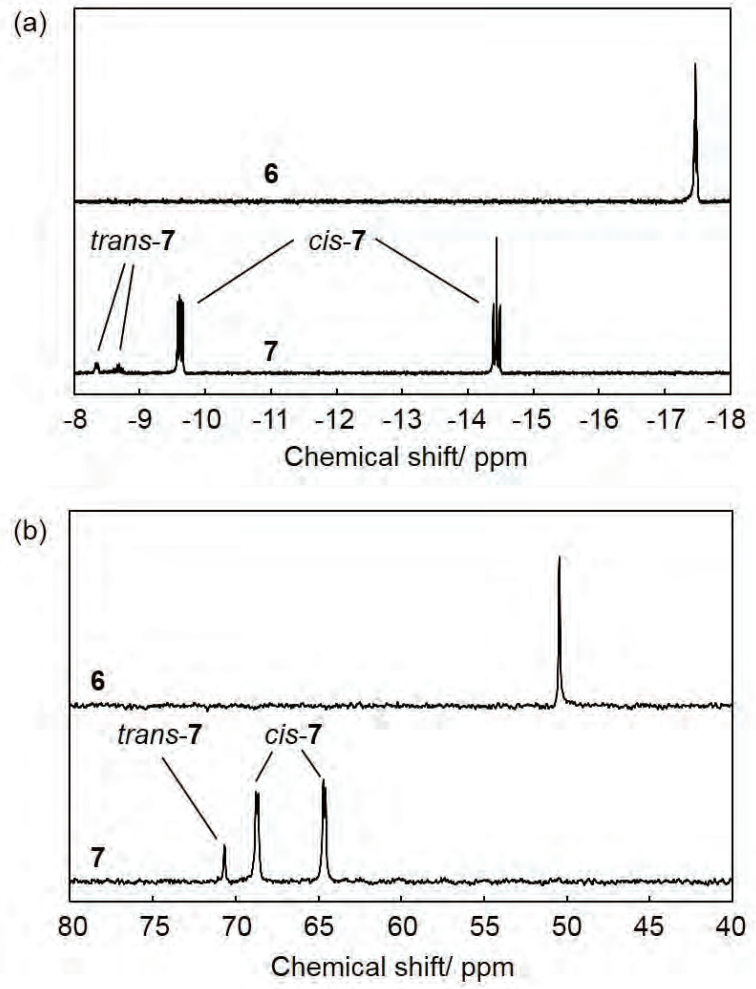

Figure 3-2 (a) ^{1}H NMR (500 MHz, C_6D_6) and (b) ^{31}P NMR (202 MHz, C_6D_6) of [Ru(η^6-C_6Me_6)($S_2C_6H_4$)RuClH(PPh_3)$_2$] (**6**) and [Ru(η^6-C_6Me_6)($S_2C_6H_4$) RuH_2(PPh_3)$_2$] (**7**)

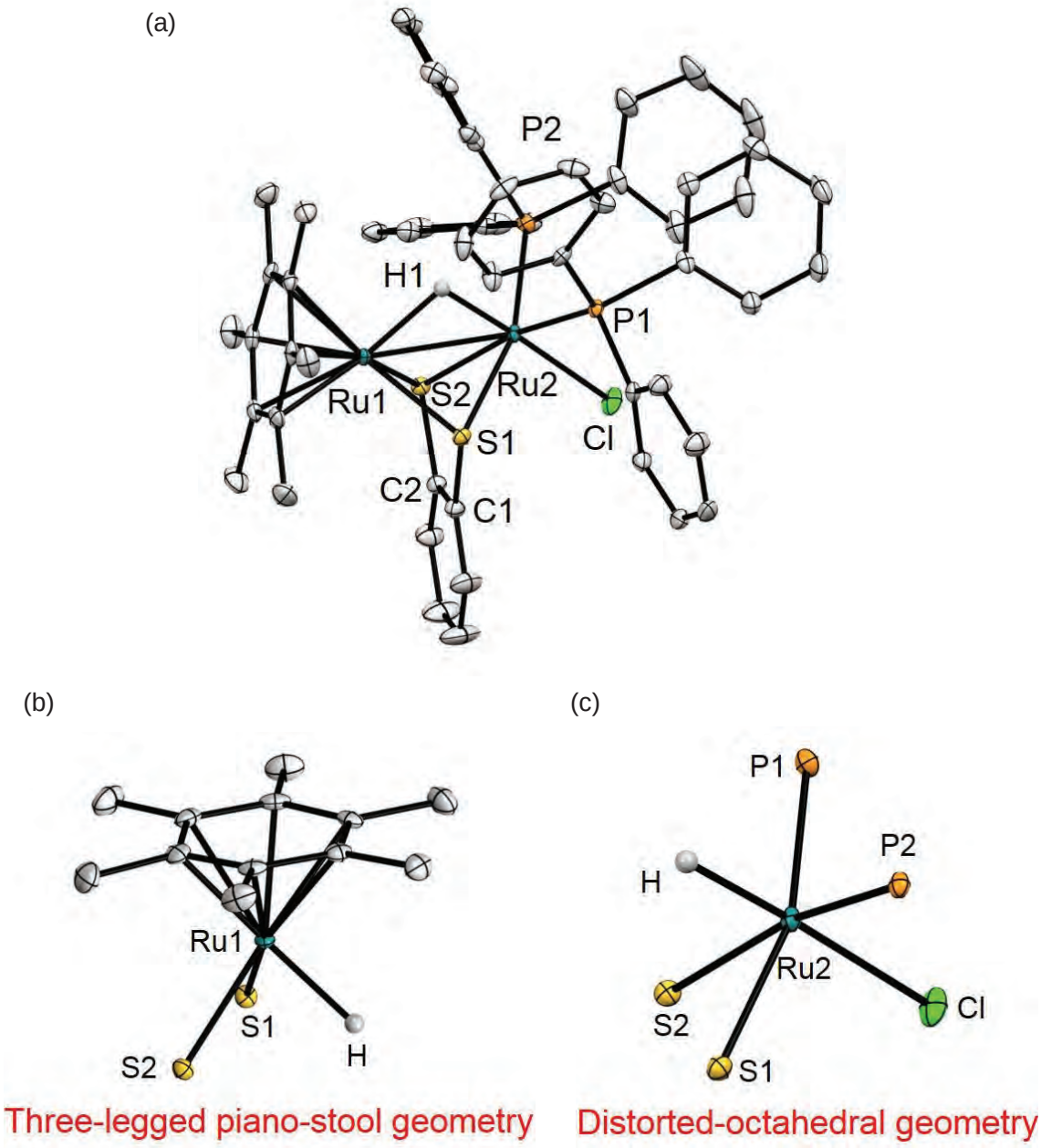

Figure 3-3. (a) ORTEP drawing of **6** with thermal ellipsoids shown at 50 % probably level. Hydrogen atoms, excluding the bridging hydride is omitted for clarity. (b) Three-legged piano-stool structure around Ru1. (c) A distorted-octahedral geometry around Ru2.

3-2-2 Synthesis of [Ru(η^6-C_6Me_6)($S_2C_6H_4$) $RuH_2(PPh_3)_2$] (**7**)

The reaction of **6** with excess KOH in *i*-PrOH produced the dihydride ruthenium dinuclear complex [Ru(η^6-C_6Me_6)($S_2C_6H_4$)$RuH_2(PPh_3)_2$] **7** which was isolated as orange solid in 83% yield (Scheme 3-2). Reaction mechanism of this ligand exchange reaction is expected to be same manner that is reported previously.[21] In other words, chloride ligand is eliminated by KOH and unsaturated complex is generated as an intermediate. Then, proton of alcohol coordinated to unsaturated compound. The reaction product was estimated to contain a mixture of *cis*- and *trans*- dihydride isomers in a 10:1 molar ratio from the proton ratio in ^{1}H NMR spectra. In ^{1}H NMR spectrum of **7**, the triplet signal at −14.44 ppm (J_{HH} = 25 Hz) is assigned to the bridged hydride of the *cis*-isomer and the double doublets at −9.61 ppm (J_{HP} = 16 Hz, $J_{H\text{-}H}$ = 25 Hz) are assigned to the terminal hydride of the *cis*-isomer (Figure 3-2 (a)) similar to the assignments reported for rhodium-ruthenium heteronuclear complex [Rh(η^5-C_5Me_5)($S_2C_6H_4$)$RuH_2(PPh_3)_2$].[17] In general, bridged hydrides is usually observed at high magnetic field than terminal hydrides in ^{1}H NMR spectroscopy.[22] In the ^{31}P NMR spectrum, the doublet signals at 64 ppm and 68 ppm are assigned to the chemically inequivalent triphenylphosphine ligands of *cis*-isomer and the singlet at 70 ppm is assigned to the chemically equivalent triphenylphosphine ligands of *trans*-isomer (Figure 3-2 (b)) present in the solution. The dihydride complex **7** exhibited thermal stability up to 110 °C which is in line with earlier observation reported for Rh-Ru dihydride complex.[17]

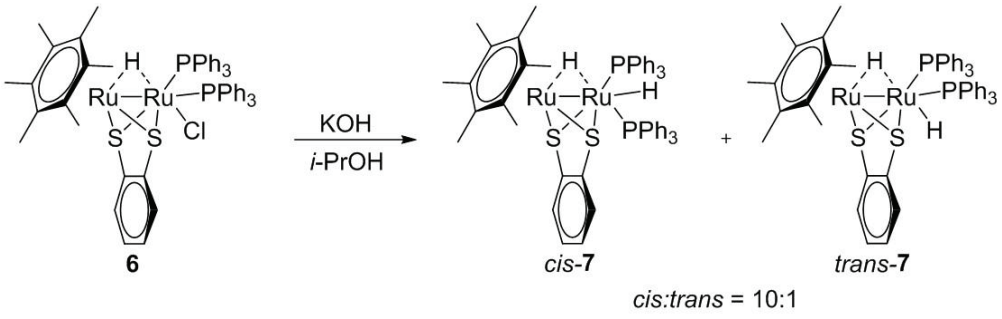

Scheme 3-2 Synthesis of dihydride ruthenium dinuclear complex [Ru(η^6-C_6Me_6)($S_2C_6H_4$) $RuH_2(PPh_3)_2$] (**7**).

The molecular structure of *cis*-**7** was successfully determined by single crystal X-ray diffraction analysis. Single crystals of *cis*-**7** isomer were obtained by recrystallization in a mixed solvent of dichloromethane and hexane to determine the molecular structure of *cis*-**7** using single crystal X-ray diffraction analysis (Figure 3-4 (a), Table 1). Unfortunately, single crystals of *trans*-**7** isomer could not be isolated despite using various ways of recrystallization. The *cis*-**7** isomer exhibits a structural similarity with **6** around the metal center where Ru1 is ligated to a hexamethylbenzene in a three-legged piano-stool geometry (Figure 3-4 (b)) and Ru2 coordinates with two triphenylphosphine ligands in a distorted-octahedral geometry (Figure 3-4 (c)). The terminal hydride ligand is in *cis* conformation to the bridged hydride in the crystal structure. The Ru–P bond lengths of **6** is expected to be shorter than that of *cis*-**7** because of the inductive effect of the chloride ligand of **6**. However, this bond lengths of **6** is longer than that of *cis*-**7** in nature. In fact, the Ru2–P1 and Ru2–P2 bond lengths of **6** (2.3106(4) Å and 2.3122(5) Å) are slightly longer than those of *cis*-**7** (2.2599(7) Å and 2.2626(7) Å). Therefore, steric hindrance of ligands has greatly affected on the bond lengths around metals compared with trans effect. The Ru–Ru bond length of **6** (2.7819(2) Å) and *cis*-**7** isomer (2.8052(3) Å) are longer than that of the $[Ru_2(CO)_6(C_6H_4S_2)]$ complex (2.650(2) Å).[23] Additionally, the Ru–H–Ru angles of **6** and *cis*-**7** (**6**: 101°, *cis*-**7**: 105°) are less than 180°. These results indicate that Ru–H–Ru bonds of **6** and *cis*-**7** are a three-center two-electron bond. In general, the bent M–H–M geometry (less than 180°) implies a closed three-centered two-electron bond, with an M–M bond distance that is longer than that in a simple two-center two-electron metal-metal bond.[24] Propanedithiolate ruthenium complex $[Ru_2(S_2C_3H_6)(\mu\text{-}H)(H)(CO)_3(PCy_3)_2]$, the heteronuclear complex $[Rh(\eta^5\text{-}C_5Me_5)(S_2C_6H_4)RuH_2(PPh_3)_2]$, and the rhodium dinuclear complex salt $[Rh_2(\eta^5\text{-}C_5Me_5)_2(\mu\text{-}H)(SC_3H_7)_2][OTf]$ are nominated as examples of such structural features around **M–**H–M.[7, 17, 25]

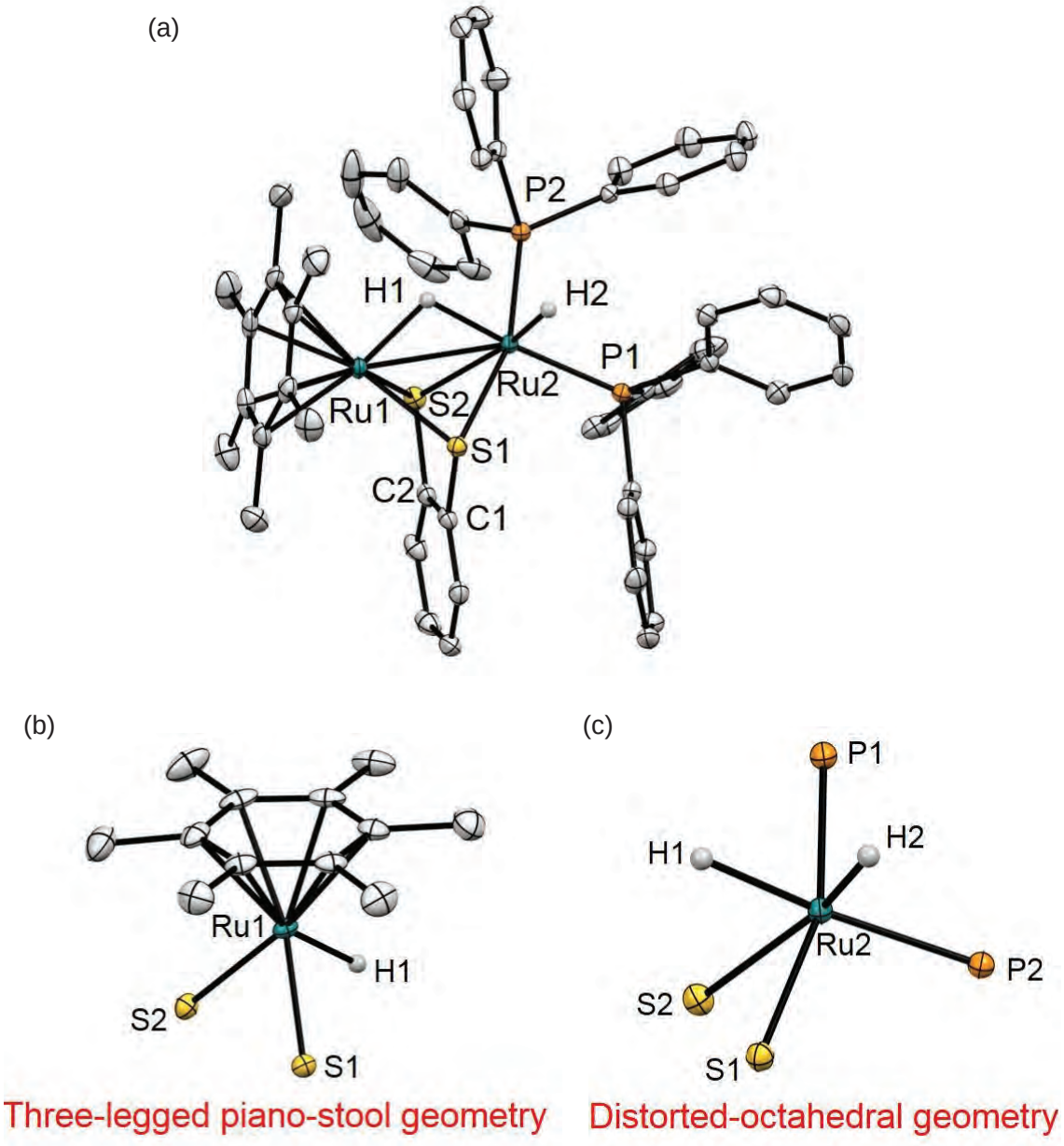

Figure 3-4. (a) ORTEP drawing of *cis*-**7** isomer with thermal ellipsoids shown at 50 % probably level. Hydrogen atoms, excluding the bridging and terminal hydrides, are omitted for clarity. (b) Three-legged piano-stool structure around Ru1. (c) A distorted-octahedral geometry around Ru2.

3-2-3 Reaction of [Ru(η^6-C_6Me_6)($S_2C_6H_4$) $RuH_2(PPh_3)_2$] (**7**) with CO

A study to investigate the reactivity of the dihydride complex **7** was performed. **7** was reacted with CO at room temperature for 30 min, which resulted in the formation of a dicarbonyl complex [Ru(η^6-C_6Me_6)($S_2C_6H_4$) $Ru(CO)_2(PPh_3)$] (**8**) isolated as reddish purple solid in 55% yield (Scheme 3-3). ^{1}H NMR spectrum of **8** shows the absence of signals derived from two hydride ligands in dinuclear complex **7**, which suggests that coordination of carbon monoxide to metal center induces reductive elimination of H_2 from **7**, as previously encountered for [(*i*Pr-PONOP)$Ru(CO)_2$] (*i*Pr-PONOP = $C_3H_5N(OP^iPr_2)_2$) and [(η^5-C_5Me_5)$Rh(S_2C_6H_4)Ru(CO)_2(PPh_3)$] (Scheme 3-4).[17, 26] This observation was further reinforced by IR spectrum of **8**, which displays two strong absorption bands at 2054 and 1944 cm^{-1} attributed to the terminal carbonyl ligands. Surprisingly, when reaction time between **7** with CO was increased to 1 day, a tetracarbonyl complex $[Ru_2(CO)_4(PPh_3)_2(S_2C_6H_4)]$ (labeled **9** in Scheme 3-3) was obtained as yellow solid (86% yield) at room temperature. Therefore, **7** seems to react with two equivalents of carbon monoxide to generated **8** with reductive elimination of dihydrogen in the first step. Then, **8** is probably reacted with revealed triphenylphosphine and additional two equivalents of carbon monoxide. Finally, **9** is generated with elimination reaction of hexamethylbenzene. The molecular structure of **9** was determined by single-crystal X-ray diffraction analysis (Figure 3-5 and Table 3-1). A facile substitution reaction between benzene moiety and CO led to the formation of this tetracarbonyl complex **9** that is analogous to the substitution reaction reported between dithiolate ruthenium complex ligated to *p*-cymene [(*p*-cymene)$Ru(SC_8H_{11})_2$] and CO to form pentacarbonyl complex $[Ru_2(CO)_5(SC_8H_{11})_4]$ (Scheme 3-5).[18] **9** could be also obtained by the reaction of $[Ru_2(CO)_4(MeCN)_4(PPh_3)_2][PF_6]_2$ with *o*-benzenedithiol in the presence of trimethylamine (Scheme 3-6).[27]

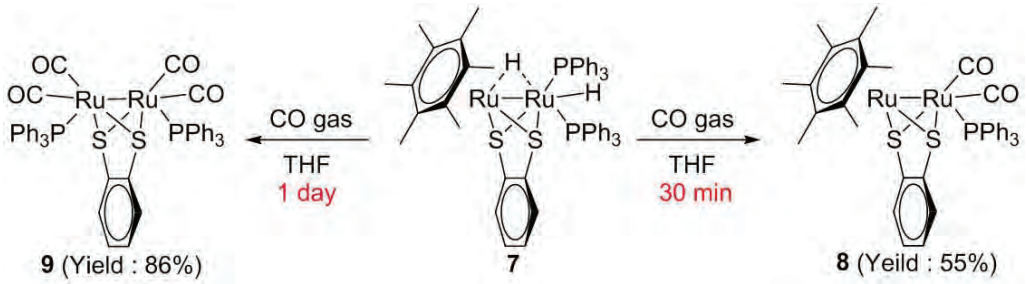

9 (Yield : 86%) **7** **8** (Yeild : 55%)

Scheme 3-3

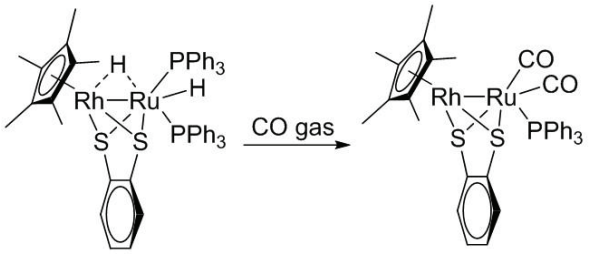

Scheme 3-4

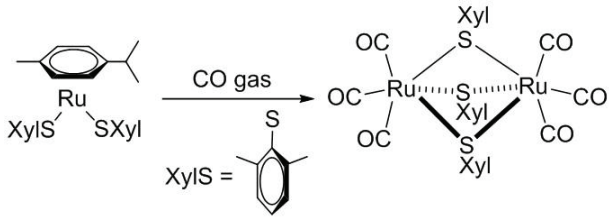

Scheme 3-5

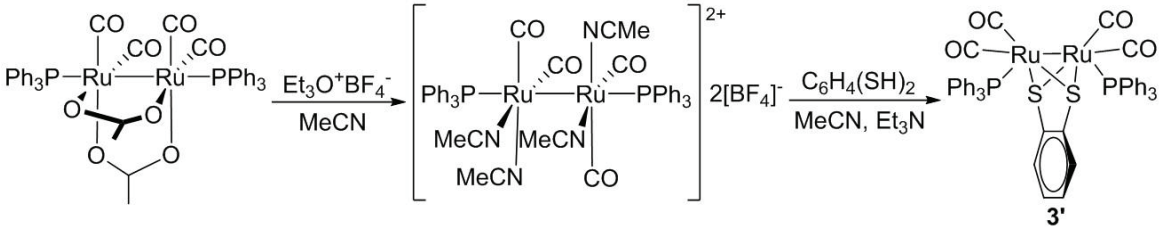

Scheme 3-6

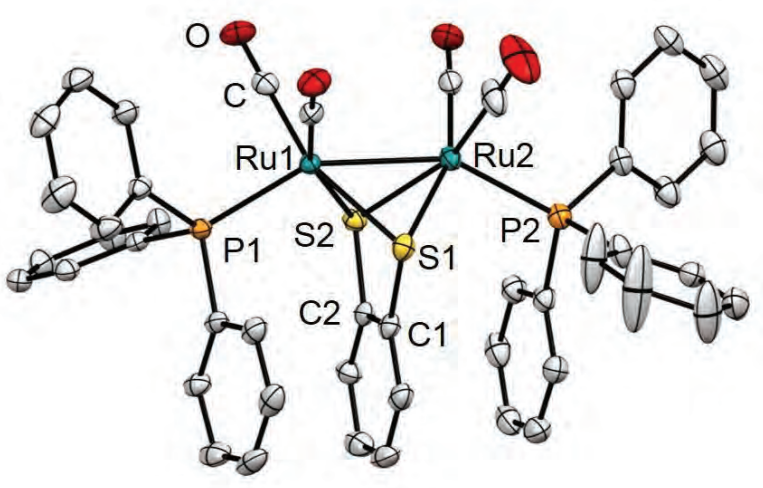

Figure 3-5. ORTEP drawing of **9** with thermal ellipsoids shown at 50 % probably level. Hydrogen atoms are omitted for clarity.

3-2-4 Reaction of [Ru(η^6-C_6Me_6)($S_2C_6H_4$)$RuH_2(PPh_3)_2$] (**7**) with CO_2

An investigation of the reaction of **7** with CO_2 was also performed. An *i*-PrOH solution of **7** was stirred under CO_2 atmosphere at room temperature for 24 h. The solution was then concentrated under reduced pressure to obtain a deep brown solid and a distillate. The ^{1}H NMR spectrum of the deep brown solid shows no signals for bridged hydride (Figure 3-6 (a)). Moreover, a few non-identified signals make it more difficult to estimate the structure. The ^{31}P NMR spectrum shows only a singlet peak at 27.5 ppm assigned to the phosphorus atom in the chemically equivalent triphenylphosphine ligands (Figure 3-6 (b)). These spectral data suggest that the deep brown solid might be a ruthenium complex ligated triphenylphosphine ligands without hydride ligand. Unfortunately, it is difficult to characterize a product because of the difficulty on purification. On the other hand, the distillate, when analyzed by GC-MS (Figure 3-7), shows the formation of formic acid. Consequently, it is inferred that the two hydrides in **7** reduced CO_2 under the ambient condition to generate formic acid.

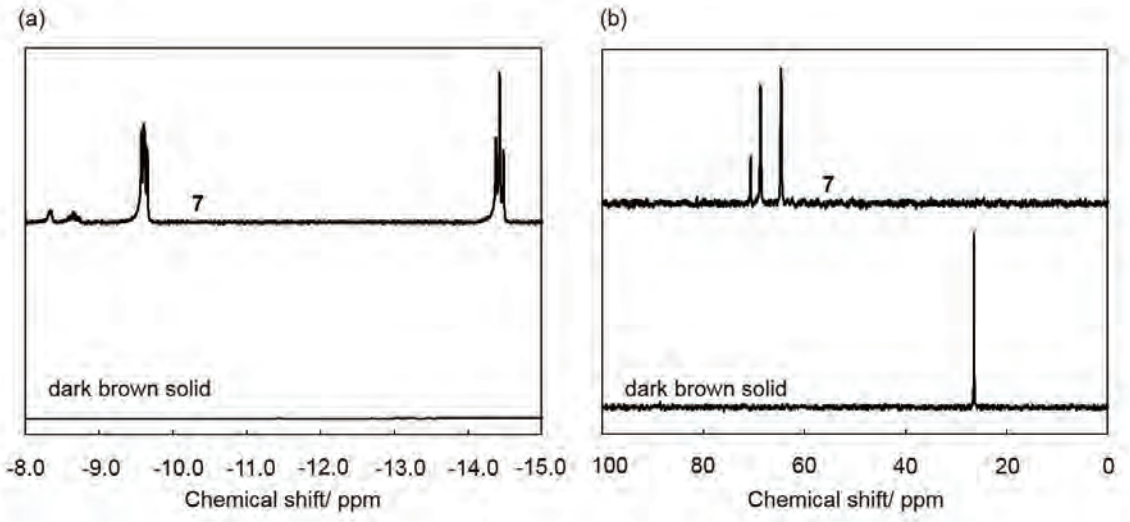

Figure 3-6. (a) ^{1}H NMR (500 MHz, C_6D_6) and (b) ^{31}P NMR (202 MHz, C_6D_6) of [Ru(η^6-C_6Me_6)($S_2C_6H_4$)$RuH_2(PPh_3)_2$] (**7**) and dark brown solid.

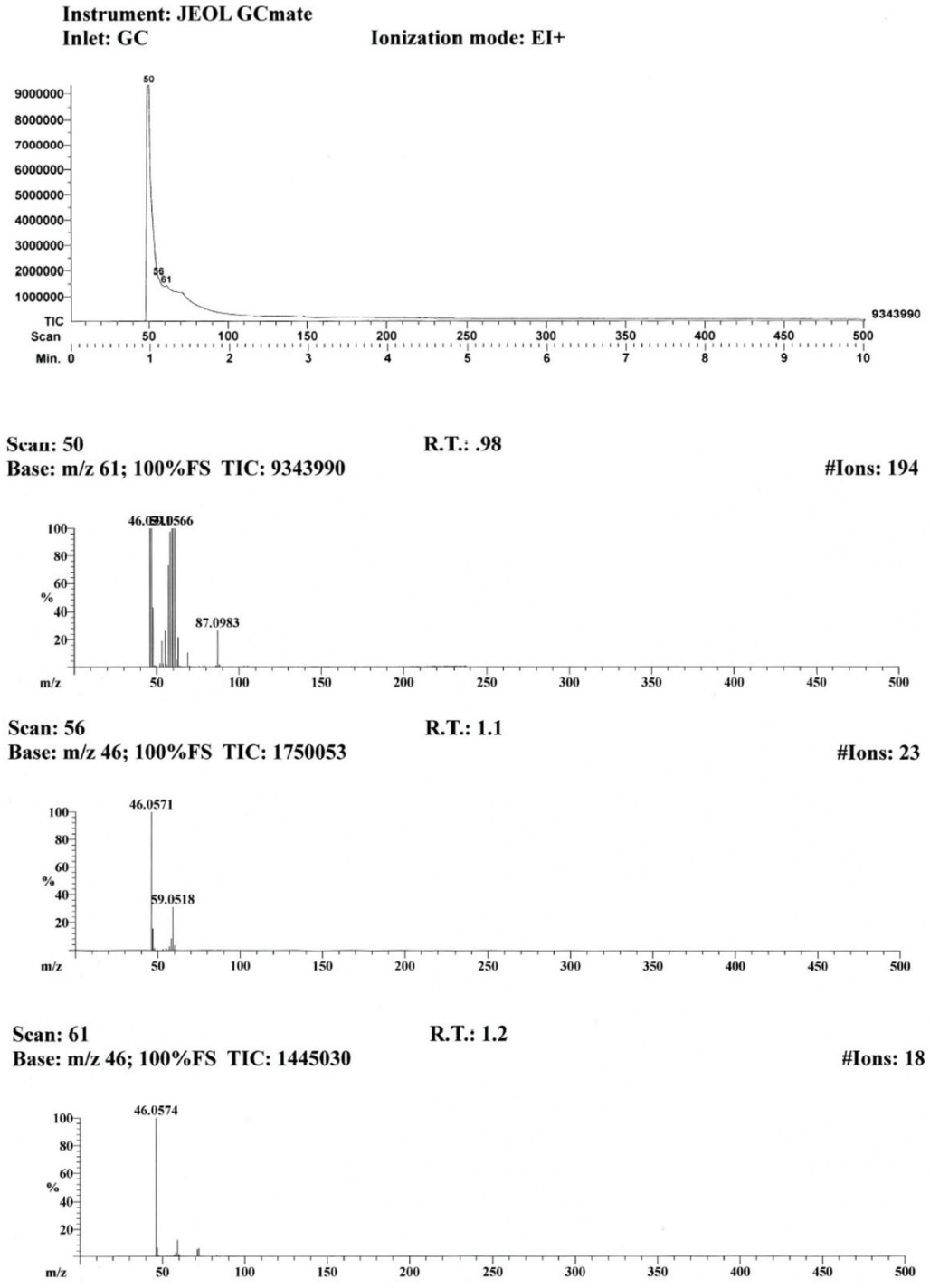

Figure 3-7. GC-MS spectra of distillate.

3-3 Experimental Section

3-3-1 General

Tetrahydrofuran (THF), diethyl ether (Et_2O), hexane, isopropyl alcohol (*i*-PrOH), and toluene were purchased from KANTO Chemicals. Chloroform and methanol were purchased from Godo Co., Ltd. Dichloromethane was purchased from Wako Pure Chemical Industries, Ltd. Toluene and THF were distilled using Na, dried over 4 Å molecular sieves, and degassed with N_2 before use. Isopropyl alcohol and methanol were dried over 3 Å molecular sieves and degassed with N_2 before use. Other solvents were distilled over calcium hydride, dried over 4 Å molecular sieves, and degassed with N_2 prior to use. Other chemicals were obtained from commercial sources. Complexes [(η^6-C_6Me_6)Ru($S_2C_6H_4$)] (**1**) and [RuClH(PPh_3)$_3$] (**5**) were prepared using literature methods as reported previously.[18, 19]

All NMR spectra were recorded on an ECP-500 (500 MHz) spectrometer. ^{1}H NMR (500 MHz), ^{13}C{^{1}H} NMR (126 MHz), and ^{31}P{^{1}H} NMR (202 MHz) spectra were measured using tetramethylsilane as an internal standard. IR spectra were recorded using a JASCO FT-IR 6100 spectrometer. High-resolution electrospray ionization mass spectra (HR-ESI MS) were recorded on a JEOL JMS-T100CS "AccuTOF CS" spectrometer. Elemental analyses were performed using a PerkinElmer 2400II CHNS analyzer.

For structural determination, crystal data were collected using a Bruker AXS SMART APEX CCD X-ray diffractometer equipped with a rotating-anode X-ray generator emitting graphite-monochromatic Mo-Kα (0.7107 Å) and Cu-Kα radiation (1.5418 Å). Empirical absorption corrections and Lorentzian polarization correction were performed using equivalent reflections and the SADABS program, respectively.[28] All data were collected with SMART and Bruker SAINTPLUS (Version 6.45) software packages. The structures were solved using the SHELXS-97[29] program and refined against F^2 using SHELEXL-97.[30] CCDC No. 1564973, 1564974, 1564975 and 1564976 contains the supplementary crystallographic data for **2**, **3**, *cis*-**4** and **6**. These data can be obtained free of charge from the Cambridge Crystallographic Data Center. via http://www.ccdc.cam.ac.uk/conts/retrieving.html. The crystal structure of **9** was previously reported in reference 27; however, it has not been registered with the Cambridge Crystallographic Data Center. So, we added the crystal structure data of **9**.

Table 3-1 Summary of crystal data

	5-toluene	**6**	***cis*-7·2($C_2H_4Cl_2$)**	**9**
Emprical formula	$C_{61}H_{54}ClP_3Ru$	$C_{54}H_{53}ClP_2Ru_2S_2$	$C_{58}H_{62}Cl_4P_2Ru_2S_2$	$C_{46}H_{34}O_4P_2Ru_2S_2$
Formula weight	1016.47	1065.61	1229.08	978.93
T (K)	103	100	103	103
Wavelength (Å)	0.71073	1.54178	0.71073	0.71073
Crystal system	Monoclinic	Monoclinic	Monoclinic	Triclinic
Space group	*P*2(1)/*c*	*P*2(1)/*c*	*P*2(1)/*c*	*P*-1
a (Å)	19.4960(11)	11.7576(4)	17.6233(9)	10.1045(7)
b (Å)	14.2087(8)	21.0538(8)	12.4625(6)	10.9753(7)
c (Å)	19.5837(11)	19.3395(7)	24.3631(12)	21.0868(14)
α (deg)	90	90	90	101.1160(10)
β (deg)	116.001(1)	104.2580(10)	93.5080(10)	93.8020(10)
γ (deg)	90	90	90	113.8270(10)
V (Å^3)	4875.9(5)	4639.9(3)	5340.9(5)	2071.8(2)
Z	4	4	4	2
D_{calc} (g m^{-3})	1.385	1.525	1.529	1.569
F (000)	2104	2176	2512	984
Reflection collected	23209	75958	30377	12507
Independent refrections (R_{int})	8624 (0.0678)	9182 (0.0356)	10891 (0.0237)	8254 (0.0199)
R_1 ($I > 2\sigma(I)$)	0.0757	0.0199	0.0318	0.0321
w*R*2 (all data)	0.153	0.0457	0.0838	0.0797
Goodness of fit (GOF) on F^2	1.185	1.077	1.026	1.011

3-3-2 Synthesis of [Ru(η^6-C_6Me_6)($S_2C_6H_4$)RuClH(PPh_3)$_2$] (**6**)

Complexes **1** (0.081 g, 0.20 mmol) and **5** (0.19 g, 0.20 mmol) were suspended in THF (40 mL) and stirred at room temperature for 24 h. The crude product was then concentrated under reduced pressure, washed with Et_2O, and collected by filtration. The final product was dried under reduced pressure to obtain complex **6** as dark green solid (yield: 0.16 g, 72%). Single crystals suitable for X-ray crystallographic analysis were obtained by recrystallization from chloroform/hexane at −30 °C.

Experimental data for **6**: ^{1}H NMR (500 MHz, C_6D_6) δ (ppm): −17.49 (t, J_{HP} = 12 Hz, 1H, RuHRu), 1.65 (s, 18H, C_6Me_6), 6.60 (dd, J= 3.0, 6.0 Hz, 2H, $S_2C_6H_4$), 6.92–6.99 (m, 18H, Ph),7.36 (dd, J= 3.0, 6.0 Hz, 2H, $S_2C_6H_4$), 7.60–7.64 (m, 12H, Ph). ^{31}P {^{1}H} NMR (202 MHz, C_6D_6) δ (ppm) (Figure S2): 50.5 (s). IR (KBr): (ν C-H) 3052, 2907 cm^{-1}, (ν P-C) 1631 cm^{-1}. LRMS (LR-ESI-TOF) *m/z*: Calcd. for $C_{54}H_{53}P_2Ru_2S_2$ 1031[M-Cl]$^+$, Found: 1031. Anal. Calcd for $C_{54}H_{53}ClP_2Ru_2S_2$: C, 60.86; H, 5.01. Found: C, 60.50; H, 5.05%.

3-3-3 Synthesis of [Ru(η^6-C_6Me_6)($S_2C_6H_4$)RuH_2(PPh_3)$_2$] (**7**)

The hydride complex **6** (0.11 g, 0.10 mmol) and KOH (0.060 g, 1.1 mmol) were suspended in *i*-PrOH (10 mL) and heated at 60 °C for 2 h. The suspension was filtered and washed with methanol followed by extraction with toluene and reprecipitation from methanol.

Finally, the precipitate was filtered and dried under reduced pressure to obtain complex **7** (*cis*/*trans* mixture) as orange solid (yield: 84 mg, 83%). The mixture was recrystallized from dichloromethane/hexane at room temperature to give *cis*-**7** isomer.

Experimental data for **7**: ^{1}H NMR for *cis*-**7** (500 MHz, C_6D_6) δ (ppm): −14.43 (t, J_{HH} = 25 Hz, 1H, RuHRu), −9.61 (dd, J_{HP} = 16 Hz, J_{HH} = 25 Hz, 1H, RuH), 1.73 (s, 18H, C_6Me_6), 6.01 (t, J_{HH} = 7.5 Hz, 1H, $S_2C_6H_4$), 6.24 (d, J_{HH} = 7.5 Hz, 1H, $S_2C_6H_4$), 6.35 (d, J_{HH} = 7.5 Hz, 1H, $S_2C_6H_4$), 7.32 (d, J_{HH} = 7.5 Hz, 1H, $S_2C_6H_4$), 6.89–7.75 (m, Ph). ^{31}P {^{1}H} NMR for *cis*-**7** (202 MHz, C_6D_6) δ (ppm): 63.7 (d, J_{PP} = 65 Hz), 67.7 (d, J_{PP} = 65 Hz). ^{1}H NMR for *trans*-**7** (500 MHz, C_6D_6) δ (ppm): −8.74–−8.59 (m, 1H, RuH), −8.35–−8.33 (m, 1H, RuH), 1.83 (s, 18H, C_6Me_6), 6.89–7.75 (m, Ph). ^{31}P {^{1}H} NMR for *trans*-**7** (202 MHz, C_6D_6) δ (ppm): 69.7 (s). HRMS (HR-ESI-TOF) *m/z*: Calcd. for $C_{54}H_{53}P_2Ru_2S_2$ 1031.11509 $[M-H]^+$, Found: 1031.11547.

3-3-4 Synthesis of [Ru(η^6-C_6Me_6)($S_2C_6H_4$) $Ru(CO)_2(PPh_3)$] (**8**)

THF solution (10 mL) of **7** (0.052 mg, 0.050 mmol) was stirred at room temperature for 30 min under CO atmosphere. The solution was then concentrated under reduced pressure. The crude product was purified by aluminum gel column chromatography using toluene as eluent. The second reddish purple fraction that eluted from the column was collected. Subsequently, the solvent was evaporated and the final product was subjected under reduced pressure to obtain complex **8** as reddish purple solid (yield: 41 mg, 55%).

Experimental data for **5**: ^{1}H NMR (500 MHz, C_6D_6) δ (ppm): 1.69 (s, 18H, C_6Me_6), 5.70 (dd, J= 3.0, 6.0 Hz, 2H, $S_2C_6H_4$), 6.19 (dd, J= 3.0, 6.0 Hz, 2H, $S_2C_6H_4$), 6.70–7.93 (m, 30H, Ph). ^{31}P {^{1}H} NMR (202 MHz, C_6D_6) δ (ppm): 38.7 (s). IR(KBr) (Figure S9): (ν_{C-H}) 3055, 2917 cm^{-1}, ($\nu_{C\equiv O}$) 2054, 1944 cm^{-1}. HRMS (HR-ESI-TOF) *m/z*: Calcd. for $C_{38}H_{37}O_2P_1Ru_2S_2$ 825.01560 $[M+H]^+$, Found: 825.01397.

3-3-5 Synthesis of [$Ru_2(CO)_4(PPh_3)_2(S_2C_6H_4)$] (**9**)

THF solution (10 mL) of **7** (0.052 mg, 0.050 mmol) was stirred at room temperature for 24 h under CO atmosphere. The solution was then concentrated under reduced pressure. The crude product was purified by aluminum gel column chromatography using toluene as eluent. The first pale yellow fraction that eluted from the column was collected and the solvent was evaporated. The final product was dried under reduced pressure to obtain complex **9** as yellow solid (42 mg, 86%).

Experimental data for **9**: ^{1}H NMR (500 MHz, C_6D_6) δ (ppm): 5.71 (dd, 2H, J= 3.0, 6.0 Hz, $S_2C_6H_4$), 6.21 (dd, J= 3.0, 6.0 Hz, 2H, $S_2C_6H_4$), 6.91–7.00 (m, 18H, Ph), 7.62–7.66 (m,

12H, Ph). $^{31}P\{^{1}H\}$ NMR (202 MHz, C_6D_6) δ (ppm): 38.4 (s). IR(KBr) (Figure S9): (ν_{C-H}) 3052 cm^{-1}, ($\nu_{C\equiv O}$) 2006, 1972, 1942 cm^{-1}. LRMS (LR-ESI-TOF) *m*/*z*: Calcd. for $C_{46}H_{34}O_4P_2Ru_2S_2$ 980 $[M+H]^+$, Found: 980.

3-3-6 Reaction of $[Ru(\eta^6\text{-}C_6Me_6)(S_2C_6H_4)\ RuH_2(PPh_3)_2]$ (**7**) and CO_2

The dihydride complex **7** (0.052 mg, 0.050 mmol) was suspended in *i*-PrOH (10 mL) and stirred at room temperature for 24 h under CO_2 atmosphere. The solution was then concentrated under reduced pressure to collect the crude product and the distillate. The crude product was washed with hexane, filtered and subjected to reduced pressure to obtain a dark brown solid (16 mg). On the other hand, the distillate was confirmed to contain formic acid by GC-MS.

3-4 References

[1] H. D. Kaesz, R. B. Saillant, *Chem. Rev.* **1972**, *72*, 231–281.

[2] L. C. Po, N. S. Man, J. Guochen, L. Zhenyang, *Coord. Chem. Rev.* **2007**, *251*, 2223–2237.

[3] R. H. Morris, *Coord. Chem. Rev.* **2008**, *252*, 2381–2394.

[4] W. Wang, Y. Himeda, J. T. Muckerman, G. F. Manbeck, E, Fujita, *Chem. Rev.* **2015**, *115*, 12936–12973.

[5] D. Mellmann, P. Sponholz, H. Junge, M. Beller, *Chem. Soc. Rev.* **2016**, *45*, 3954–3988.

[6] A. S. Weller, J. S. McIndoe, *Eur. J. Inorg. Chem.* **2007**, 4411–4423.

[7] A. K. Justice, R. C. Linck, T. B. Raunchfuss, S. R. Wilson, *J. Am. Chem. Soc.* **2004**, *126*, 13214–13215.

[8] N. A. Arnet, T. R. Dugan, F. S. Menges, B. Q. Mercado, W. W. Brennessel, E. Bill, M. A. Johnson, P. L. Holland, *J. Am. Chem. Soc.* **2015**, *137*, 13220–13223.

[9] *Dithiolene Chemistry: Synthesis, Properties, and Applications (Progress in Inorganic Chemistry vol. 52)*, (ed. by E. I. Stiefel) Wiley, Hoboken, NJ, **2004**.

[10] R. Eisenberg, *Prog. Inorg. Chem.* **1970**, *12*, 295–369.

[11] R. P. Burns, C. A. McAuliffe, *Adv. Inorg. Chem. Radiochem.* **1979**, *22*, 303–348.

[12] M. Fourmigue, *Coord. Chem. Rev.* **1998**, *178–180*, 823–864.

[13] A. Sugimori, T. Akiyama, M. Kajitani, T. Sugiyama, *Bull. Chem. Soc. Jpn.* **1999**, *72*, 879–908.

[14] R. Sakamoto, S. Tsukada, H. Nishihara, *Dalton Trans.* **2012**, *41*, 10123–10135.

[15] M. Sakurada, M. Kajitani, K. Dohki, T. Akiyama A. Sugimori, *J. Organomet. Chem.* **1992**, *423*, 141–161.

[16] M. Nomura, M. Fujii, K. Fukuda, T. Sugiyama, Y. Yokoyama, M. Kajitani, *J. Organomet. Chem.* **2005**, *690*, 1627–1637.

[17] S. Takemoto, D. Shimadzu, K. Kamikawa, H. Matsuzaka, R. Nomura, *Organometallics* **2006**, *25*, 982–988.

[18] K. Mashima, H. Kaneyoshi, S. Kaneko, A. Mikami, K. Tani, A. Nakamura, *Organometallics* **1997**, *16*, 1016–1025.

[19] R. Abbel, K. Abdur-Rashid, F. Faatz, A. Hadzovic, A. J. Lough, R. H. Morris, *J. Am. Chem. Soc.* **2005**, *127*, 1870–1882.

[20] S. Tsukada, T. Sagawa, T. Gunji, *Chem. Asian J.* 10 (2015) 1881–1883.

[21] E. Alberico, A. J. J. Lennox, L. K. Vogt, J. Jiao, W. Baumann, H.-J. Drexler, M. Nielsen, A. Spannenberg, M. P. Checinski, H. Junge, M. Beller, *J. Am. Chem. Soc.* **2016**, *138*, 14890–14904.

[22] D. S. Moore, S. D. Robinson, *Chem. Soc. Rev.* **1983**, *12*, 415–452.

[23] J. A. Cabeza, M. A. Martinez-Garcia, V. Riera, *Organometallics* **1998**, *17*, 1471–1477.
[24] J. F. Hartwig, *Organotransition Metal Chemistry from Bonding to Catalysis*, Universal Science Books, **2010**.
[25] T. Iwasa, H. Shimada, A. Takami, H. Matsuzaki, Y. Ishii, M. Hidai, *Inorg. Chem.* **1999**, *38*, 2851–2859.
[26] H. Salem, L. J. W. Shimon, Y. Diskin-Posner, G. Leitus, Y. Bem-David, D. Milstein, *Organometallics* **2009**, *28*, 4791–4806.
[27] K. Shiu, C. Li, T. Chan, *Organometallics* **1995**, *14*, 524–529.
[28] G. M. Sheldrick, *SADABS*, *Program for area detector absorption correction*, University of Göttingen, Germany, **1996**.
[29] G. M. Sheldrick, *SHELXS–97*, *Program for crystal structure solution*, University of Göttingen, Germany, **1997**.
[30] G. M. Sheldrick, *SHELXL–97*, *Program for crystal structure refinement*, University of Göttingen, Germany, **1997**.

Chapter 4

Synthesis of mononuclear ruthenium dithiolene complexes and reactivity with carbon monoxide

4-1 Introduction

Metalladithiolene complexes of transition metals comprise a five-membered planar ring with a metal center, two sulfur atoms, and two unsaturated carbon atoms. The quasi-aromaticity of the metal-containing five-membered ring stabilizes a 16-electron unsaturated coordination state at the metal center.[1–6] Because of the peculiar electronic structure, metalladithiolenes have been studied extensively in relation to topics such as composites. Kambe et al. reported the preparation of π-conjugated nickel bis(dithiolene) complex nanosheets and control of the oxidation state of the nanosheet via chemical oxidation and reduction.[7, 8] This dithiolene nanosheet has potential as an organic two-dimensional topological insulator.[9] Begum et al. reported carbon-nanotube-based composites of gadolinium and platinum dithiolenes and their photoluminescence.[10] Wang and Stiefel proposed separation and purification of olefins using $Ni[S_2C_2(CF_3)_2]_2$.[11] To apply metal complexes for advanced materials, it is better to prepare a sheet, coating film, or self-standing film from a metal complex powder to maintain the reactivity.

The 16-electron unsaturated coordination state at the metal center of the metalladithiolene ring enables reactions with Lewis bases: in other words, the metal center of the dithiolene ring undergoes addition reactions.[5] For example, $[(\eta^6\text{-}C_6Me_6)Ru(S_2C_6H_4)]$ (**1**) reacts with H_2NNH_2 and *t*-BuCN at the ruthenium center.[12, 13] The cobaltadithiolene complex is also known to undergo reversible addition and dissociation reactions. Dissociation of the phosphine adduct complex $[(\eta^5\text{-}C_5H_5)Co(PBu_3)(S_2C_2(CN)_2)]$, which is synthesized from the reaction of $[(\eta^5\text{-}C_5H_5)Co(S_2C_2(CN)_2)]$ with PBu_3, proceeds via singlet oxygen to give $[(\eta^5\text{-}C_5H_5)Co(S_2C_2(CN)_2)]$ and the corresponding phosphine oxide.[14] Yu and co-workers also reported electrochemically controlled reversible binding of PPh_3 to $[M(S_2C_2(C_6H_4\text{-}p\text{-}OCH_3)_2)_2]_2$ (M = Fe or Co).[15] All of the above reactions were performed only in the solution state.

In this report, therefore, we describe novel CO addition and dissociation on the ruthenium center of **1** in both solution and solid states. we also demonstrate the preparation of a **1**/polysiloxane self-standing hybrid film and its CO gas addition.

4-2 Results and discussion

4-2-1 Carbon monoxide addition reaction to Ru complexes

Reaction of **1** with 1 atm of CO gas in tetrahydrofuran (THF) for 6 h gave [(η^6-C_6Me_6)Ru(CO)($S_2C_6H_4$)] (**3**) quantitatively (Scheme 4-1). In the ^{13}C NMR of **3**, a signal at 178.7 ppm is assigned to the carbonyl ligand. The IR spectrum of **3** (in KBr) shows strong absorption band at 1951 cm^{-1}, which we attribute to the carbonyl ligand. CO adduct **2** is an air-stable complex. This CO addition reaction also occurred in the solid state. Under neat conditions, **1** converted to **2** in 60% yield after 1 h and in 95% yield after 24 h, as estimated by ^1H NMR spectroscopy. For [(η^5-C_5Me_5)Co($S_2C_6H_4$)],[16] which contains a 16-electron coordinatively unsaturated metal center with the same electron count as **1**, the CO addition reaction didn't occur (Scheme 4-2).

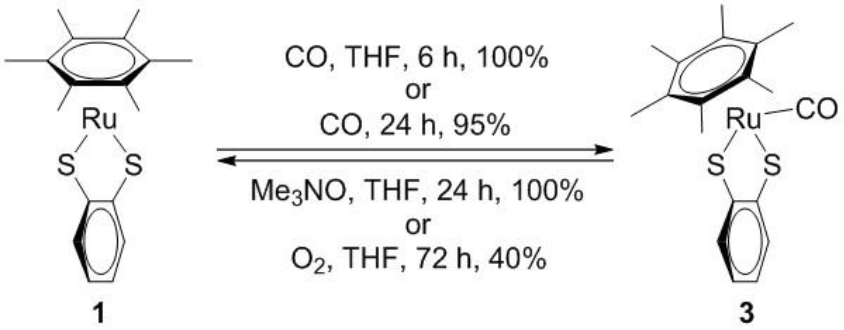

Scheme 4-1 Addition and dissociation reactions of **1** and **3**.

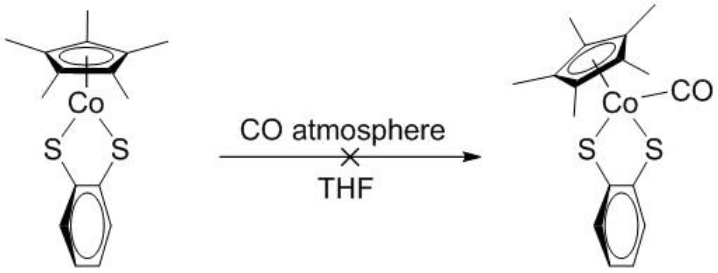

Scheme 4-2. Addition reaction of [(η^5-C_5Me_5)Co($S_2C_6H_4$)] with CO gas.

4-2-2 Carbon monoxide elimination reaction of Ru carbonyl complexes

The CO ligand could be dissociated from **3** by reaction with oxidants (Scheme 4-1). Treatment of **3** with excess Me_3NO as an oxidant in THF under an inert atmosphere gave **1** quantitatively via removal of the CO ligand from the metal center. O_2 gas could also be used as an oxidant: under O_2 atmosphere, **3** converted to **1** in a 40% yield after 72 h. In both cases, the CO ligand was removed as CO_2, as observed by a gas detector tube. Thermogravimetry and differential thermal analysis (TG-DTA) of **3** indicated that a weight loss (~11%) occurred at 102–147 °C (Figure 4-1): this weight loss was ascribed to the release of CO from **3** to generate **1**. Then, a dramatic weight loss (~55%) was observed at 251–281 °C, which corresponded to the combustion of **1**. TG-DTA of **1** revealed combustion at the same temperature.

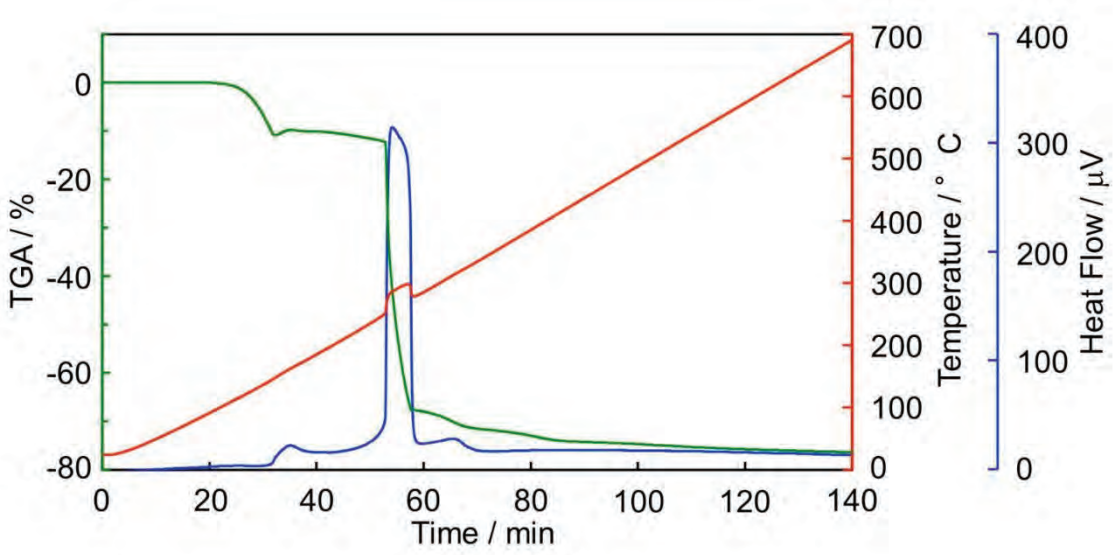

Figure 4-1. TG-DTA traces of **3** (5 ^{0}C / min, air atmosphere).

4-2-3 Crystal structures

Single crystals of **1** and **3** were obtained by recrystallization in mixed solvents of dichloromethane / hexane and dichloromethane / toluene, respectively. The molecular structure of **1** and **3** were determined using single-crystal X-ray diffraction analysis (Table 4-1, Figure 4-2, Figure 4-3). The Ru–S bond distances in **3** are about 0.1 Å longer than those in **1** [2.340(16) and 2.350(16) Å, respectively. The distance between the Ru atom and the C_6Me_6 plane in **3** (1.810 Å) is also longer than that in **1** (1.684 Å). These elongations were ascribed to the decrease in π-donation from the thiolato ligand to the metal center due to the addition of CO. The C–O distance didn't differ greatly from that of a free CO molecule (1.128 Å)[17] and a ruthenium carbonyl porphyrin complex, *i.e.*, [Ru(CO)(TPP)(EtOH)] [1.16(3) Å].[18] The dihedral angle between the benzendithiolato ligand and the S1–Ru–S2 plane was 5.3°, which indicates that the RuS_2C_2 ring was almost planar. The CO ligand was vertically coordinated to the Ru center of the dithiolene ring: therefore, the Ru–C3–O angle was close to 180°. The C_6Me_6 ligand inclined from perpendicular toward the RuS_2C_2 ring. The angle between the C_6Me_6 ligand and the RuS_2C_2 ring was 55°. The ligands on the central metal were coordinated in a piano-stool geometry. These structural features of **3** resemble those of $[(\eta^6\text{-}C_6Me_6)Ru(S_2C_6H_4)]_2(\mu_2\text{-}NH_2NH_2)$[6] and $[(\eta^6\text{-}C_6Me_6)Ru(CN^tBu)(S_2C_6H_4)]$.[13]

Table 4-1 Summary of crystal data.

	1	**3**
emprical formula	$C_{18}H_{22}RuS_2$	$C_{20.17}H_{23.33}ORuS_2$
formula wt.	403.55	446.91
temp. (K)	103	103
wavelength (Å)	0.71073	0.71073
cryst. syst.	Monoclinic	Hxagonal
space group	*P*2(1)/*c*	*R*-3
a (Å)	8.4709(16)	36.246(3)
b (Å)	14.131(3)	36.246(3)
c (Å)	13.925(3)	7.8970(13)
α (deg)	90	90
β (deg)	95.246(3)	90
γ (deg)	90	120
V (Å^3)	1660.0(5)	8984.9(18)
Z	4	18
D_{calc} (Mg m^{-3})	1.615	1.487
F(000)	824	4110
cryst. color	black	orange
cryst. size (mm)	0.08 0.07 0.07	0.10 0.02 0.01
data completeness	0.997	1.000
*R*1	0.0309	0.0615
w*R*2	0.0749	0.1492
S	1.093	1.221

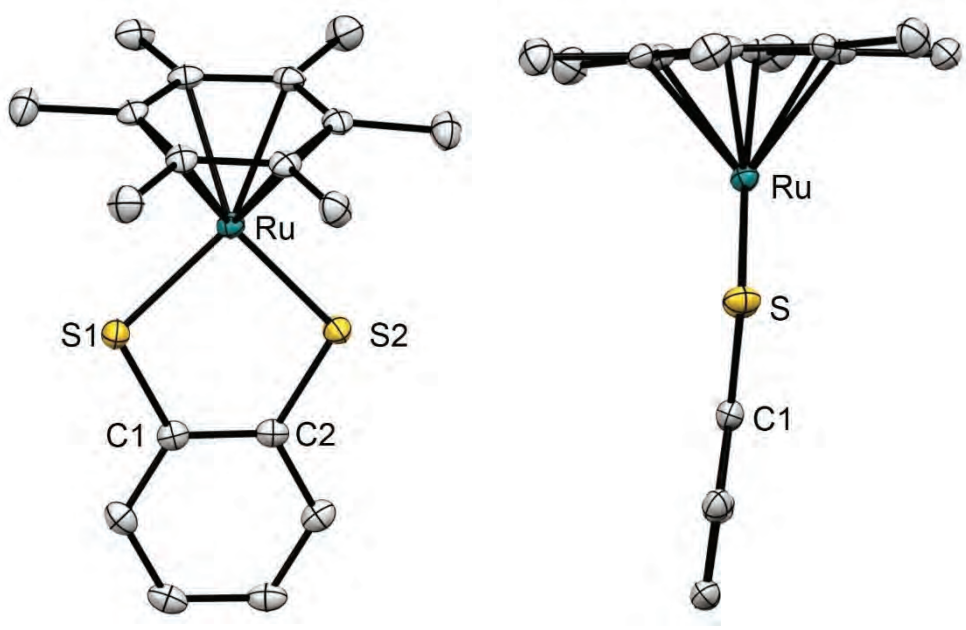

Figure 4-2. ORTRP drawing of **1** (left: oblique view; right: side view) with thermal elipsoids ahown at 50% probablity level. Hydrogen atoms are omitted for clarity.

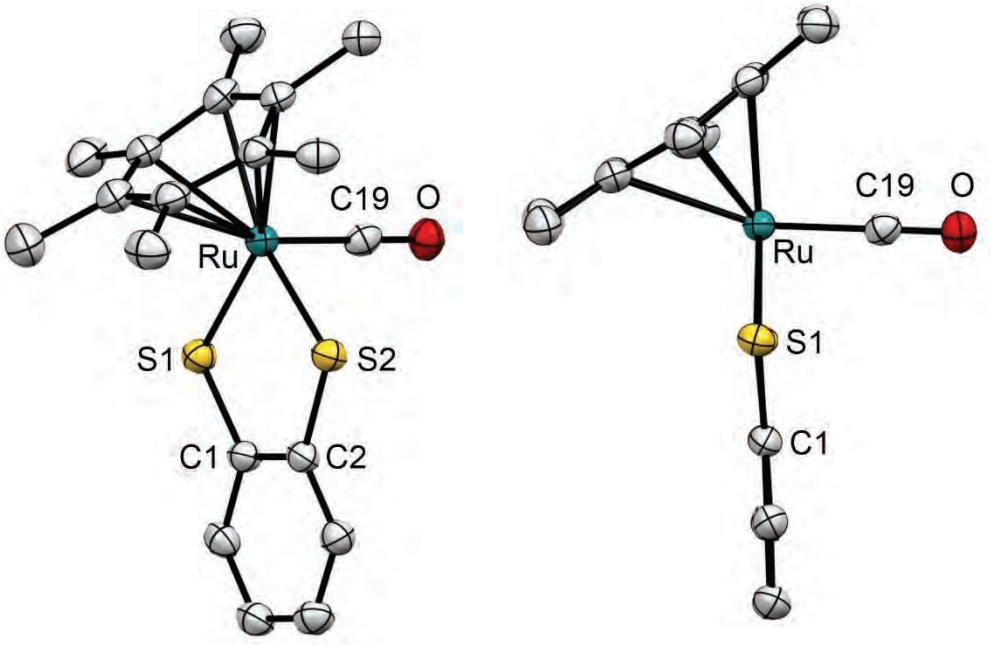

Figure 4-3. ORTRP drawing of **2** (left: oblique view; right: side view) with thermal elipsoids ahown at 50% probablity level. Hydrogen atoms are omitted for clarity.

4-2-4 UV-Vis spectra of **1** and **3**

The absorption spectrum of **1** exhibited two strong peaks at 563 and 435 nm. In the spectrum of **3**, each peak was less intense (Figure 4-4). To investigate the differences in the absorption spectra, excited-state calculations using time-dependent density functional theory were performed for **1** and **3** at the B3LYP/Lanl2DZ (Ru) and 6-31G(d,p) (other atoms) levels. The highest occupied molecular orbital (HOMO), the lowest unoccupied molecular orbital (LUMO), HOMO−1 and LUMO+1 of **1** and **3** are shown in Figure 4-5. The peaks at 563 and 435 nm in the spectrum of **1** were attributed to highest occupied molecular orbital (HOMO)–lowest unoccupied molecular orbital (LUMO) and HOMO−1–LUMO transitions, respectively (Figure 4-6, Figure 4-7, Table 4-2, Table 4-3). The HOMO and HOMO−1 were located mainly on the dithiolene ring (Figure 4-5), whereas the LUMO was based on the *d* orbital of the Ru atom. Therefore, the absorption peaks of **1** were attributed to a ligand-to-metal charge-transfer transition that is commonly observed in 16-electron metalladithiolene complexes.[13] In contrast, the HOMO of **3** was similar to the LUMO of **1** because the vacant *d* orbital of **1** was filled with electrons upon the addition of the CO ligand (Figure 4-5). The decrease in ε for **3** was the result of the structural changes around ruthenium that formed the piano-stool geometry of **3**. A similar color change associated with the change in geometry was reported for the addition of $P(OMe)_3$ to a cobaltadithiolene complex, i.e., $[(\eta^5\text{-}C_5H_5)Co(S_2C_2(COOMe)_2)]$.[19]

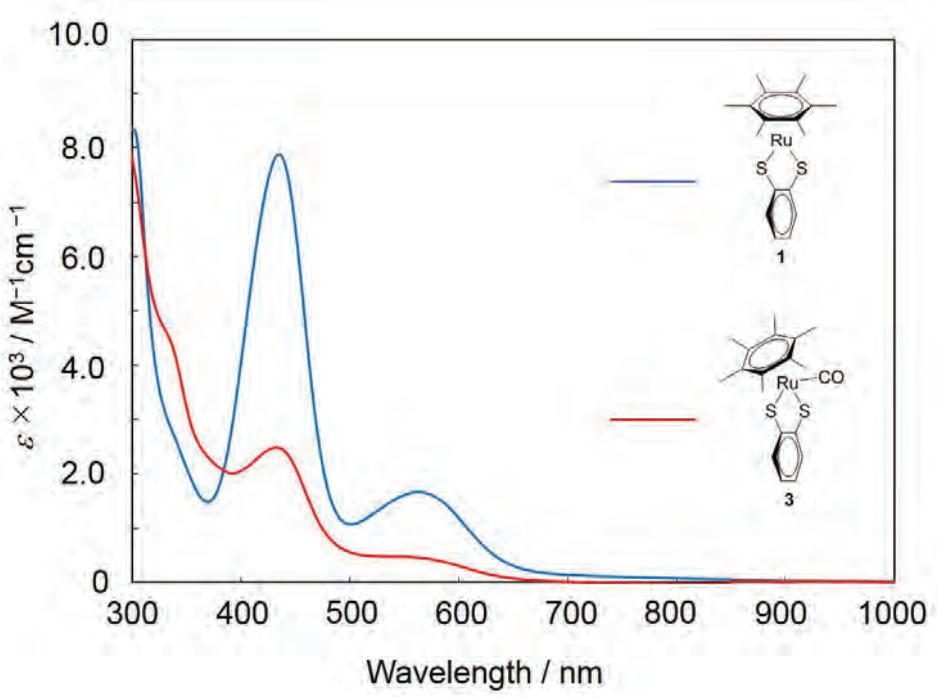

Figure 4-4. UV/Vis/NIR spectra of **1** and **3** in THF.

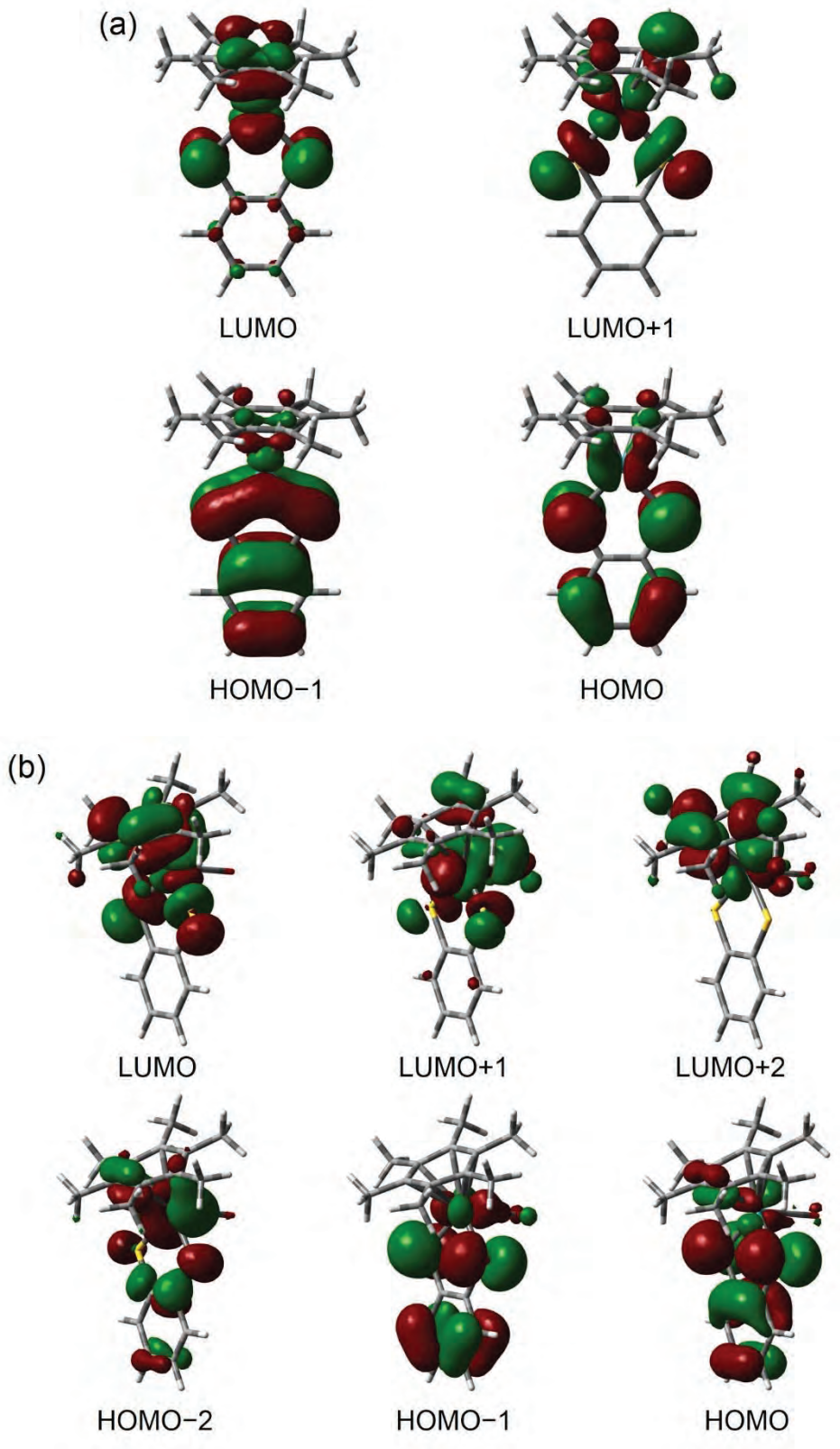

Figure 4-5. Molecular orbital of **1** (a) and **3** (b). The contour plots are shown with an isovalue of 0.030.

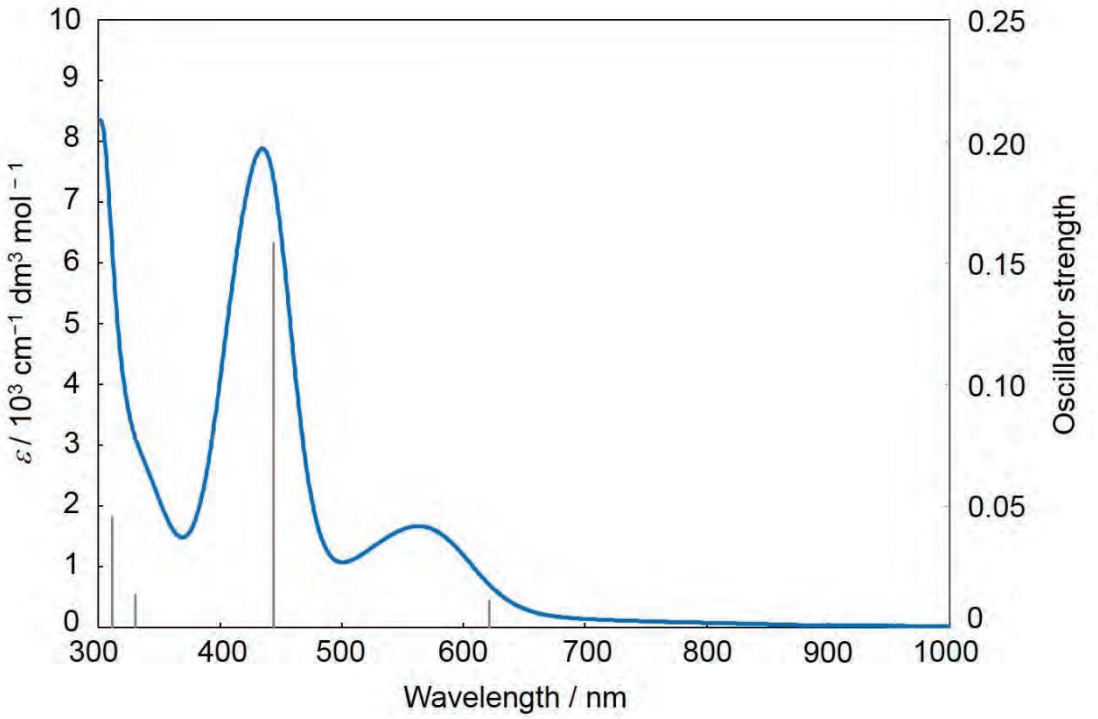

Figure 4-6. An observed UV/Vis/NIR spectrum and calculated excitation energy of **1**.

Table 4-2. Selected excitation energies and oscillator strength of **1** obtained by experiment and DFT method.

energy/ eV (found) (nm)	energy/ eV (calcd.) (nm)	oscillator strength	configuration	CI coef.
2.85 (435)	2.79 (444)	0.1580	HOMO−5 -> LUMO+1 HOMO−1 -> LUMO	0.12076 0.68888
2.20 (564)	2.00 (621)	0.0111	HOMO−4 -> LUMO HOMO−2 -> LUMO+1 HOMO -> LUMO	0.20568 0.12004 0.65588

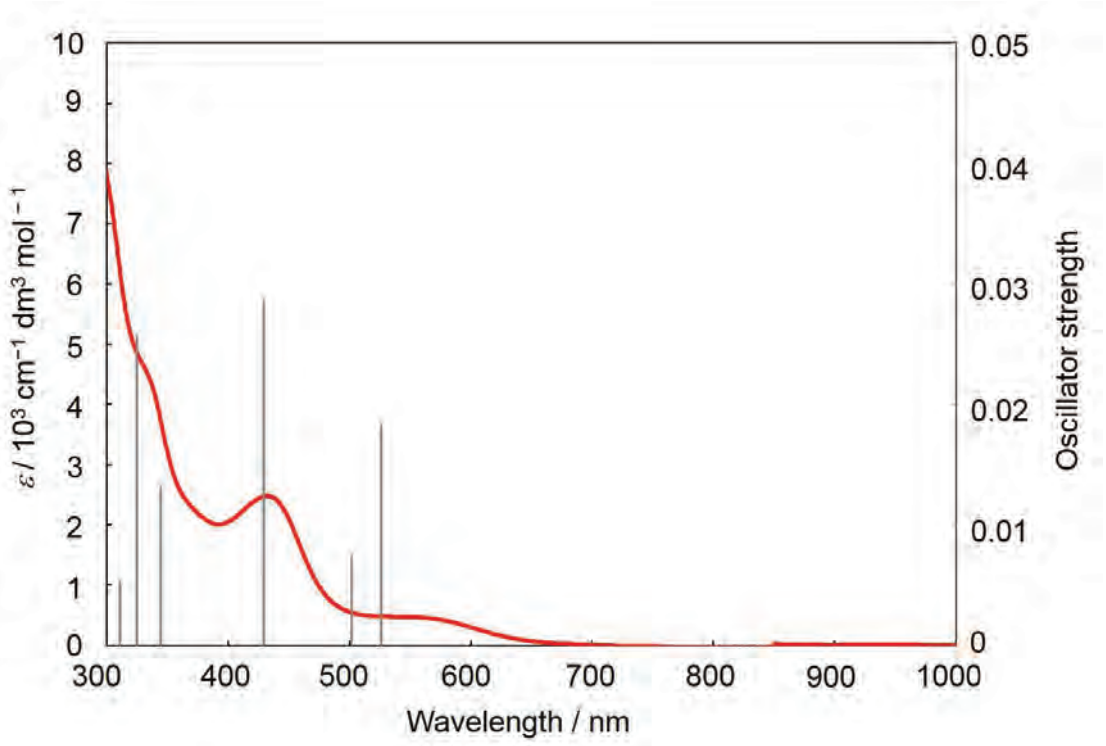

Figure 4-7. An observed UV/Vis/NIR spectrum and calculated excitation energy of **3**.

Table 4-2. Selected excitation energies and oscillator strength of **3** obtained by experiment and DFT method.

energy/ eV (found) (nm)	energy/ eV (calcd.) (nm)	oscillator strength	configuration	CI coef.
2.87 (432)	2.88 (429)	0.0287	HOMO -> LUMO+2	0.69410
2.19 (565)	2.36 (526)	0.0183	HOMO−3 -> LUMO HOMO−1 -> LUMO+1 HOMO -> LUMO+1	0.10552 −0.46481 0.50267

4-2-5 Electrochemical properties of **1** and **3**

Figure 4-8 shows the cyclic voltammograms of **1** and **3** which was analyzed in acetonitrile under argon atmosphere at room temperature. **1** presents two reversible redox peaks at −1.95 V and 0.01 V. On the other hand, **3** presents an irreversible reduction peak at −2.01 V and a reversible redox peak at 0.02 V. The electron density distribution of the LUMO+1 of **3** suggests cleavage of the carbonyl ligand and decomposition during the reduction phase (Figure 4-5 (f)).

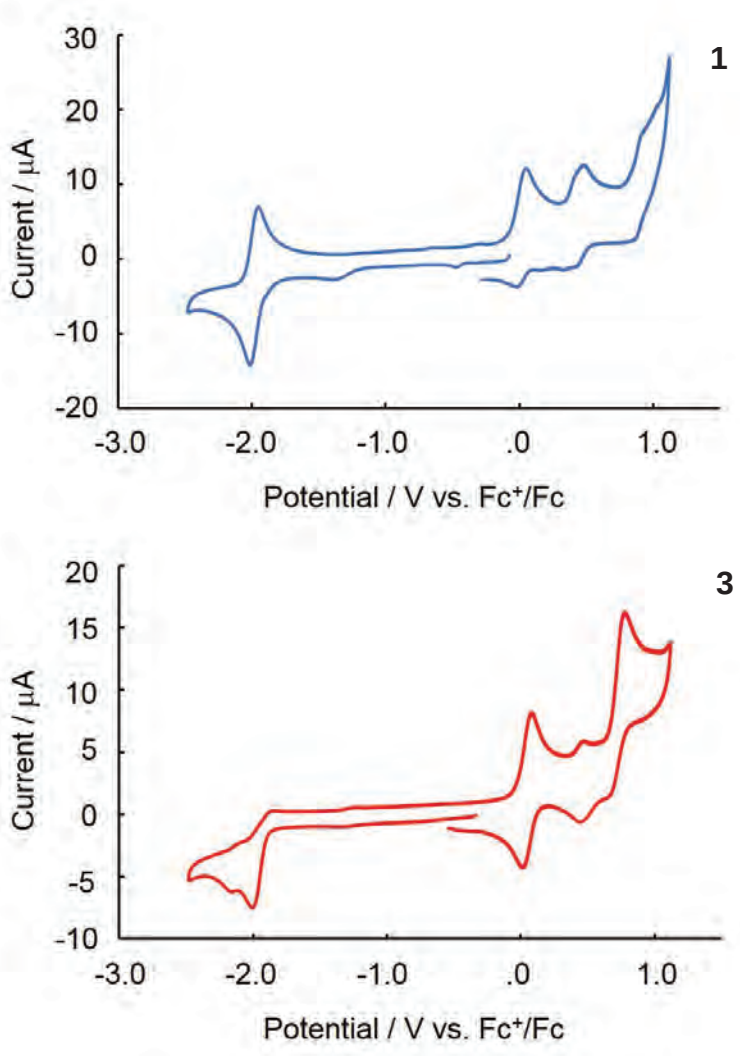

Figure 4-8. Cyclic voltammograms of 1 and 3 (W.E.: GC, R.E.: Ag^{+}/Ag, C.E.: Pt, Fc^{+}/Fc as an internal reference. Sample: 0.5 mM complex and 0.1 M *n*-Bu_4NClO_4-CH_3CN. Temp.: 298 K. Scan rate: 100 mV/s).

4-2-6 Preparation of Ru complex and polymer nanocomposite

Next, a self-standing hybrid film of **1** was prepaired. Hybridization of a functionalized molecule with an organic or inorganic polymer matrix is a useful method of preparing thin and self-standing films. Organic–inorganic hybrid materials of functionalized organic molecules, for example, C_{60} derivatives, have been reported.[20–23] On the other hand, to the best of our knowledge, there have been few reports of metal complex/polymer matrix hybrids.[24–28] In our case, a polymer for gas absorption requires high transparency, heat resistance, and gas permeability. Therefore, we selected polysiloxane for its superior properties. Polysiloxane was synthesized via hydrolytic polycondensation of tetraethoxysilane (TEOS) in the presence of hydrogen chloride and under nitrogen flow. Polyethoxysiloxane (PEOS) was isolated as a highly viscous and transparent liquid. The weight-average molecular weight was 18800 when the H_2O/TEOS molar ratio was 1.70.

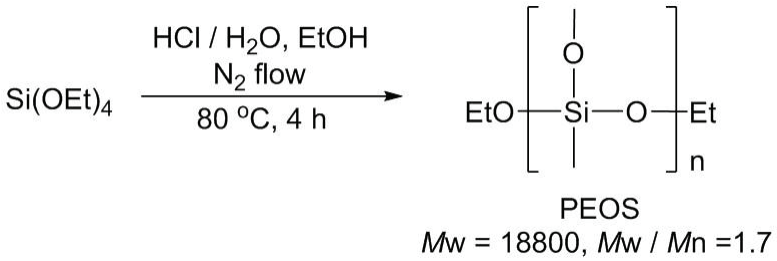

Scheme 4-3. Preparation of PEOS in the presence of hydrogen chloride and under nitrogen flow.

The **1**/PEOS self-standing hybrid film was prepared by standing a mixture of PEOS and **1**/THF solution stand for 6 h at room temperature (Figure 4-9). Figure 4-10 shows the uniform **1**/PEOS self-standing hybrid film with a thickness of 0.658 mm. The differences in the UV–vis spectra of the **1**/PEOS nanocomposite and **3**/PEOS nanocomposite are shown in Figure 4-9. The intensities of the two strong peaks for the **1**/PEOS hybrid at 563 and 433 nm immediately decreased after exposure to CO gas for 10 min. In other words, the **1**/PEOS nanocomposite easily converted to the **3**/PEOS self-standing nanocomposite during CO gas exposure. The color change upon conversion of the **1**/PEOS nanocomposite to the **3**/PEOS nanocomposite was easily recognized by visual observation (Figures 4-10).

We also investigated the dissociation of the CO ligand from **3** in the nanocomposite film. The CO ligand was not dissociated from **3** in the nanocomposite film under exposure to O_2 gas for one week at room temperature. On the other hand, the color of the

nanocomposite film changed by heating for 1 h at 180 °C under nitrogen atmosphere. This result indicated that the CO ligand was dissociated. However, the nanocomposite film was broken down by internal CO gas evolution during heating.

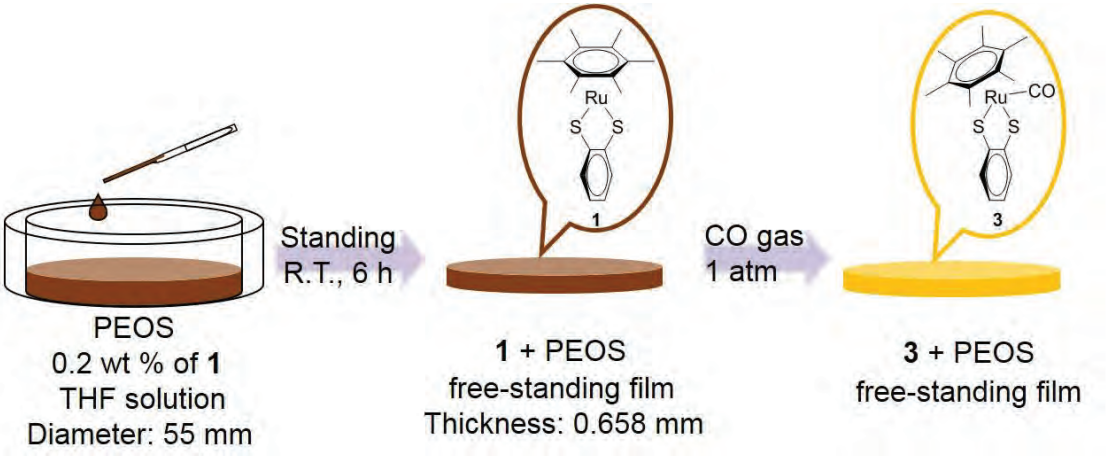

Figure 4-9. Preparation of **1**/PEOS nanocomposite film and exposure of this film to CO atmosphere.

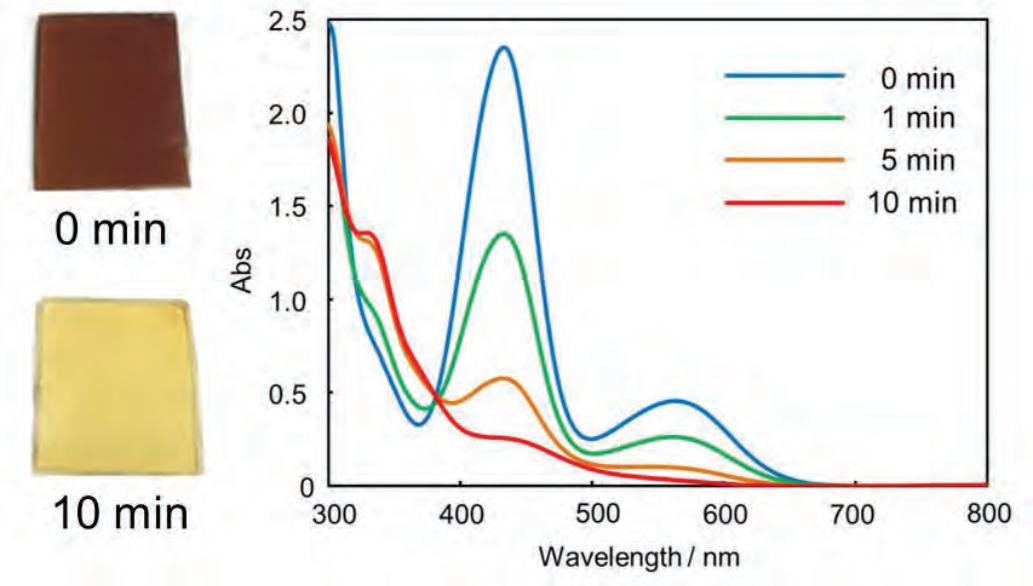

Figure 4-10. UV–Vis spectra of **1**/PEOS nanocomposite film under CO atmosphere and photographs of self-standing film.

4-3 Experimental Section

4-3-1 General

Tetrahydrofuran, dichloromethane, ethanol, toluene, and benzene were purchased from KANTO Chemicals. Tetrahydrofuran was distilled from Na, dried over 4 Å molecular sieves, and degassed with nitrogen before use. Ethanol was distilled from Mg, dried over 3 Å molecular sieves, and degassed with nitrogen before use. Other solvents were distilled from calcium hydride, dried over 4 Å molecular sieves, and degassed with nitrogen before use. Hydrochloric acid (6 mol/L) was purchased from Wako Pure Chemical Industries. Tetraethoxysilane was purchased from Shin-Etsu Silicone. Trimethylamine *N*-oxide was purchased from Tokyo Chemical Industry Co. Ltd. $[(\eta^6\text{-}C_6Me_6)Ru(S_2C_6H_4)]$ (**1**) was prepared according to literature methods.[13]

All NMR spectra were recorded on an ECP-500 (500 MHz) spectrometer. ^1H NMR (500 MHz) and $^{13}C\{^1H\}$ NMR (126 MHz) spectra were measured using tetramethylsilane as an internal standard. IR spectra were recorded using a JASCO FT-IR 6100 spectrometer, and UV-Vis-NIR spectra were recorded using a JASCO V670 spectrometer. Melting points were recorded using a Bibby Stuart Scientific SMP3 instrument. All melting points are uncorrected. HR-ESI MS was recorded on a JEOL JMS-T100CS "AccuTOF CS" spectrometer. TG-DTA curves were recorded on a NETZSCH Japan TG-DTA2020SE instrument.

For structural determination, crystal data were collected using a Bruker AXS SMART APEX CCD X-ray diffractometer equipped with a rotating-anode X-ray generator emitting graphite-monochromatic Mo-Kα radiation (0.7107 Å). Empirical absorption corrections using equivalent reflections and Lorentzian polarization correction were performed using the SADABS program.[29] All data were collected with SMART and Bruker SAINTPLUS (Version 6.45) software packages. The structures were solved using the SHELXS-97[30] program and refined against F^2 using SHELEXL-97.[31] CCDC 1049889 (**1**) and 1049890 (**3**) contain supplementary crystallographic data for this paper. These data can be obtained free of charge from The Cambridge Crystallographic Data Centre via www.ccdc.cam.ac.uk/conts/retrieving.html.The crystal structure of **1** was previously reported in reference 13; however, it has not been registered with the Cambridge Crystallographic Data Center. Therefore, we deposited the structure of **1**.

The three-parameterized Becke-Lee-Yang-Parr (B3LYP) hybrid exchange-correlation functional was employed for the theoretical calculations. A mixture of basis sets (i.e., Lanl2DZ for Mo, 6-31G(d,p) for H, C, O, S, and P)[32-34] was used. Initial structures were taken from the relevant single-crystal X-ray models. The TDDFT method was used to calculate the excited states related to the absorption spectra. Solvent effects were

evaluated by means of the conductor-like polarized continuum model (CPCM). This calculation was implemented using the Gaussian 09W (Revision-A.02) program.[35]

4-3-2 Synthesis of [(η^6-C_6Me_6)Ru(CO)($S_2C_6H_4$)] (**3**)

[(η^6-C_6Me_6)Ru($S_2C_6H_4$)] (**1**) (81 mg, 0.20 mmol) was dissolved in THF (10 mL) and stirred for 6 h at room temperature under a CO atmosphere. The solution was then concentrated under reduced pressure. The product was washed with benzene and **3** was obtained as an orange powder (85 mg, 99%). Single crystals suitable for X-ray crystallographic analysis were obtained by recrystallization from dichloromethane/toluene at −30 °C.

^{1}H NMR (500 MHz, CD_2Cl_2) δ (ppm): 2.15 (s, 18H, $C_6(CH_3)_6$), 6.61–6.64 (m, 2H, $S_2C_6H_4$), 7.11–7.14 (m, 2H, $S_2C_6H_4$). ^{13}C{^{1}H} NMR (126 MHz, CD_2Cl_2) δ 15.7 (s), 109.1 (s), 121.4 (s), 126.9 (s), 143.2 (s), 178.7 (s). IR (KBr, ν/cm^{-1}) 3046 (aryl) 2911(methyl), 1951 ($\nu_{C\equiv O}$); HRMS (HR-ESI-TOF) *m/z* Calcd. for $C_{19}H_{22}ORuS_2Na$: 455.00532 $[M+Na]^+$, Found: 455.00584.

4-3-3 Solid-state reaction of [(η^6-C_6Me_6)Ru($S_2C_6H_4$)] (**1**) with CO gas

[(η^6-C_6Me_6)Ru($S_2C_6H_4$)] (**1**) (40 mg, 0.10 mmol) was stirred for 24 h at room temperature under CO atmosphere. The product was washed with benzene and **3** was obtained as an orange powder (39 mg, 92%).

4-3-4 Reaction of [(η^6-C_6Me_6)Ru(CO)($S_2C_6H_4$)] (**3**) with Me_3NO

[(η^6-C_6Me_6)RuCO($S_2C_6H_4$)] (**2**) (43 mg, 0.10 mmol) and Me_3NO (30 mg, 0.40 mmol) were suspended in THF (10 mL) and stirred for 24 h at room temperature. **3** quantitatively converted to [(η^6-C_6Me_6)Ru($S_2C_6H_4$)] (**1**), as estimated by ^{1}H NMR spectroscopy.

4-3-5 Reaction of [(η^6-C_6Me_6)Ru(CO)($S_2C_6H_4$)] (**3**) with O_2 gas

[(η^6-C_6Me_6)RuCO($S_2C_6H_4$)] (**3**) (43 mg, 0.10 mmol) was dissolved in THF (10 mL) and stirred for 72 h at room temperature under O_2 atmosphere. The solution was then concentrated under reduced pressure. **3** converted to [(η^6-C_6Me_6)Ru($S_2C_6H_4$)] (**1**) in a 40% yield, as estimated by ^{1}H NMR spectroscopy.

4-3-6 Preparation of polysiloxane

An aqueous HCl solution mixture of 6 N HCl aq. (1.9 g) and H_2O (1.6 g)] was added to a mixture of tetraethoxysilane (21 g, 0.10 mol) and ethanol (9.2 g, 0.21mol) in a 200 mL

three-necked flask equipped with a stirrer and N_2 gas inlet and outlet tubes at 0 °C in a H_2O/TEOS molar ratio of 1.70. The mixture was stirred at 0 °C for 10 min at room temperature and then heated at 80 °C for 4 h with stirring at a rate of 150 rpm under a N_2 stream (360 mL/min flow rate). A 20 wt% solution was prepared by dissolving polysiloxane in THF, and the solution was filtered under reduced pressure. The filtrate was evaporated and polysiloxane was obtained as a colorless viscous liquid (9.67 g, Mw = 18800, Mw/Mn = 1.69).

4-3-7 Preparation of **1**/polysiloxane self-standing hybrid film

A 20wt% solution was prepared by dissolving polysiloxane in THF. A 10 g aliquot of the solution was cast onto a polytetrafluoroethylene shale with a 55 mm diameter, and **1** (4 mg) was mixed into the solution. The mixture was left to stand at room temperature for 6 h to form the **1**/polysiloxane hybrid film.

4-4 References

[1] Dithiolene Chemistry: Synthesis, Properties, and Applications (Progress in Inorganic Chemistry vol. 52), ed. by E. I. Stiefel, Wiley, Hoboken, NJ, 2004.

[2] R. Eisenberg, Prog. *Inorg. Chem.* **1970**, *12*, 295–369.

[3] R. P. Burns, C. A. McAuliffe, *Adv. Inorg. Chem. Radiochem.* **1979**, *22*, 303–348.

[4] M. Fourmigue, *Coord. Chem. Rev.* **1998**, *178–180*, 823–864.

[5] A. Sugimori, T. Akiyama, M. Kajitani, T. Sugiyama, *Bull. Chem. Soc. Jpn.* **1999**, *72*, 879–908.

[6] R. Sakamoto, S. Tsukada, H. Nishihara, *Dalton Trans.* **2012**, *41*, 10123–10135.

[7] T. Kambe, R. Sakamoto, K. Hoshiko, K. Takada, M. Miyachi, J.-H. Ryu, S. Sasaki, J. Kim, K. Nakazato, M. Takata, H. Nishihara, *J. Am. Chem. Soc.* **2013**, *135*, 2462–2465.

[8] T. Kambe, R. Sakamoto, T. Kusamoto, T. Pal, N. Fukui, K. Hoshiko, T. Shimojima, Z. Wang, T. Hirahara, K. Ishizaki, S. Hasegawa, F. Liu, H. Nishihara, *J. Am. Chem. Soc.* **2014**, *136*, 14357–14360.

[9] Z. F. Wang, N. Su, F. Liu, *Nano Lett.* **2013**, *13*, 2842–2845.

[10] A. Begum, K. M. Tripathi, S. Sarkar, *Chem. Eur. J.* **2014**, *20*, 16657–16661.

[11] K. Wang, E. I. Stiefel, *Science* **2001**, *291*, 106–109.

[12] K. Mashima, S. Kaneko, K. Tani, H. Kaneyoshi, A. Nakamura, *J. Organomet. Chem.* **1997**, *545–546*, 345–356.

[13] K. Mashima, H. Kaneyoshi, S. Kaneko, A. Mikami, K. Tani, A. Nakamura, *Organometallics* **1997**, *16*, 1016–1025.

[14] H. Hatano, M. Kajitani, T. Akiyama, Y. Sakaguchi, J. Nakamura, H. Hayashi, A. Sugimori, *Chem. Lett.* **1990**, 1089–1092.

[15] R. Yu, K. Arumugam, A. Manepalli, Y. Tran, R. Schmehl, H. Jacobsen, J. P. Donahue, *Inorg. Chem.* **2007**, *46*, 5131–5133.

[16] M. Nomura, M. Fourmigue, *Inorg. Chem.* **2008**, *47*, 1301–1312.

[17] O. R. Gilliam, C. M. Johnson, W. Gordy, *Phys. Rev.* **1950**, *78*, 140–144.

[18] J. J. Bonnet, S. S. Easton, G. R. Easton, R. H. Holm, J. A. Ibers, *J. Am. Chem. Soc.* **1973**, *95*, 2141–2149.

[19] M. Kajitani, A. Igarashi, H. Hatano, T. Akiyama, A. Sugimori, S. Matsumoto, Y. Iguchi, H. Boennemann, K. Shimizu, G. P. Satô, *J. Organomet. Chem.* **1995**, *485*, 31–36.

[20] T. Gunji, M. Ozawa, Y. Abe, R. West, *J. Sol-Gel Sci. Technol.* **2001**, *22*, 219–224.

[21] T. Gunji, Y. Sakai, Y. Suyama, K. Arimitsu, Y. Abe, *J. Sol-Gel Sci. Technol.* **2004**, *32*, 43–46.

[22] T. Gunji, Y. Sakai, K. Arimitsu, Y. Abe, *J. Polym. Sci. Part A Polym. Sci.* **2007**, *45*, 3273–3279.

[23] T. Gunji, K. Hirama, S. Tsukada, Y. Abe, *J. Sol-Gel Sci. Technol.* **2014**, *72*, 80–84.
[24] T. Itoh, T. Akitsu, *Polyhedron* **2010**, *29*, 477–487.
[25] Y. Aritake, T. Takanashi, A. Yamazaki, T. Akitsu, *Polyhedron* **2011**, *30*, 886–94.
[26] Y. Aritake, T. Akitsu, *RSC Adv.* **2012**, *2*, 2975–2980.
[27] M. Ito, T. Akitsu, *Contemp. Eng. Sci.* **2014**, *7*, 869–877.
[28] N. Hariu, M. Ito, T. Akitsu, *Contemp. Eng. Sci.* **2015**, *8*, 57–70.
[29] G. M. Sheldrick, *SADABS*, *Program for area detector absorption correction*, University of Göttingen, Germany, 1996.
[30] G. M. Sheldrick, *SHELXS–97*, *Program for crystal structure solution*, University of Göttingen, Germany, 1997.
[31] G. M. Sheldrick, *SHELXL–97*, *Program for crystal structure refinement*, University of Göttingen, Germany, 1997.
[32] A. D. Becke, *Phys. Rev. A* **1988**, *38*, 3098-3100.
[33] A. D. Becke, *J. Chem. Phys.* **1993**, *98*, 5648-5652.
[34] J. P. Perdew, Y. Wang, *Phys. Rev. B* **1992**, *45*, 13244-13249.
[35] M. J. Frisch, G. W. Trucks, H. B. Schlegel, G. E. Scuseria, M. A. Robb, J. R. Cheeseman, G. Scalmani, V. Barone, B. Mennucci, G. A. Petersson, H. Nakatsuji, M. Caricato, X. Li, H. P. Hratchian, A. F. Izmaylov, J. Bloino, G. Zheng, J. L. Sonnenberg, M. Hada, M. Ehara, K. Toyota, R. Fukuda, J. Hasegawa, M. Ishida, T. Nakajima, Y. Honda, O. Kitao, H. Nakai, T. Vreven, J. A. Montgomery, Jr., J. E. Peralta, F. Ogliaro, M. Bearpark, J. J. Heyd, E. Brothers, K. N. Kudin, V. N. Staroverov, R. Kobayashi, J. Normand, K. Raghavachari, A. Rendell, J. C. Burant, S. S. Iyengar, J. Tomasi, M. Cossi, N. Rega, J. M. Millam, M. Klene, J. E. Knox, J. B. Cross, V. Bakken, C. Adamo, J. Jaramillo, R. Gomperts, R. E. Stratmann, O. Yazyev, A. J. Austin, R. Cammi, C. Pomelli, J. W. Ochterski, R. L. Martin, K. Morokuma, V. G. Zakrzewski, G. A. Voth, P. Salvador, J. J. Dannenberg, S. Dapprich, A. D. Daniels, O. Farkas, J. B. Foresman, J. V. Ortiz, J. Cioslowski, D. J. Fox, *Gaussian 09, Revision A.02*, Gaussian, Inc.; Wallingford CT, 2009.

Chapter 5

Conclusion

5-1 Conclusion

In chapter 1, the back ground of this work was shown.

In chapter 2, the ruthenium-diiron dithiolene complex [(η^6-C_6Me_6)Ru(CO)(μ-CO)$_2$Fe$_2$(μ-bdt)(CO)$_4$] (**2**) was synthesized and two crystallographic isomers were isolated, which depend on the recrystallization temperature: specifically, **2** and its isomer (**2'**) were obtained at –30 ºC and room temperature, respectively. A single crystal of **2** was converted to **2'** by standing in hexane at room temperature for one week. A single crystal of **2'** didn't convert to **2** in hexane at –30 ºC. However, **2** could be obtained by the recrystallization of **2'** from a mixed solvent of dichloromethane and hexane. These results indicated that **2** was the most stable form in solvent. The isomerization took place because of the stability of the **2'** packing structure compared with that of **2**. Additionally, **2** was found to act as a catalyst for proton reduction: catalytic proton reduction occurred at a potential of –2.1 V and 250 μA in acetic acid (50 equiv). These results demonstrate the successful synthesis of new mixed-metal complexes containing a diiron unit that can activate dihydrogen.

In chapter 3, the two homonuclear hydride complexes the hydride bridged ruthenium dinuclear complex [Ru(η^6-C_6Me_6)($S_2C_6H_4$)RuClH(PPh_3)$_2$] (**6**) and the dihydride ruthenium dinuclear complex [Ru(η^6-C_6Me_6)($S_2C_6H_4$) $RuH_2(PPh_3)_2$] (**7**) were synthesized. **7** was obtained as a mixture of *cis*- and *trans*-dihydride isomers in a 10:1 molar ratio as estimated from ^{1}H NMR spectral data. The crystal structures of **6** and *cis*-**7** isomer were determined using single crystal X-ray diffraction analysis. A study was performed to investigate the reactivity of the dihydride complex **7**. The reaction of **7** with CO for 30 minutes produced a dicarbonyl complex [Ru(η^6-C_6Me_6)($S_2C_6H_4$)Ru(CO)$_2$(PPh_3)] (**8**), while a one day exposure of **7** to CO atmosphere on account of a facile substitution reaction between benzene moiety and CO, produced a tetracarbonyl complex [$Ru_2(CO)_4(PPh_3)_2(S_2C_6H_4)$] (**9**). The reaction of **7** with CO_2 under ambient condition led to the generation of formic acid as one of the product. These results contribute to the quest for synthesis and characterization of group 8 transition metal complexes containing hydride ligand.

In chapter 4, the novel CO addition and dissociation on the ruthenium center of [(η^6-C_6Me_6)Ru($S_2C_6H_4$)] **1** were shown. [(η^6-C_6Me_6)Ru(CO)($S_2C_6H_4$)] **3** was obtained by the addition of CO gas to **1** in both solution and solid states. The addition of CO to **1** and dissociation from **3** occurred readily. The molecular structure of **1** and **3** were determined using single-crystal X-ray diffraction analysis. The absorption spectrum of **1** exhibited two strong peaks at 563 and 435 nm, In the spectrum of **3**, each peak was less intense. The decrease in ε for **3** was the result of the structural changes around ruthenium that

formed the piano-stool geometry of **3**. The preparation of a uniform **1**/polysiloxane self-standing hybrid film and the reaction of **1** with CO gas in that film was also demonstrated. The **1**/polysiloxane hybrid film responded quickly to CO gas with a color change that was easily recognized by visual observation.

In chapter 5, a summary of the results in chapter 2, chapter 3 and chapter 4 was shown.

Finally, the novel ruthenium dithiolene complexes showed unique structures, reactivity and properties such as isomerization in single crystal, electrocatalytic proton reduction, reduction of carbon dioxide, and reversible addition and dissociation of carbon monoxide. Hence, I believe that the properties and reactivities were made progress on the cluster chemistry and bioinorganic chemistry.

5-2 Publication list

Chapter 2: S. Tsukada, T. Sagawa, and T. Gunji「Carbon Monoxide Addition to Ruthenium-Dithiolene Complex and Polysiloxane Hybrid Film Formation」*Chem. Asian J.* **2015**, *10*, 1881–1883.

Chapter 3: T. Sagawa, S. Tsukada, K. Yamamoto and Gunji, T.「Structural and Electrochemical Properties of a Ruthenium–Diiron Dithiolene Complex」*Eur. J. Inorg. Chem. I.* **2017**, *32*, 3823–3828.

Chapter 4: T. Sagawa, S. Tsukada, K. Yamamoto and Gunji, T.「Synthesis and reactivity of hydride-bridged ruthenium dithiolene complexes」*Polyhedron* **2018**, *139*, 196–200.

Other papers not induced in this dissertation

1) R. Hayami, K. Wada, T. Sagawa, S. Tsukada, and T. Gunji「Preparation and properties of organic-inorganic films using [Ti(μ_3-O)(O^iPr)$_5$(μ-O^iPr)$_3$($PhPO_3$)$_3$]·thf」*Polym. J.* **2017**, *49*, 223–228.

2) R. Hayami, K. Wada, I. Nishikawa, T. Sagawa, K. Yamamoto, S. Tsukada, and T. Gunji「Preparation and properties of organic–inorganic hybrid materials using titanium phosphonate cluster」*Polym. J.,* **2017***, 49,* 665–669.

5-3 Acknowledgement

This thesis is a summary of my reserach from 2015 to 2018 at Tokyo University of Science under the direction of Professor Takahiro Gunji.

I would like to express my special application and thanks to Professor Takahiro Gunji who provided helpful comments and suggestion. I am also deeply grateful to former Assistant Professor Satoru Tsukada and Assistant Professor Kazuki Yamamoto, who provided sincere encouragement.

Furthermore, I would like to thank the present and the past members of Gunji group: Mr. Ryohei Hayami, Mr. Iori Abe, Mr. Takahiro Igarashi, Mr. Minoru Sato, Ms. Yuki Inomata, Ms. Saya Iwabuchi, Mr. Satoshi Kimura, Ms. Yukiko Tachi, Ms. Shiori Watanabe, Mr. Akihiro Nakamura, Mr. Yuta Miyase, Mr. Keito Otsu, Mr. Kohei Okamoto, Mr. Ayumu Kato, Mr. Takashi Kokaji, Ms. Midori Takemasa, Mr. Yusuke Mitsutani, Mr. Keisuke Wada, Mr. Takayuki Abe, Mr. Tetsuro Izumiya, Mr. Nagato Endo, Mr. Masahiro Ohashi, Mr. Takuya Ogawa, Ms. Kagari Shimamura, Mr. Yudai Suzuki, Ms. Izumi Nishikawa, Mr. Tatsuya Chishima, Mr. Yu Watanabe, Mr. Hoshina Kazuhiro, Ms. Yuzuko Ideno, Mr. Naoki Mizushima, Ms. Erina Oda, Mr. Ibuki Saito, Mr. Koichi Sakamoto, and Ms. Asami Suda for their kindness and collaboration.

Special thanks are given to my family who supported a financial aid and a life deeply.

Supporting Information

S1 Crystal data

S1-1 Atomic coordination and atomic displacement parameter

(1) [(η^6-C_6Me_6)Ru($S_2C_6H_4$)] **1**

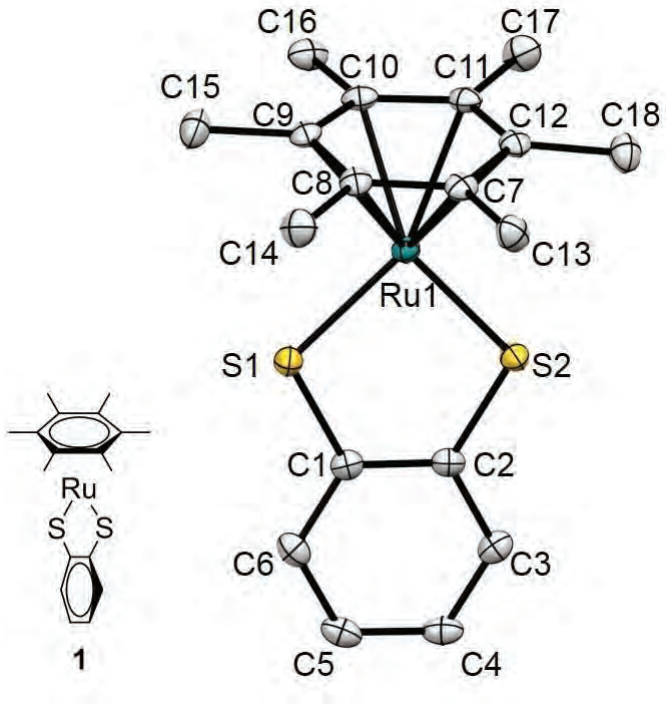

Table S1. Atomic coordination of **1**.

	x	y	z
Ru1	0.21611(3)	0.828143(18)	0.280135(17)
S1	0.09956(9)	0.90601(6)	0.15077(5)
S2	0.05628(9)	0.91180(6)	0.37127(5)
C3	-0.1503(3)	1.0596(2)	0.3280(2)
H3	-0.1633	1.0623	0.3950
C5	-0.2130(4)	1.1193(2)	0.1671(2)
H5	-0.2685	1.1630	0.1246
C9	0.3699(3)	0.7349(2)	0.1977(2)
C12	0.3658(3)	0.7621(2)	0.4018(2)
C4	-0.2303(4)	1.1229(2)	0.2660(2)
H4	-0.2974	1.1692	0.2905
C8	0.4609(3)	0.8088(2)	0.2448(2)
C10	0.2677(4)	0.6796(2)	0.2516(3)
C2	-0.0496(3)	0.9909(2)	0.2931(2)

C6	-0.1153(4)	1.0523(2)	0.1314(2)
H6	-0.1042	1.0495	0.0642
C7	0.4592(3)	0.8227(2)	0.3475(2)
C15	0.3702(4)	0.7197(3)	0.0900(2)
H15A	0.2789	0.7521	0.0565
H15B	0.3637	0.6519	0.0758
H15C	0.4683	0.7454	0.0682
C13	0.5638(4)	0.8985(3)	0.3961(2)
H13A	0.5390	0.9058	0.4630
H13B	0.5450	0.9585	0.3617
H13C	0.6752	0.8803	0.3950
C18	0.3572(4)	0.7796(3)	0.5085(2)
H18A	0.2531	0.7600	0.5268
H18B	0.3730	0.8471	0.5223
H18C	0.4401	0.7429	0.5455
C11	0.2703(4)	0.6916(2)	0.3545(2)
C1	-0.0327(3)	0.9883(2)	0.1941(2)
C14	0.5589(4)	0.8732(3)	0.1873(3)
H14A	0.6629	0.8445	0.1818
H14B	0.5726	0.9345	0.2200
H14C	0.5047	0.8826	0.1228
C17	0.1716(4)	0.6264(3)	0.4121(3)
H17A	0.2198	0.6224	0.4787
H17B	0.1677	0.5632	0.3831
H17C	0.0638	0.6517	0.4117
C16	0.1604(4)	0.6065(2)	0.2020(3)
H16A	0.1377	0.6235	0.1339
H16B	0.0611	0.6037	0.2328
H16C	0.2126	0.5445	0.2068

Table S2. Atomic displacement parameter of **1**.

	U11	U22	U33	U23	U13	U12
Ru1	0.01321(14)	0.01460(15)	0.01610(15)	-0.00013(10)	0.00247(10)	0.00120(9)
S1	0.0202(4)	0.0204(4)	0.0155(4)	-0.0003(3)	0.0018(3)	0.0031(3)
S2	0.0180(4)	0.0208(4)	0.0172(4)	0.0023(3)	0.0040(3)	0.0050(3)

C3	0.0143(14)	0.0196(17)	0.0245(17)	-0.0031(14)	0.0046(13)	-0.0017(13)
C5	0.0145(15)	0.0190(17)	0.0302(19)	0.0068(15)	-0.0003(13)	-0.0009(13)
C9	0.0146(14)	0.0190(17)	0.0208(16)	-0.0005(14)	0.0036(12)	0.0064(13)
C12	0.0141(14)	0.0193(17)	0.0196(16)	0.0018(14)	0.0014(12)	0.0055(13)
C4	0.0143(15)	0.0168(17)	0.0328(19)	0.0021(15)	0.0038(13)	0.0006(13)
C8	0.0125(14)	0.0211(17)	0.0207(16)	0.0003(14)	0.0016(12)	0.0036(13)
C10	0.0144(15)	0.0152(16)	0.0263(17)	0.0000(14)	0.0020(13)	0.0038(12)
C2	0.0136(14)	0.0148(16)	0.0215(16)	0.0005(14)	0.0008(12)	-0.0008(12)
C6	0.0178(15)	0.0224(17)	0.0214(17)	0.0045(14)	0.0009(13)	-0.0028(13)
C7	0.0118(14)	0.0198(17)	0.0216(17)	-0.0001(14)	-0.0004(12)	0.0040(12)
C15	0.0248(17)	0.034(2)	0.0201(17)	-0.0066(16)	0.0026(14)	0.0032(15)
C13	0.0253(17)	0.0245(19)	0.0220(17)	0.0001(15)	-0.0025(14)	-0.0027(15)
C18	0.0224(16)	0.034(2)	0.0191(17)	0.0001(16)	0.0035(13)	0.0029(15)
C11	0.0164(15)	0.0151(16)	0.0228(17)	0.0028(14)	0.0041(13)	0.0041(13)
C1	0.0128(14)	0.0162(16)	0.0203(16)	-0.0006(14)	0.0016(12)	-0.0020(12)
C14	0.0243(17)	0.028(2)	0.0275(18)	0.0017(16)	0.0088(14)	-0.0004(15)
C17	0.0274(17)	0.0235(19)	0.032(2)	0.0012(16)	0.0110(15)	-0.0025(15)
C16	0.0193(16)	0.0199(18)	0.0311(19)	-0.0014(15)	-0.0047(14)	0.0006(14)

(2) $[(\eta^6\text{-}C_6Me_6)Ru(CO)(\mu\text{-}CO)_2Fe_2(\mu\text{-bdt})(CO)_4]$ **2**

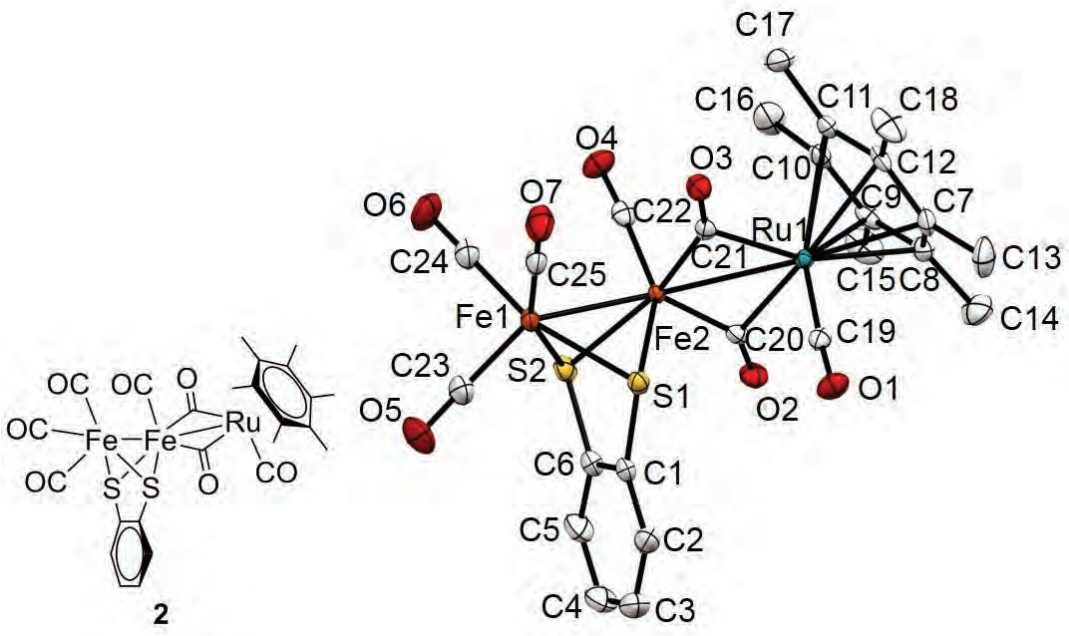

Table S3. Atomic coordination of **2**.

	x	y	z
Ru1	1.003576(12)	0.738815(12)	0.154939(7)
Fe2	0.80517(2)	0.74317(2)	0.083215(15)
Fe1	0.61644(3)	0.82801(3)	0.055265(16)
S1	0.68119(4)	0.77895(4)	0.16528(2)
S2	0.65623(4)	0.63664(5)	0.03806(3)
C7	1.17207(17)	0.75311(18)	0.21421(11)
O2	0.88897(12)	0.51198(13)	0.12064(8)
O3	0.90062(12)	0.97040(13)	0.12037(8)
O4	0.87159(15)	0.77603(14)	-0.05772(8)
C20	0.88712(16)	0.61227(18)	0.11712(10)
O7	0.66091(15)	1.07266(15)	0.08620(10)
O1	0.89757(15)	0.74538(13)	0.29019(8)
C21	0.89192(16)	0.86961(18)	0.11694(10)
C8	1.17049(17)	0.63924(18)	0.18468(11)
C22	0.84898(18)	0.76266(17)	-0.00180(12)
C10	1.13468(17)	0.7245(2)	0.06866(11)
C19	0.93485(18)	0.74179(17)	0.23778(11)
O6	0.60702(17)	0.87115(19)	-0.09424(9)
C13	1.1930(2)	0.7670(2)	0.29206(13)
H13A	1.2733	0.7746	0.3044
H13B	1.1646	0.6991	0.3153
H13C	1.1546	0.8363	0.3069
C24	0.61093(19)	0.8543(2)	-0.03571(12)
C12	1.16157(16)	0.85183(18)	0.17032(11)
O5	0.37666(15)	0.8150(2)	0.07336(13)
C1	0.61276(16)	0.64290(19)	0.17278(11)
C25	0.64383(18)	0.9773(2)	0.07430(12)
C17	1.1314(2)	0.9417(2)	0.05138(14)
H17A	1.2057	0.9675	0.0408
H17B	1.0942	1.0036	0.0752
H17C	1.0872	0.9222	0.0081
C11	1.14207(16)	0.83682(19)	0.09747(11)
C4	0.5076(2)	0.4312(3)	0.17514(17)

H4	0.4714	0.3584	0.1762
C3	0.5184(2)	0.4982(3)	0.23419(15)
H3	0.4897	0.4711	0.2756
C14	1.1943(2)	0.5350(2)	0.23056(14)
H14A	1.1253	0.4913	0.2342
H14B	1.2237	0.5603	0.2769
H14C	1.2495	0.4857	0.2103
C2	0.57101(18)	0.6054(2)	0.23364(13)
H2	0.5781	0.6519	0.2743
C6	0.60195(17)	0.5754(2)	0.11327(12)
C9	1.15016(17)	0.62560(18)	0.11256(11)
C5	0.5495(2)	0.4693(2)	0.11325(15)
H5	0.5419	0.4233	0.0724
C15	1.1481(2)	0.5056(2)	0.08206(15)
H15A	1.2245	0.476	0.0825
H15B	1.1145	0.5082	0.0341
H15C	1.104	0.4547	0.1097
C23	0.46919(19)	0.8203(2)	0.06574(13)
C18	1.1722(2)	0.9724(2)	0.19981(15)
H18A	1.1005	1.0125	0.192
H18B	1.2293	1.0148	0.1768
H18C	1.1936	0.9682	0.2498
C16	1.1249(2)	0.7064(3)	-0.00917(12)
H16A	1.1108	0.7806	-0.0326
H16B	1.0631	0.6534	-0.022
H16C	1.1946	0.6733	-0.0234

Table S4. Atomic displacement parameter of **2**.

	U11	U22	U33	U23	U13	U12
Ru1	0.01125(8)	0.01309(8)	0.01090(8)	-0.00074(5)	0.00040(5)	-0.00084(5)
Fe2	0.00792(14)	0.01541(15)	0.00945(15)	-0.00117(11)	-0.00018(11)	-0.00097(11)
Fe1	0.01182(15)	0.02779(19)	0.01556(16)	0.00347(13)	-0.00120(12)	0.00060(13)
S1	0.0148(2)	0.0247(2)	0.0141(2)	0.00025(18)	0.00103(18)	0.00130(19)
S2	0.0179(2)	0.0285(3)	0.0180(2)	-0.0035(2)	-0.00241(19)	-0.0054(2)
C7	0.0118(9)	0.0280(12)	0.0197(11)	-0.0008(8)	-0.0034(8)	0.0026(8)

O2	0.0240(8)	0.0174(8)	0.0272(8)	-0.0015(6)	0.0010(6)	-0.0042(6)
O3	0.0198(7)	0.0171(8)	0.0274(8)	-0.0002(6)	0.0015(6)	0.0018(6)
O4	0.0391(10)	0.0299(9)	0.0181(8)	0.0020(6)	0.0072(7)	0.0031(7)
C20	0.0144(9)	0.0206(11)	0.0140(9)	-0.0026(8)	0.0021(7)	-0.0047(8)
O7	0.0361(10)	0.0277(10)	0.0447(11)	0.0034(8)	-0.0091(8)	0.0051(8)
O1	0.0355(9)	0.0297(9)	0.0164(8)	0.0000(6)	0.0080(7)	0.0010(7)
C21	0.0124(9)	0.0227(11)	0.0128(9)	0.0008(8)	0.0032(7)	0.0030(8)
C8	0.0143(9)	0.0198(10)	0.0269(11)	0.0042(9)	0.0033(8)	0.0037(8)
C22	0.0191(10)	0.0175(10)	0.0226(11)	-0.0025(8)	-0.0002(8)	-0.0007(8)
C10	0.0120(9)	0.0311(12)	0.0186(10)	-0.0020(9)	0.0027(8)	-0.0021(8)
C19	0.0188(10)	0.0158(10)	0.0163(10)	0.0006(7)	-0.0009(8)	-0.0008(8)
O6	0.0461(11)	0.0694(14)	0.0190(9)	0.0104(9)	-0.0019(8)	0.0057(10)
C13	0.0314(13)	0.0526(16)	0.0210(12)	-0.0055(11)	-0.0094(10)	0.0097(12)
C24	0.0202(11)	0.0392(14)	0.0273(12)	0.0049(10)	-0.0020(9)	0.0023(10)
C12	0.0089(9)	0.0182(10)	0.0283(11)	-0.0039(8)	-0.0020(8)	-0.0021(8)
O5	0.0156(9)	0.0871(18)	0.0780(16)	0.0257(14)	0.0057(9)	0.0033(10)
C1	0.0114(9)	0.0280(11)	0.0234(11)	0.0069(9)	-0.0013(8)	-0.0001(8)
C25	0.0187(10)	0.0350(14)	0.0228(11)	0.0070(10)	-0.0029(8)	0.0061(9)
C17	0.0242(12)	0.0339(13)	0.0425(14)	0.0210(11)	0.0080(10)	0.0023(10)
C11	0.0097(9)	0.0239(11)	0.0244(11)	0.0045(9)	0.0016(8)	-0.0004(8)
C4	0.0272(13)	0.0396(15)	0.0638(19)	0.0196(14)	-0.0036(13)	-0.0134(11)
C3	0.0264(13)	0.0526(17)	0.0431(15)	0.0252(13)	0.0041(11)	-0.0038(12)
C14	0.0345(13)	0.0303(13)	0.0446(15)	0.0164(12)	0.0065(11)	0.0104(11)
C2	0.0190(11)	0.0442(14)	0.0273(12)	0.0133(11)	0.0042(9)	0.0033(10)
C6	0.0144(10)	0.0296(12)	0.0257(11)	0.0050(9)	-0.0023(8)	-0.0032(9)
C9	0.0139(9)	0.0192(10)	0.0291(11)	-0.0068(9)	0.0059(8)	-0.0012(8)
C5	0.0257(12)	0.0346(14)	0.0444(15)	0.0042(11)	-0.0066(11)	-0.0106(10)
C15	0.0304(13)	0.0245(12)	0.0499(16)	-0.0153(11)	0.0110(11)	0.0008(10)
C23	0.0193(12)	0.0445(15)	0.0331(13)	0.0120(11)	0.0008(9)	0.0036(10)
C18	0.0304(13)	0.0219(12)	0.0522(16)	-0.0136(11)	-0.0001(11)	-0.0053(10)
C16	0.0297(13)	0.0601(18)	0.0207(12)	-0.0068(12)	0.0052(10)	-0.0029(12)

(3) [(η^6-C_6Me_6)Ru(CO)(μ-CO)$_2$Fe$_2$(μ-bdt)(CO)$_4$] **2'**

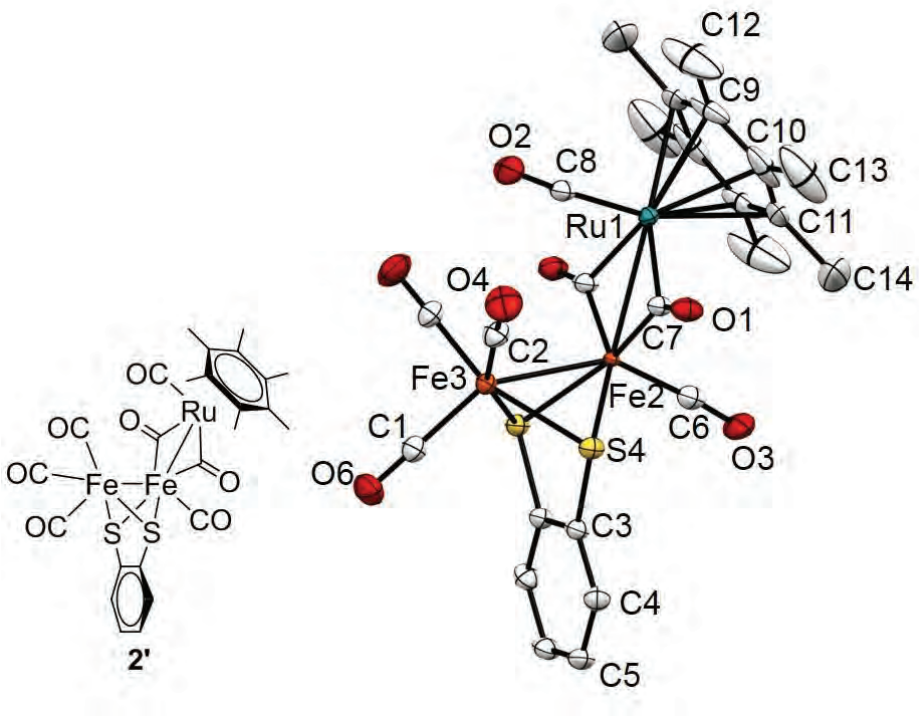

Table S5. Atomic coordination of **2'** .

	x	y	z
Ru1	0.37746(4)	0.25	0.34837(4)
Fe2	0.33202(7)	0.25	0.52518(7)
Fe3	0.15906(8)	0.25	0.54857(8)
S4	0.25588(10)	0.12816(12)	0.61864(9)
O1	0.3409(3)	0.0308(4)	0.4379(3)
O2	0.1825(5)	0.25	0.2832(5)
C7	0.3446(4)	0.1281(5)	0.4450(4)
C4	0.2717(4)	0.1334(5)	0.8080(4)
H4	0.2721	0.0545	0.8079
O4	0.1040(4)	0.0704(5)	0.4257(4)
O3	0.5112(5)	0.25	0.6161(5)
C3	0.2655(4)	0.1917(5)	0.7277(4)
C2	0.1251(4)	0.1427(6)	0.4729(4)
C10	0.4848(6)	0.1330(6)	0.2775(6)
C6	0.4430(6)	0.25	0.5775(6)
C1	0.0616(6)	0.25	0.6261(6)

C5	0.2773(4)	0.1929(6)	0.8902(4)
H5	0.2811	0.1539	0.9465
C8	0.2568(6)	0.25	0.3116(6)
C9	0.4337(5)	0.1915(7)	0.2118(5)
O6	0.0007(5)	0.25	0.6740(5)
C11	0.5311(5)	0.1915(7)	0.3457(5)
C14	0.5848(7)	0.1266(12)	0.4151(7)
H14A	0.5503	0.0603	0.4329
H14B	0.5957	0.1729	0.4691
H14C	0.6436	0.1043	0.3886
C12	0.3815(7)	0.1309(12)	0.1380(7)
H12A	0.3166	0.151	0.1415
H12B	0.3882	0.0507	0.1467
H12C	0.4056	0.1518	0.0779
C13	0.4861(9)	0.0074(8)	0.2718(9)
H13A	0.5477	-0.0197	0.286
H13B	0.469	-0.0159	0.21
H13C	H	0.4425	-0.0233

Table S6. Atomic displacement parameter of **2'** .

	U11	U22	U33	U23	U13	U12
Ru1	0.0136(3)	0.0190(4)	0.0122(3)	0	-0.0008(2)	0
Fe2	0.0098(5)	0.0126(5)	0.0067(5)	0	0.0009(4)	0
Fe3	0.0146(6)	0.0229(6)	0.0153(6)	0	-0.0007(4)	0
S4	0.0224(7)	0.0172(7)	0.0160(7)	-0.0002(5)	0.0007(5)	-0.0010(6)
O1	0.037(3)	0.021(2)	0.020(2)	-0.0017(18)	0.0017(18)	-0.003(2)
O2	0.020(3)	0.086(6)	0.027(4)	0	-0.007(3)	0
C7	0.021(3)	0.028(4)	0.013(3)	0.000(2)	0.001(2)	0.001(3)
C4	0.023(3)	0.023(3)	0.022(3)	0.004(2)	0.002(2)	0.000(2)
O4	0.042(3)	0.047(3)	0.041(3)	-0.016(3)	-0.010(2)	-0.005(3)
O3	0.027(4)	0.068(5)	0.023(3)	0	-0.009(3)	0
C3	0.019(3)	0.025(3)	0.014(3)	-0.001(2)	0.002(2)	-0.001(2)
C2	0.022(3)	0.036(4)	0.023(3)	-0.001(3)	-0.005(2)	-0.002(3)
C10	0.054(5)	0.020(3)	0.064(5)	0.006(3)	0.045(4)	0.005(3)
C6	0.029(5)	0.024(5)	0.019(4)	0	0.004(4)	0

C1	0.021(4)	0.030(5)	0.023(4)	0	-0.002(4)	0
C5	0.024(3)	0.039(4)	0.015(3)	0.005(3)	0.002(2)	0.001(3)
C8	0.022(5)	0.040(6)	0.014(4)	0	0.001(3)	0
C9	0.032(3)	0.062(5)	0.024(3)	-0.017(3)	0.016(3)	-0.020(3)
O6	0.027(4)	0.056(5)	0.034(4)	0	0.008(3)	0
C11	0.026(3)	0.075(5)	0.028(3)	0.019(4)	0.015(3)	0.023(4)
C14	0.071(6)	0.146(8)	0.057(5)	0.048(6)	0.021(4)	0.065(6)
C12	0.074(6)	0.139(8)	0.053(5)	-0.050(5)	0.019(4)	-0.056(6)
C13	0.111(7)	0.031(4)	0.125(7)	0.003(5)	0.078(6)	0.009(5)

(4) [(η^6-C_6Me_6)Ru(CO)($S_2C_6H_4$)] **3**

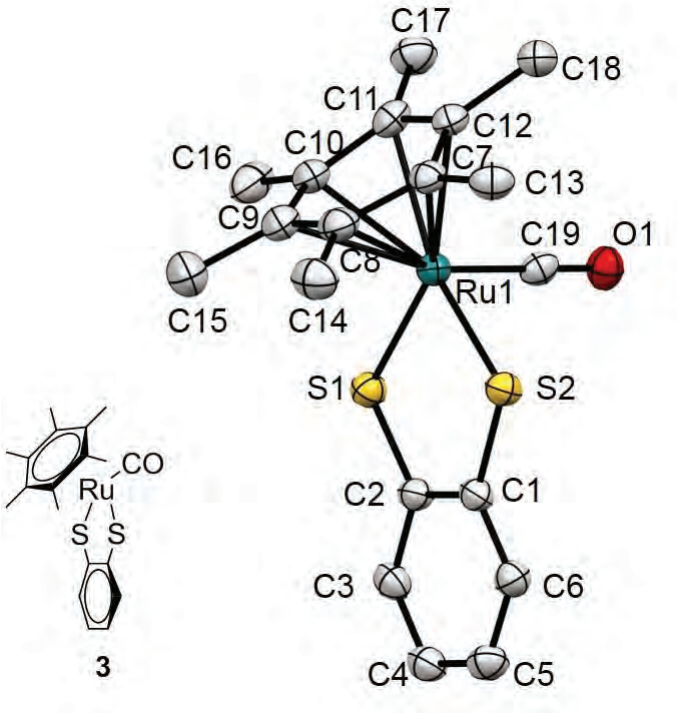

Table S7. Atomic coordination of **3**.

	x	y	z
C39A	0.0511(16)	0.0674(16)	-0.135(6)
H39A	0.0362	0.0837	-0.1411
H39B	0.0368	0.0425	-0.2097
H39C	0.0807	0.0854	-0.1723
C40A	0.0504(10)	0.0526(10)	0.048(3)

C41A	0.0339(10)	0.0667(9)	0.176(4)
H41A	0.0211	0.0833	0.148
C42A	0.0362(10)	0.0565(10)	0.343(3)
H42A	0.025	0.0661	0.4306
C43A	0.0550(10)	0.0322(10)	0.384(3)
H43A	0.0565	0.0252	0.4985
C44A	0.0714(10)	0.0182(10)	0.256(4)
H44A	0.0842	0.0016	0.2838
C45A	0.0691(10)	0.0284(10)	0.088(3)
H45A	0.0803	0.0188	0.0012
Ru1	0.019031(15)	0.226391(15)	0.38437(6)
S1	0.09102(5)	0.27751(5)	0.35087(19)
S2	0.03467(5)	0.17989(5)	0.2342(2)
O1	0.00204(14)	0.25768(14)	0.0613(5)
C12	-0.0477(2)	0.2001(2)	0.4916(8)
C11	-0.0336(2)	0.1708(2)	0.5227(8)
C10	0.0028(2)	0.1832(2)	0.6333(8)
C9	0.0281(2)	0.2254(2)	0.6836(8)
C8	0.0168(2)	0.2565(2)	0.6283(7)
C7	-0.0221(2)	0.2432(2)	0.5441(7)
C15	0.0681(2)	0.2406(3)	0.7840(9)
H15A	0.0611	0.2357	0.9048
H15B	0.087	0.2711	0.7641
H15C	0.0824	0.225	0.749
C14	0.0448(2)	0.3023(2)	0.6783(8)
H14A	0.0369	0.3068	0.792
H14B	0.041	0.3207	0.5974
H14C	0.0746	0.3094	0.678
C13	-0.0375(2)	0.2743(2)	0.5061(9)
H13A	-0.0548	0.2747	0.601
H13B	-0.0548	0.2654	0.4028
H13C	-0.013	0.3029	0.49
C18	-0.0897(2)	0.1856(2)	0.4053(9)
H18A	-0.1123	0.176	0.4906
H18B	-0.0959	0.162	0.3284

H18C	-0.0884	0.2093	0.3406
C17	-0.0583(2)	0.1258(2)	0.4561(9)
H17A	-0.0794	0.1076	0.5406
H17B	-0.0387	0.1151	0.4334
H17C	-0.0729	0.1255	0.3512
C16	0.0134(3)	0.1489(3)	0.6817(10)
H16A	0.0018	0.1377	0.794
H16B	0.0444	0.1612	0.6837
H16C	0.001	0.1258	0.5984
C19	0.00822(19)	0.24532(19)	0.1836(8)
C1	0.1128(2)	0.2537(2)	0.2205(7)
C6	0.1551(2)	0.2772(2)	0.1702(8)
H6A	0.1716	0.3064	0.2006
C5	0.1734(2)	0.2584(2)	0.0766(8)
H5A	0.2024	0.2747	0.0433
C4	0.1497(2)	0.2160(2)	0.0311(8)
H4A	0.1626	0.203	-0.0316
C3	0.1077(2)	0.1926(2)	0.0765(8)
H3A	0.0915	0.1637	0.042
C2	0.08814(19)	0.2107(2)	0.1733(7)

Table S8. Atomic displacement parameter of **3**.

	U11	U22	U33	U23	U13	U12
C39A	0.045(11)	0.039(11)	0.046(11)	-0.003(8)	0.002(8)	0.015(8)
C40A	0.045(7)	0.045(7)	0.050(8)	0.000(6)	-0.002(6)	0.017(6)
C41A	0.045(8)	0.043(8)	0.054(8)	-0.002(6)	-0.001(6)	0.020(6)
C42A	0.048(8)	0.047(8)	0.054(8)	-0.003(6)	0.000(6)	0.018(6)
C43A	0.047(8)	0.050(8)	0.053(8)	-0.002(6)	-0.001(6)	0.019(6)
C44A	0.042(8)	0.045(8)	0.052(8)	-0.001(6)	-0.002(6)	0.024(6)
C45A	0.040(8)	0.045(8)	0.051(8)	0.001(6)	-0.001(6)	0.021(6)
Ru1	0.0231(3)	0.0257(3)	0.0250(3)	0.00066(19)	0.00151(19)	0.0126(2)
S1	0.0252(8)	0.0269(8)	0.0312(8)	-0.0024(6)	0.0002(6)	0.0136(7)
S2	0.0274(8)	0.0259(8)	0.0328(8)	-0.0005(6)	0.0027(6)	0.0134(7)
O1	0.034(2)	0.032(2)	0.033(2)	0.0022(19)	-0.0042(19)	0.014(2)
C12	0.031(3)	0.033(3)	0.027(3)	0.005(2)	0.007(2)	0.013(2)

C11	0.030(3)	0.036(3)	0.031(3)	0.007(2)	0.009(2)	0.018(3)
C10	0.038(3)	0.039(3)	0.033(3)	0.008(2)	0.011(2)	0.022(3)
C9	0.032(3)	0.048(3)	0.029(3)	0.006(3)	0.007(2)	0.023(3)
C8	0.029(3)	0.036(3)	0.023(3)	0.002(2)	0.004(2)	0.018(2)
C7	0.030(3)	0.032(3)	0.027(3)	0.004(2)	0.008(2)	0.017(2)
C15	0.042(4)	0.058(4)	0.033(3)	-0.001(3)	-0.003(3)	0.031(3)
C14	0.029(3)	0.039(4)	0.035(3)	-0.006(3)	-0.002(3)	0.016(3)
C13	0.032(3)	0.036(4)	0.041(3)	0.005(3)	0.007(3)	0.019(3)
C18	0.028(3)	0.046(4)	0.041(3)	0.001(3)	0.000(3)	0.016(3)
C17	0.045(4)	0.035(4)	0.044(4)	0.001(3)	0.015(3)	0.015(3)
C16	0.054(4)	0.050(4)	0.051(4)	0.012(3)	0.008(3)	0.034(4)
C19	0.022(3)	0.027(3)	0.027(3)	-0.002(2)	0.001(2)	0.008(3)
C1	0.030(3)	0.032(3)	0.026(3)	0.002(2)	0.002(2)	0.020(2)
C6	0.029(3)	0.034(3)	0.029(3)	0.003(2)	0.001(2)	0.017(3)
C5	0.025(3)	0.041(3)	0.034(3)	0.001(3)	0.000(2)	0.017(3)
C4	0.035(3)	0.042(3)	0.029(3)	0.000(2)	0.000(2)	0.026(3)
C3	0.035(3)	0.035(3)	0.030(3)	0.000(2)	-0.003(2)	0.023(3)
C2	0.026(3)	0.033(3)	0.026(3)	0.002(2)	0.002(2)	0.018(2)

(5) $[Fe_2(CO)_6(S_2C_6H_4)]$ **4**

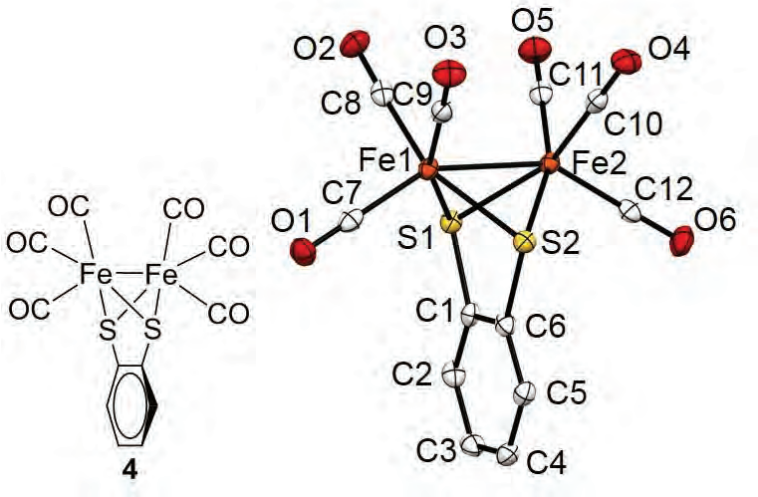

Table S9. Atomic coordination of **4**.

	x	y	z
Fe1	1.12564(3)	0.214532(19)	0.33823(2)

Fe2	0.89079(3)	0.312377(19)	0.22712(2)
S2	0.96107(6)	0.17908(3)	0.16231(4)
S1	0.86453(6)	0.21962(3)	0.36574(4)
O4	1.07518(18)	0.41487(10)	0.09884(11)
O6	0.54977(18)	0.32716(11)	0.06316(12)
O2	1.26995(18)	0.33160(11)	0.53357(12)
O5	0.88388(18)	0.46737(11)	0.37252(12)
C8	1.2131(2)	0.28486(14)	0.45941(16)
O3	1.41268(18)	0.26846(11)	0.25863(12)
O1	1.26560(18)	0.03620(10)	0.42336(12)
C1	0.7600(2)	0.12500(14)	0.28586(15)
C10	1.0042(2)	0.37477(14)	0.14826(15)
C5	0.7291(2)	0.03555(14)	0.11972(16)
C3	0.5624(2)	0.00235(14)	0.24484(16)
C2	0.6393(2)	0.07380(14)	0.31448(16)
C9	1.2999(2)	0.24669(14)	0.28729(15)
C11	0.8885(2)	0.40784(14)	0.31554(15)
C12	0.6795(3)	0.32173(14)	0.12915(16)
C4	0.6060(3)	-0.01640(15)	0.14847(17)
C7	1.2092(2)	0.10466(15)	0.39257(15)
C6	0.8048(2)	0.10590(13)	0.18951(15)
H1	0.614(2)	0.0870(14)	0.3807(17)
H2	0.760(2)	0.0224(14)	0.0552(17)
H3	0.556(2)	-0.0623(15)	0.1036(16)
H4	0.479(3)	-0.0345(15)	0.2627(17)

Table S10. Atomic displacement parameter of **4**.

	U11	U22	U33	U23	U13	U12
Fe1	0.01192(14)	0.01900(17)	0.01505(14)	0.00056(10)	0.00365(11)	0.00032(11)
Fe2	0.01281(15)	0.01770(16)	0.01451(14)	0.00100(10)	0.00399(11)	0.00017(11)
S2	0.0154(2)	0.0195(3)	0.0155(2)	-0.00032(18)	0.00620(18)	-0.00101(19)
S1	0.0145(2)	0.0201(3)	0.0149(2)	0.00025(18)	0.00560(17)	-0.00027(19)
O4	0.0324(8)	0.0310(9)	0.0254(7)	-0.0005(7)	0.0142(7)	-0.0106(7)
O6	0.0177(7)	0.0417(10)	0.0261(7)	0.0065(7)	-0.0005(6)	-0.0010(7)
O2	0.0264(8)	0.0344(9)	0.0216(7)	-0.0070(7)	0.0062(6)	-0.0040(7)

O5	0.0304(8)	0.0271(9)	0.0314(8)	-0.0072(7)	0.0127(7)	-0.0012(7)
C8	0.0155(9)	0.0236(11)	0.0203(10)	0.0049(9)	0.0079(8)	0.0023(8)
O3	0.0227(8)	0.0329(9)	0.0353(8)	-0.0022(7)	0.0166(7)	-0.0042(7)
O1	0.0276(8)	0.0213(8)	0.0315(8)	0.0040(6)	0.0070(6)	0.0039(7)
C1	0.0146(9)	0.0185(10)	0.0162(8)	0.0021(7)	0.0015(7)	0.0023(8)
C10	0.0172(9)	0.0209(11)	0.0177(9)	-0.0037(8)	0.0029(8)	0.0012(8)
C5	0.0173(9)	0.0218(11)	0.0176(9)	0.0002(8)	0.0023(8)	0.0022(8)
C3	0.0164(10)	0.0214(11)	0.0297(10)	0.0062(9)	0.0049(8)	-0.0020(9)
C2	0.0172(9)	0.0246(12)	0.0202(9)	0.0042(8)	0.0077(8)	0.0021(8)
C9	0.0194(10)	0.0189(11)	0.0184(9)	-0.0020(8)	0.0022(8)	0.0012(8)
C11	0.0148(9)	0.0239(11)	0.0205(9)	0.0044(9)	0.0061(8)	0.0006(8)
C12	0.0213(11)	0.0192(11)	0.0210(10)	0.0032(8)	0.0096(9)	-0.0018(8)
C4	0.0184(10)	0.0197(11)	0.0250(10)	0.0004(9)	-0.0010(8)	-0.0014(9)
C7	0.0147(9)	0.0269(13)	0.0183(9)	-0.0030(8)	0.0057(8)	-0.0026(9)
C6	0.0132(9)	0.0192(11)	0.0202(9)	0.0040(8)	0.0042(7)	0.0022(8)

(6) $[RuClH(PPh_3)_3]$ **5**

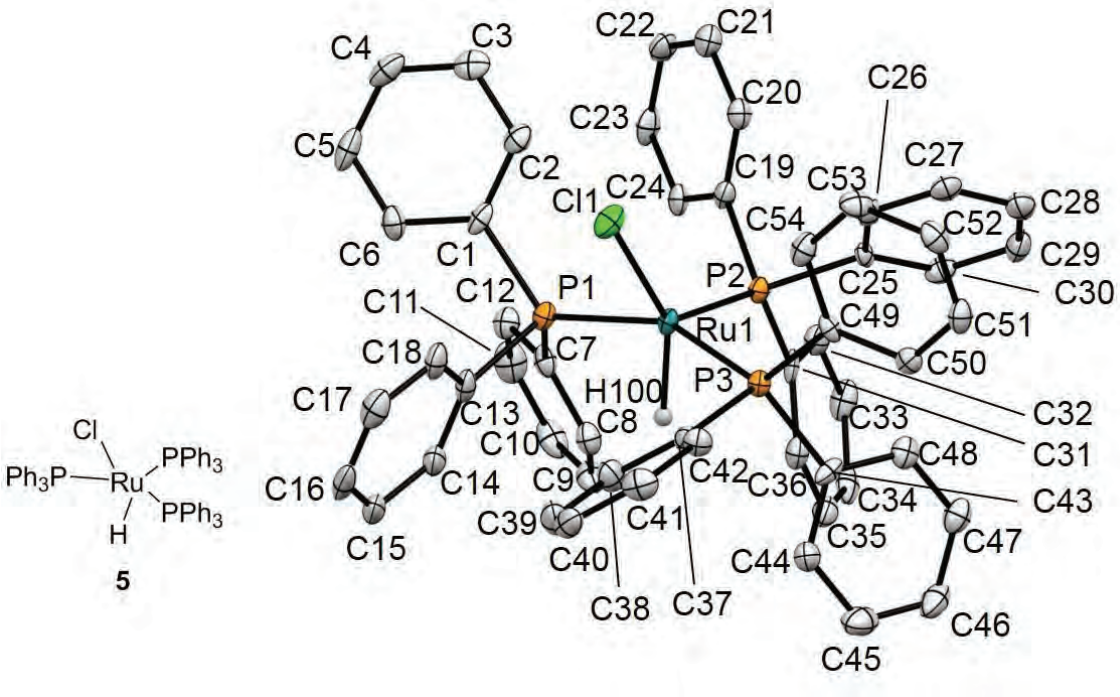

Table S11. Atomic coordination of **5**.

	x	y	z
Ru1	0.73791(3)	1.00721(3)	0.49646(3)
P1	0.76328(9)	0.99906(11)	0.62393(9)
P2	0.72003(10)	0.85543(11)	0.47162(9)
P3	0.76070(10)	1.06145(11)	0.39469(9)
Cl1	0.63848(10)	1.12362(11)	0.47162(9)
C25	0.6698(3)	0.8290(4)	0.3690(3)
C51	0.6485(4)	1.0893(4)	0.1605(4)
H51	0.6593	1.0792	0.1183
C31	0.7983(4)	0.7687(4)	0.5022(3)
C1	0.6892(4)	1.0089(4)	0.6574(3)
C2	0.6144(4)	0.9849(4)	0.6100(4)
H2	0.6009	0.9675	0.5588
C50	0.7039(4)	1.0710(4)	0.2333(4)
H50	0.7523	1.0482	0.2402
C19	0.6533(4)	0.8050(4)	0.5054(4)
C44	0.9094(4)	1.0331(5)	0.4065(4)
H44	0.9227	1.0905	0.4342
C8	0.8082(4)	0.8537(4)	0.7354(4)
H8	0.7648	0.8692	0.7433
C24	0.5753(4)	0.8194(4)	0.4622(4)
H24	0.5575	0.8495	0.4142
C36	0.8682(4)	0.7958(4)	0.5060(4)
H36	0.8755	0.8592	0.4953
C21	0.6255(4)	0.7308(4)	0.6010(4)
H21	0.6429	0.7002	0.6488
C53	0.5629(4)	1.1383(5)	0.2116(4)
H53	0.5144	1.1614	0.2043
C40	0.8683(4)	1.3541(5)	0.4788(4)
H40	0.8917	1.4135	0.4966
C20	0.6778(4)	0.7608(4)	0.5754(4)
H20	0.7308	0.7511	0.606
C49	0.6902(4)	1.0855(4)	0.2968(3)
C52	0.5774(4)	1.1221(4)	0.1491(4)

H52	0.539	1.1335	0.0991
C54	0.6187(4)	1.1208(4)	0.2847(4)
H54	0.6083	1.1329	0.327
C14	0.8969(4)	1.0979(5)	0.7241(4)
H14	0.921	1.0382	0.7386
C26	0.6175(4)	0.8936(4)	0.3214(3)
H26	0.6066	0.9484	0.3426
C6	0.7074(4)	1.0366(4)	0.7320(4)
H6	0.758	1.0554	0.7648
C37	0.8014(4)	1.1795(4)	0.4257(4)
C18	0.7884(4)	1.1915(5)	0.6494(4)
H18	0.7373	1.1964	0.6114
C28	0.5961(4)	0.8009(5)	0.2129(4)
H28	0.5719	0.7923	0.1593
C48	0.8184(4)	0.9168(4)	0.3379(4)
H48	0.7678	0.8932	0.3178
C29	0.6460(4)	0.7337(5)	0.2590(4)
H29	0.655	0.678	0.2374
C35	0.9276(4)	0.7320(5)	0.5251(4)
H35	0.9751	0.7518	0.5273
C32	0.7884(4)	0.6748(4)	0.5160(4)
H32	0.7403	0.6539	0.5115
C43	0.8357(3)	1.0010(4)	0.3783(3)
C10	0.9199(4)	0.7594(5)	0.7667(4)
H10	0.9531	0.7106	0.796
C41	0.8202(4)	1.3416(4)	0.4030(4)
H41	0.8098	1.3927	0.3686
C47	0.8729(4)	0.8673(5)	0.3267(4)
H47	0.8597	0.81	0.2989
C22	0.5485(4)	0.7451(5)	0.5575(4)
H22	0.5129	0.7239	0.5752
C34	0.9177(4)	0.6400(5)	0.5408(3)
H34	0.9587	0.5965	0.5547
C7	0.8228(4)	0.9030(4)	0.6822(4)
C30	0.6828(4)	0.7472(4)	0.3368(4)

H30	0.7171	0.7008	0.3684
C23	0.5233(4)	0.7902(5)	0.4885(4)
H23	0.4704	0.8014	0.459
C17	0.8283(5)	1.2722(5)	0.6835(4)
H17	0.8045	1.3321	0.6694
C12	0.8869(4)	0.8784(4)	0.6714(4)
H12	0.8974	0.9107	0.6346
C13	0.8219(4)	1.1032(4)	0.6699(4)
C42	0.7871(4)	1.2545(4)	0.3768(4)
H42	0.754	1.2464	0.3243
C9	0.8567(4)	0.7818(5)	0.7772(4)
H9	0.846	0.7479	0.8133
C39	0.8825(4)	1.2802(5)	0.5289(4)
H39	0.915	1.2891	0.5814
C38	0.8497(4)	1.1934(5)	0.5030(4)
H38	0.8598	1.1427	0.5377
C16	0.9022(5)	1.2655(5)	0.7377(4)
H16	0.9294	1.3209	0.7617
C4	0.5781(4)	1.0114(4)	0.7102(4)
H4	0.5402	1.0116	0.7283
C11	0.9351(4)	0.8074(5)	0.7139(4)
H11	0.9788	0.7916	0.7066
C15	0.9373(4)	1.1792(5)	0.7576(4)
H15	0.9891	1.1751	0.7942
C27	0.5812(4)	0.8803(4)	0.2443(4)
H27	0.5459	0.9258	0.2126
C3	0.5593(4)	0.9859(4)	0.6362(4)
H3	0.5082	0.969	0.6032
C45	0.9651(4)	0.9833(6)	0.3955(4)
H45	1.0158	1.0068	0.4155
C46	0.9469(4)	0.9003(5)	0.3557(4)
H46	0.9848	0.8659	0.3482
C33	0.8488(4)	0.6109(4)	0.5363(4)
H33	0.842	0.5473	0.5471
C5	0.6524(4)	1.0367(4)	0.7581(4)

H5	0.6653	1.0543	0.8091
C55	0.1221(5)	0.0520(6)	0.9827(5)
C57	0.0758(5)	-0.0638(6)	0.8839(5)
H57	0.0515	-0.1226	0.8658
C58	0.0981(5)	-0.0114(7)	0.8392(5)
H58	0.0894	-0.0328	0.7901
C56	0.0876(5)	-0.0338(6)	0.9539(5)
H56	0.0718	-0.0726	0.9839
C59	0.1329(5)	0.0721(7)	0.8659(5)
H59	0.1489	0.109	0.8351
C60	0.1455(5)	0.1046(6)	0.9361(5)
H60	0.1704	0.1633	0.9535
C61	0.1350(6)	0.0850(8)	1.0593(5)
H61A	0.0963	0.0575	1.0726
H61B	0.1313	0.1538	1.0593
H61C	0.1858	0.0654	1.0967
H100	0.827(3)	0.991(4)	0.535(3)

Table S12. Atomic displacement parameter of **5**.

	U11	U22	U33	U23	U13	U12
Ru1	0.0185(3)	0.0088(2)	0.0145(2)	0.0004(2)	0.0095(2)	0.0009(2)
P1	0.0214(9)	0.0141(7)	0.0166(8)	-0.0004(7)	0.0105(7)	0.0014(8)
P2	0.0175(9)	0.0132(7)	0.0130(8)	0.0003(6)	0.0079(8)	0.0003(7)
P3	0.0177(9)	0.0135(7)	0.0138(8)	-0.0002(6)	0.0076(8)	0.0003(7)
Cl1	0.0287(10)	0.0244(8)	0.0250(9)	0.0058(7)	0.0164(8)	0.0083(7)
C25	0.015(4)	0.018(3)	0.007(3)	-0.001(2)	0.004(3)	-0.003(3)
C51	0.031(4)	0.021(3)	0.016(3)	0.000(3)	0.012(3)	0.000(3)
C31	0.029(4)	0.011(3)	0.012(3)	-0.003(2)	0.011(3)	0.004(3)
C1	0.029(4)	0.007(3)	0.025(3)	0.003(3)	0.020(3)	0.005(3)
C2	0.024(4)	0.015(3)	0.026(3)	0.000(3)	0.014(3)	0.004(3)
C50	0.020(4)	0.011(3)	0.022(4)	0.000(3)	0.011(3)	-0.002(3)
C19	0.024(4)	0.015(3)	0.018(3)	-0.003(3)	0.014(3)	-0.003(3)
C44	0.022(4)	0.027(3)	0.019(3)	-0.004(3)	0.009(3)	-0.002(3)
C8	0.025(4)	0.016(3)	0.020(3)	0.001(3)	0.010(3)	0.003(3)
C24	0.024(4)	0.016(3)	0.017(3)	-0.001(3)	0.009(3)	0.001(3)

C36	0.029(4)	0.016(3)	0.018(3)	-0.002(3)	0.013(3)	0.000(3)
C21	0.040(5)	0.017(3)	0.018(3)	0.002(3)	0.019(4)	0.000(3)
C53	0.018(4)	0.026(3)	0.021(4)	0.006(3)	0.006(3)	0.003(3)
C40	0.030(4)	0.018(3)	0.042(5)	-0.012(3)	0.024(4)	-0.008(3)
C20	0.025(4)	0.014(3)	0.017(3)	-0.004(3)	0.010(3)	0.001(3)
C49	0.018(4)	0.012(3)	0.009(3)	0.002(2)	0.002(3)	-0.002(3)
C52	0.025(4)	0.022(3)	0.015(3)	0.004(3)	0.004(3)	-0.002(3)
C54	0.032(4)	0.015(3)	0.025(4)	0.001(3)	0.018(4)	0.002(3)
C14	0.028(4)	0.028(4)	0.021(4)	-0.009(3)	0.015(4)	-0.005(3)
C26	0.022(4)	0.021(3)	0.018(3)	-0.003(3)	0.013(3)	-0.003(3)
C6	0.030(4)	0.015(3)	0.019(3)	-0.003(3)	0.010(3)	-0.002(3)
C37	0.017(4)	0.016(3)	0.021(3)	-0.006(3)	0.013(3)	-0.002(3)
C18	0.038(5)	0.025(4)	0.020(4)	-0.003(3)	0.020(4)	-0.001(3)
C28	0.023(4)	0.028(4)	0.022(4)	-0.002(3)	0.012(3)	-0.007(3)
C48	0.025(4)	0.019(3)	0.017(3)	0.004(3)	0.009(3)	0.004(3)
C29	0.031(4)	0.021(3)	0.025(4)	-0.005(3)	0.018(4)	-0.002(3)
C35	0.023(4)	0.027(4)	0.019(4)	-0.002(3)	0.009(3)	0.005(3)
C32	0.025(4)	0.021(3)	0.019(3)	-0.001(3)	0.012(3)	0.000(3)
C43	0.018(3)	0.022(3)	0.015(3)	0.009(3)	0.011(3)	0.010(3)
C10	0.032(5)	0.018(3)	0.020(4)	0.001(3)	-0.001(4)	0.006(3)
C41	0.028(4)	0.016(3)	0.036(4)	0.004(3)	0.016(4)	0.000(3)
C47	0.033(5)	0.022(3)	0.024(4)	0.003(3)	0.016(4)	0.006(3)
C22	0.027(4)	0.027(4)	0.025(4)	-0.004(3)	0.018(4)	-0.006(3)
C34	0.030(4)	0.028(4)	0.010(3)	0.000(3)	0.003(3)	0.012(3)
C7	0.025(4)	0.012(3)	0.016(3)	-0.002(3)	0.006(3)	0.001(3)
C30	0.020(4)	0.019(3)	0.026(4)	0.004(3)	0.012(3)	0.004(3)
C23	0.027(4)	0.027(4)	0.024(4)	-0.005(3)	0.013(3)	0.000(3)
C17	0.045(5)	0.015(3)	0.037(4)	0.000(3)	0.029(4)	0.000(3)
C12	0.027(4)	0.021(3)	0.016(3)	-0.001(3)	0.008(3)	-0.001(3)
C13	0.033(4)	0.016(3)	0.018(3)	-0.004(3)	0.018(4)	-0.005(3)
C42	0.023(4)	0.014(3)	0.021(3)	0.002(3)	0.011(3)	-0.002(3)
C9	0.048(5)	0.021(3)	0.025(4)	0.003(3)	0.017(4)	-0.005(3)
C39	0.036(5)	0.032(4)	0.025(4)	-0.010(3)	0.018(4)	-0.014(3)
C38	0.030(4)	0.029(4)	0.019(4)	-0.001(3)	0.013(4)	-0.008(3)
C16	0.047(5)	0.025(4)	0.040(5)	-0.016(3)	0.037(5)	-0.016(4)

C4	0.035(4)	0.017(3)	0.042(4)	0.006(3)	0.030(4)	0.005(3)
C11	0.021(4)	0.025(4)	0.025(4)	-0.003(3)	0.003(3)	0.009(3)
C15	0.029(4)	0.041(4)	0.029(4)	-0.019(3)	0.020(4)	-0.011(4)
C27	0.021(4)	0.022(3)	0.024(4)	0.004(3)	0.014(3)	-0.001(3)
C3	0.022(4)	0.012(3)	0.037(4)	0.005(3)	0.013(3)	0.006(3)
C45	0.020(4)	0.050(5)	0.026(4)	0.004(4)	0.008(3)	0.003(4)
C46	0.028(4)	0.042(4)	0.023(4)	0.003(3)	0.013(4)	0.015(4)
C33	0.044(5)	0.013(3)	0.024(4)	0.004(3)	0.020(4)	0.006(3)
C5	0.050(5)	0.016(3)	0.027(4)	0.003(3)	0.029(4)	0.007(3)
C55	0.031(5)	0.039(4)	0.034(5)	-0.003(4)	0.004(4)	0.010(4)
C57	0.065(7)	0.028(4)	0.044(6)	-0.002(4)	0.001(5)	0.000(4)
C58	0.050(6)	0.057(6)	0.036(5)	0.000(5)	0.012(4)	0.021(5)
C56	0.039(5)	0.040(5)	0.033(5)	0.015(4)	0.005(4)	-0.009(4)
C59	0.039(6)	0.069(6)	0.040(5)	0.005(5)	0.018(5)	-0.010(5)
C60	0.043(6)	0.035(5)	0.054(6)	-0.005(4)	0.008(5)	-0.018(4)
C61	0.067(8)	0.091(9)	0.042(6)	-0.020(6)	0.010(6)	0.012(6)

(7) $Ru(\eta^6\text{-}C_6Me_6)(S_2C_6H_4)RuClH(PPh_3)_2$] **6**

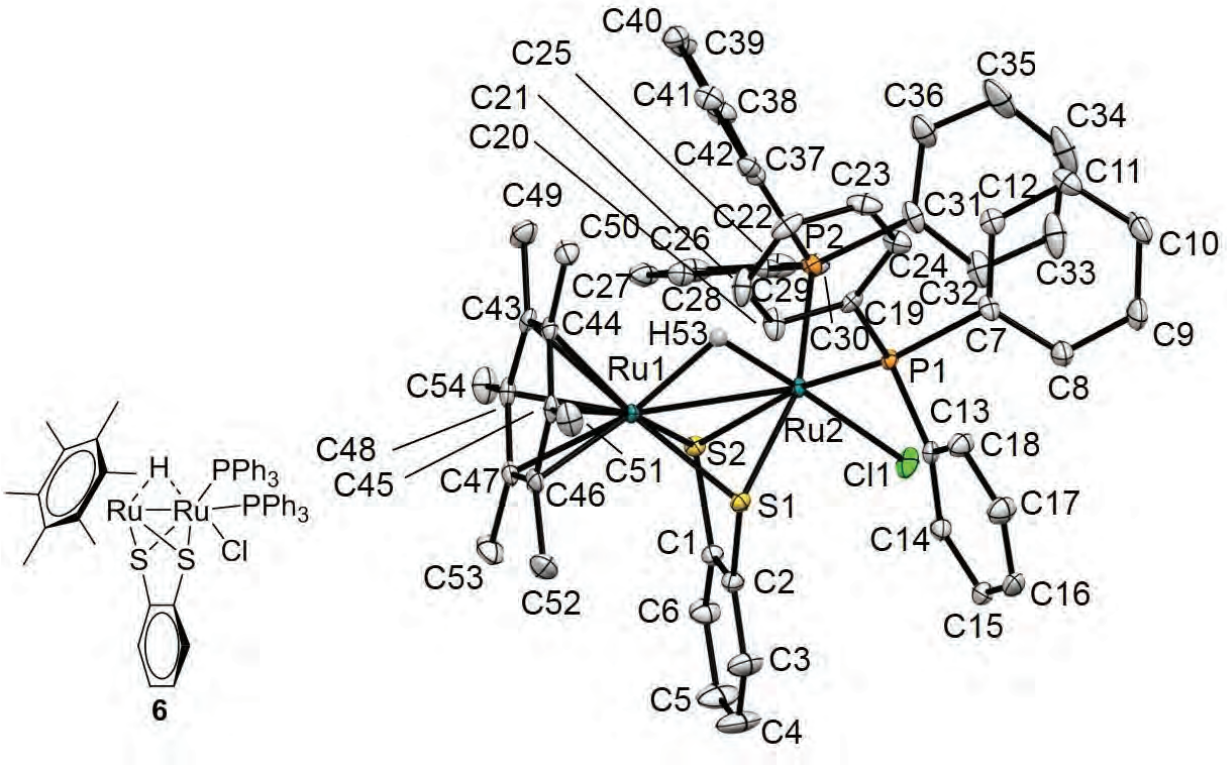

Table S13. Atomic coordination of **6**.

	x	y	z
Ru1	0.152860(11)	0.139583(6)	0.577521(7)
Ru2	0.311506(11)	0.235863(6)	0.632363(7)
S2	0.30280(4)	0.13130(2)	0.68366(2)
S1	0.11179(4)	0.22727(2)	0.64364(2)
P2	0.48580(4)	0.21700(2)	0.60079(2)
P1	0.27477(4)	0.33776(2)	0.58812(2)
Cl1	0.40068(4)	0.27896(2)	0.74993(2)
C33	0.7317(2)	0.34841(11)	0.69547(13)
H33	0.7473	0.3728	0.7381
C31	0.60996(16)	0.27333(9)	0.61632(11)
C13	0.17570(16)	0.38563(9)	0.62900(10)
C44	0.08185(16)	0.11617(9)	0.46051(9)
C7	0.39696(16)	0.39450(9)	0.59939(10)
C37	0.47055(15)	0.19678(9)	0.50599(10)
C42	0.38246(16)	0.22551(9)	0.45368(10)

H42	0.3293	0.254	0.4674
C19	0.19766(16)	0.34840(8)	0.49366(9)
C25	0.56659(16)	0.14602(9)	0.64318(10)
C17	0.05175(18)	0.47842(10)	0.62426(11)
H17	0.01	0.5129	0.5979
C45	-0.01363(15)	0.13150(8)	0.49015(10)
C46	-0.02403(15)	0.10099(9)	0.55474(10)
C41	0.37132(17)	0.21309(9)	0.38167(10)
H41	0.3109	0.2331	0.3467
C48	0.15109(16)	0.03630(8)	0.55507(10)
C2	0.13088(16)	0.19194(9)	0.72936(10)
C47	0.05544(16)	0.05190(9)	0.58619(10)
C26	0.51806(17)	0.08603(9)	0.62432(10)
H26	0.4437	0.0827	0.5912
C28	0.68477(18)	0.03562(10)	0.70260(11)
H28	0.7252	-0.0017	0.7225
C8	0.41858(18)	0.43895(10)	0.65461(11)
H8	0.3704	0.4396	0.6875
C14	0.17008(16)	0.37593(9)	0.69947(10)
H14	0.2087	0.3405	0.7254
C50	0.09413(17)	0.14785(9)	0.39279(10)
H50A	0.0385	0.1288	0.3518
H50B	0.1743	0.142	0.3876
H50C	0.0776	0.1933	0.3949
C1	0.22172(16)	0.14756(9)	0.74855(10)
C21	0.03333(18)	0.31682(9)	0.39773(11)
H21	-0.0335	0.2906	0.3807
C43	0.16586(15)	0.06834(8)	0.49322(10)
C22	0.06253(17)	0.36192(10)	0.35347(10)
H22	0.0181	0.3658	0.3055
C16	0.04978(17)	0.46965(9)	0.69489(11)
H16	0.0089	0.4987	0.7177
C38	0.54799(16)	0.15515(9)	0.48385(10)
H38	0.6089	0.1352	0.5185
C12	0.47149(16)	0.39350(9)	0.55300(10)

H12	0.4602	0.3624	0.5164
C6	0.24318(19)	0.11720(10)	0.81390(11)
H6	0.3047	0.0869	0.8269
C30	0.67446(16)	0.14979(10)	0.69314(10)
H30	0.7085	0.1901	0.7072
C36	0.68461(17)	0.27839(10)	0.57031(13)
H36	0.6683	0.255	0.527
C52	-0.11982(17)	0.12125(11)	0.58979(12)
H52A	-0.1859	0.0916	0.5765
H52B	-0.1463	0.1641	0.5739
H52C	-0.0893	0.1211	0.6417
C11	0.56151(17)	0.43739(10)	0.55982(11)
H11	0.61	0.437	0.5271
C32	0.63365(18)	0.30910(10)	0.67880(11)
H32	0.5828	0.3067	0.71
C15	0.10803(17)	0.41812(9)	0.73193(10)
H15	0.1056	0.4115	0.7801
C3	0.0612(2)	0.20583(11)	0.77557(11)
H3	-0.0013	0.2355	0.7623
C40	0.44831(17)	0.17151(10)	0.36079(10)
H40	0.4405	0.1628	0.3117
C20	0.10080(17)	0.30946(9)	0.46697(10)
H20	0.0808	0.2775	0.4966
C9	0.5101(2)	0.48235(11)	0.66196(12)
H9	0.5241	0.5124	0.6998
C23	0.15712(17)	0.40151(10)	0.37963(11)
H23	0.177	0.4331	0.3496
C27	0.57681(18)	0.03118(10)	0.65320(11)
H27	0.5433	-0.0093	0.6392
C18	0.11460(17)	0.43696(9)	0.59175(10)
H18	0.116	0.4437	0.5434
C24	0.22330(16)	0.39549(10)	0.44939(10)
H24	0.2867	0.4238	0.4671
C5	0.1730(2)	0.13168(12)	0.86071(12)
H5	0.1869	0.111	0.9057

C10	0.58072(19)	0.48185(11)	0.61445(12)
H10	0.6424	0.5119	0.6192
C29	0.73286(17)	0.09467(10)	0.72259(11)
H29	0.8062	0.0978	0.7566
C39	0.53658(17)	0.14287(10)	0.41221(11)
H39	0.5897	0.1146	0.3981
C53	0.0416(2)	0.01840(10)	0.65290(11)
H53A	0.0961	0.0369	0.6947
H53B	0.059	-0.0269	0.6498
H53C	-0.0391	0.0235	0.6574
C51	-0.10646(17)	0.17920(9)	0.45421(12)
H51A	-0.0947	0.2191	0.481
H51B	-0.1845	0.1623	0.4531
H51C	-0.1	0.1869	0.4054
C4	0.0839(2)	0.17572(12)	0.84216(13)
H4	0.0377	0.1857	0.8747
C49	0.26377(17)	0.05181(10)	0.45830(11)
H49A	0.3163	0.0208	0.4878
H49B	0.308	0.0903	0.4534
H49C	0.2304	0.0336	0.411
C35	0.78272(19)	0.31773(11)	0.58792(15)
H35	0.8334	0.3208	0.5566
C34	0.8069(2)	0.35234(12)	0.65064(15)
H34	0.8746	0.3786	0.6629
C54	0.23754(18)	-0.01363(9)	0.59116(11)
H54A	0.1983	-0.055	0.5873
H54B	0.2677	-0.0026	0.6416
H54C	0.3028	-0.0157	0.568
H53	0.245(2)	0.2030(13)	0.5506(14)

Table S14. Atomic displacement parameter of **6**.

	U11	U22	U33	U23	U13	U12
Ru1	0.00782(6)	0.00780(6)	0.00839(6)	-0.00038(5)	0.00105(5)	-0.00042(5)
Ru2	0.00850(6)	0.00827(6)	0.00687(6)	0.00009(5)	-0.00032(5)	-0.00080(5)
S2	0.01075(19)	0.0112(2)	0.00924(19)	0.00121(15)	0.00125(15)	0.00091(15)

S1	0.0115(2)	0.0100(2)	0.01130(19)	-0.00040(16)	0.00301(16)	0.00098(15)
P2	0.0083(2)	0.0116(2)	0.0112(2)	0.00094(17)	0.00002(16)	-0.00058(16)
P1	0.0113(2)	0.0089(2)	0.00729(19)	-0.00009(16)	0.00028(16)	-0.00129(16)
Cl1	0.0223(2)	0.0182(2)	0.00958(19)	-0.00165(16)	-0.00444(17)	-0.00208(17)
C33	0.0269(12)	0.0232(11)	0.0344(13)	0.0018(10)	-0.0129(10)	-0.0078(9)
C31	0.0097(8)	0.0141(9)	0.0233(10)	0.0046(8)	-0.0030(7)	-0.0012(7)
C13	0.0136(9)	0.0113(8)	0.0128(9)	-0.0034(7)	0.0032(7)	-0.0043(7)
C44	0.0130(8)	0.0119(9)	0.0110(8)	-0.0024(7)	-0.0014(7)	-0.0034(7)
C7	0.0145(9)	0.0120(9)	0.0117(8)	0.0036(7)	-0.0010(7)	-0.0023(7)
C37	0.0120(8)	0.0137(9)	0.0130(9)	0.0008(7)	0.0035(7)	-0.0026(7)
C42	0.0122(9)	0.0148(9)	0.0161(9)	0.0011(7)	0.0044(7)	0.0005(7)
C19	0.0139(9)	0.0120(9)	0.0091(8)	-0.0025(7)	0.0014(7)	0.0039(7)
C25	0.0126(8)	0.0168(9)	0.0116(8)	0.0039(7)	0.0056(7)	0.0041(7)
C17	0.0263(11)	0.0175(10)	0.0222(10)	0.0002(8)	0.0083(9)	0.0044(8)
C45	0.0098(8)	0.0107(9)	0.0155(9)	-0.0026(7)	-0.0029(7)	-0.0025(7)
C46	0.0098(8)	0.0152(9)	0.0178(9)	-0.0043(7)	0.0016(7)	-0.0049(7)
C41	0.0162(9)	0.0200(10)	0.0144(9)	0.0048(8)	0.0019(7)	0.0016(8)
C48	0.0150(9)	0.0081(8)	0.0156(9)	-0.0021(7)	-0.0030(7)	-0.0018(7)
C2	0.0188(9)	0.0130(9)	0.0123(9)	0.0001(7)	0.0051(7)	-0.0009(7)
C47	0.0176(9)	0.0115(9)	0.0136(9)	-0.0007(7)	0.0014(7)	-0.0067(7)
C26	0.0162(9)	0.0177(10)	0.0165(9)	0.0017(8)	0.0058(8)	0.0017(7)
C28	0.0254(11)	0.0249(11)	0.0215(10)	0.0107(9)	0.0129(9)	0.0126(9)
C8	0.0227(10)	0.0210(10)	0.0173(10)	-0.0033(8)	0.0056(8)	-0.0088(8)
C14	0.0183(9)	0.0143(9)	0.0130(9)	-0.0009(7)	0.0027(7)	-0.0040(7)
C50	0.0212(10)	0.0197(10)	0.0131(9)	0.0009(8)	0.0019(8)	-0.0034(8)
C1	0.0166(9)	0.0141(9)	0.0115(9)	-0.0004(7)	0.0036(7)	-0.0024(7)
C21	0.0234(10)	0.0153(10)	0.0218(10)	-0.0017(8)	-0.0086(8)	-0.0012(8)
C43	0.0125(8)	0.0109(9)	0.0128(8)	-0.0056(7)	0.0002(7)	-0.0014(7)
C22	0.0215(10)	0.0252(11)	0.0093(9)	-0.0016(8)	-0.0015(7)	0.0092(8)
C16	0.0199(10)	0.0173(10)	0.0250(10)	-0.0093(8)	0.0108(8)	-0.0031(8)
C38	0.0114(9)	0.0212(10)	0.0169(9)	0.0036(8)	0.0030(7)	0.0023(7)
C12	0.0142(9)	0.0162(9)	0.0141(9)	0.0022(7)	0.0000(7)	0.0007(7)
C6	0.0262(11)	0.0209(10)	0.0175(10)	0.0057(8)	0.0069(8)	0.0031(8)
C30	0.0141(9)	0.0217(10)	0.0137(9)	0.0028(8)	0.0037(7)	0.0021(7)
C36	0.0150(10)	0.0196(10)	0.0370(12)	0.0021(9)	0.0066(9)	-0.0014(8)

C52	0.0157(10)	0.0308(12)	0.0290(11)	-0.0061(9)	0.0101(9)	-0.0059(8)
C11	0.0160(9)	0.0257(11)	0.0192(10)	0.0070(8)	0.0032(8)	-0.0028(8)
C32	0.0179(10)	0.0195(10)	0.0236(10)	0.0048(8)	-0.0064(8)	-0.0027(8)
C15	0.0209(10)	0.0209(10)	0.0133(9)	-0.0052(8)	0.0055(8)	-0.0082(8)
C3	0.0325(12)	0.0259(11)	0.0224(11)	0.0018(9)	0.0148(9)	0.0090(9)
C40	0.0198(10)	0.0216(10)	0.0133(9)	-0.0007(8)	0.0058(8)	-0.0017(8)
C20	0.0232(10)	0.0125(9)	0.0160(9)	0.0031(7)	-0.0037(8)	-0.0024(8)
C9	0.0331(12)	0.0264(12)	0.0237(11)	-0.0090(9)	0.0048(9)	-0.0164(10)
C23	0.0166(9)	0.0318(12)	0.0150(9)	0.0083(8)	0.0051(8)	0.0038(8)
C27	0.0269(11)	0.0160(10)	0.0227(10)	0.0036(8)	0.0135(9)	0.0037(8)
C18	0.0229(10)	0.0153(9)	0.0169(9)	0.0002(8)	0.0069(8)	0.0024(8)
C24	0.0125(9)	0.0227(10)	0.0146(9)	0.0032(8)	0.0024(7)	0.0004(7)
C5	0.0462(14)	0.0372(13)	0.0173(10)	0.0105(10)	0.0153(10)	0.0082(11)
C10	0.0243(11)	0.0276(11)	0.0248(11)	0.0016(9)	0.0019(9)	-0.0155(9)
C29	0.0161(9)	0.0319(12)	0.0156(9)	0.0085(8)	0.0044(8)	0.0084(8)
C39	0.0177(9)	0.0199(10)	0.0202(10)	0.0009(8)	0.0087(8)	0.0030(8)
C53	0.0336(12)	0.0239(11)	0.0180(10)	0.0053(9)	0.0056(9)	-0.0106(9)
C51	0.0139(9)	0.0163(10)	0.0318(11)	0.0020(9)	-0.0001(8)	0.0023(8)
C4	0.0503(15)	0.0412(14)	0.0259(12)	0.0063(11)	0.0267(11)	0.0135(12)
C49	0.0163(9)	0.0249(11)	0.0229(10)	-0.0078(8)	0.0048(8)	0.0019(8)
C35	0.0152(10)	0.0304(13)	0.0607(17)	0.0068(12)	0.0111(11)	-0.0052(9)
C34	0.0166(11)	0.0296(13)	0.0584(17)	0.0076(12)	-0.0069(11)	-0.0118(9)
C54	0.0246(11)	0.0146(10)	0.0262(11)	0.0037(8)	-0.0023(9)	0.0031(8)

(8) [Ru(η⁶-C_6Me_6)($S_2C_6H_4$) $RuH_2(PPh_3)_2$] **7**

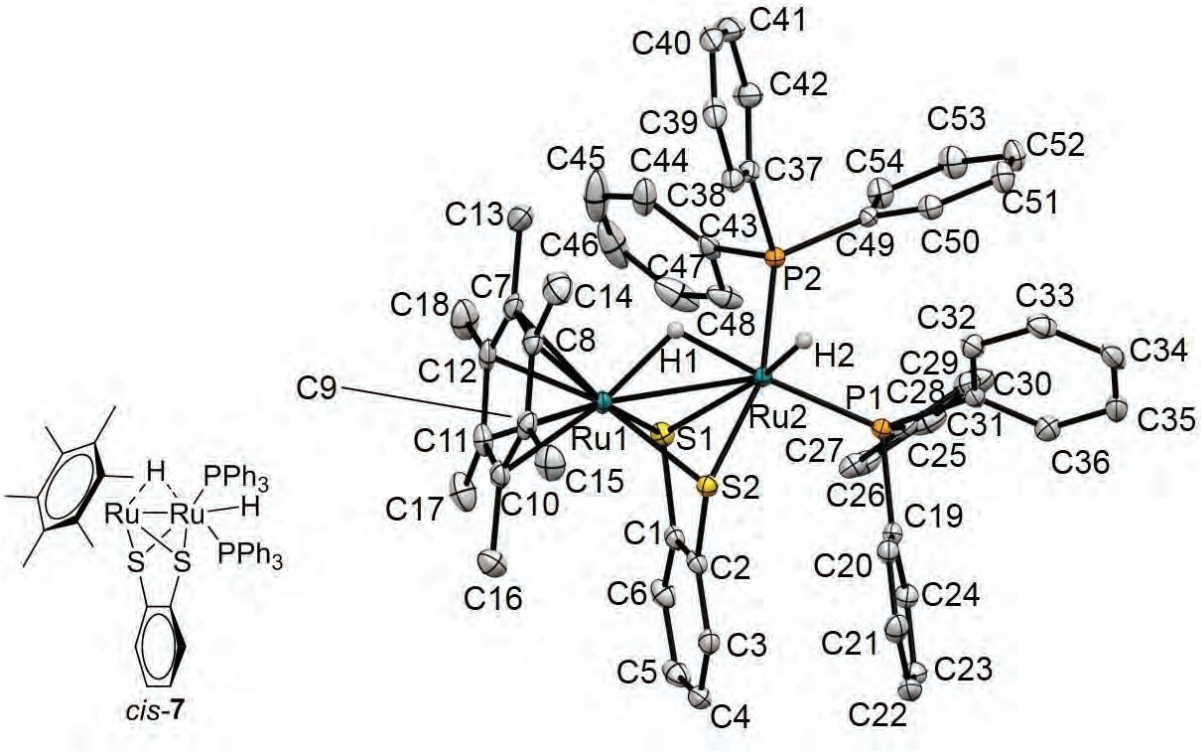

Table S15. Atomic coordination of **7**.

	x	y	z
Ru1	0.371707(12)	0.199850(16)	0.426069(8)
Ru2	0.250814(11)	0.227306(16)	0.346954(8)
S2	0.25802(4)	0.29455(5)	0.44001(3)
P1	0.15830(4)	0.33466(5)	0.30929(3)
P2	0.27512(4)	0.12975(5)	0.27170(3)
S1	0.37079(4)	0.33112(5)	0.35458(3)
C31	0.06060(15)	0.2866(2)	0.29158(11)
C26	0.24753(16)	0.4740(2)	0.25218(12)
H26	0.2736	0.4835	0.2871
C10	0.43637(16)	0.2359(2)	0.50485(11)
C43	0.36907(15)	0.1591(2)	0.24651(11)
C35	-0.06889(17)	0.3200(3)	0.25688(12)
H35	-0.1057	0.3663	0.2393
C3	0.26881(15)	0.5140(2)	0.46434(11)
H3	0.2329	0.503	0.4913
C19	0.12883(14)	0.4422(2)	0.35588(10)

C32	0.03859(16)	0.1851(2)	0.30767(11)
H32	0.0751	0.1385	0.3253
C54	0.24069(16)	0.1548(2)	0.15492(11)
H54	0.2921	0.1755	0.1517
C50	0.14003(15)	0.0967(2)	0.20959(11)
H50	0.1222	0.0768	0.2442
C40	0.28032(17)	-0.2394(2)	0.29534(13)
H40	0.2822	-0.315	0.3003
C11	0.48544(16)	0.2402(2)	0.46097(11)
C37	0.27782(15)	-0.0168(2)	0.28150(11)
C20	0.09676(15)	0.4085(2)	0.40407(11)
H20	0.092	0.3339	0.4113
C2	0.29204(15)	0.4288(2)	0.43313(10)
C21	0.07177(16)	0.4826(2)	0.44137(11)
H21	0.0501	0.4585	0.4739
C49	0.21525(15)	0.1291(2)	0.20637(10)
C25	0.18366(15)	0.4071(2)	0.24732(10)
C24	0.13477(15)	0.5517(2)	0.34611(11)
H24	0.1562	0.5761	0.3135
C44	0.43027(17)	0.0889(3)	0.24893(12)
H44	0.4246	0.0187	0.2633
C23	0.10961(16)	0.6260(2)	0.38378(12)
H23	0.1141	0.7007	0.3767
C39	0.25743(16)	-0.1741(2)	0.33691(13)
H39	0.2423	-0.2048	0.3702
C27	0.27329(17)	0.5265(2)	0.20669(12)
H27	0.3165	0.572	0.2108
C42	0.29882(19)	-0.0839(2)	0.23918(12)
H42	0.312	-0.0537	0.2053
C1	0.34567(15)	0.4447(2)	0.39387(11)
C48	0.37962(18)	0.2627(2)	0.22618(12)
H48	0.3388	0.3125	0.2251
C38	0.25651(15)	-0.0628(2)	0.33005(12)
H38	0.2411	-0.0182	0.359
C53	0.19106(17)	0.1504(2)	0.10825(12)

H53	0.2089	0.1678	0.0733
C28	0.23622(19)	0.5130(2)	0.15538(12)
H28	0.253	0.5506	0.1244
C4	0.29825(16)	0.6163(2)	0.45610(11)
H4	0.2813	0.6753	0.4768
C9	0.38988(15)	0.1421(2)	0.51123(11)
C15	0.33373(18)	0.1410(3)	0.55562(12)
H15A	0.2883	0.1008	0.5427
H15B	0.3194	0.2148	0.5642
H15C	0.357	0.1067	0.5887
C29	0.17452(19)	0.4442(2)	0.14957(12)
H29	0.1499	0.4331	0.1142
C5	0.35201(17)	0.6317(2)	0.41796(12)
H5	0.3725	0.7013	0.4129
C41	0.3006(2)	-0.1947(2)	0.24622(13)
H41	0.3158	-0.2396	0.2174
C47	0.4496(2)	0.2932(3)	0.20751(14)
H47	0.4561	0.3635	0.1935
C30	0.14827(17)	0.3912(2)	0.19500(11)
H30	0.1061	0.3439	0.1904
C36	0.00548(16)	0.3547(2)	0.26673(11)
H36	0.0191	0.4254	0.2565
C17	0.52897(18)	0.3424(3)	0.44993(14)
H17A	0.4995	0.4047	0.461
H17B	0.5374	0.3473	0.4106
H17C	0.5781	0.3412	0.4711
C51	0.09078(16)	0.0931(2)	0.16313(12)
H51	0.0395	0.0715	0.166
C52	0.11636(17)	0.1208(2)	0.11240(12)
H52	0.0824	0.1194	0.0806
C6	0.37645(16)	0.5460(2)	0.38677(11)
H6	0.4139	0.5568	0.3609
C22	0.07813(16)	0.5916(2)	0.43150(12)
H22	0.0611	0.6423	0.4572
C33	-0.03641(16)	0.1504(2)	0.29835(12)

H33	-0.0507	0.0807	0.3097
C7	0.44722(16)	0.0567(2)	0.43241(11)
C14	0.34914(19)	-0.0485(3)	0.48355(13)
H14A	0.3201	-0.0408	0.5163
H14B	0.3834	-0.1102	0.4881
H14C	0.3141	-0.0596	0.4512
C8	0.39545(16)	0.0527(2)	0.47573(11)
C16	0.43093(19)	0.3293(3)	0.54445(13)
H16A	0.4749	0.3767	0.5415
H16B	0.4303	0.302	0.5821
H16C	0.3841	0.3696	0.5353
H1	0.312(2)	0.128(3)	0.3797(15)
C34	-0.08952(17)	0.2175(3)	0.27269(13)
H34	-0.1404	0.1937	0.2658
C12	0.49270(15)	0.1487(3)	0.42545(11)
C18	0.54898(18)	0.1534(3)	0.38096(13)
H18A	0.561	0.0804	0.3693
H18B	0.5956	0.1891	0.3953
H18C	0.5268	0.1938	0.3494
C45	0.50010(19)	0.1210(4)	0.23036(13)
H45	0.5417	0.0724	0.2323
H2	0.184(2)	0.142(4)	0.3610(18)
C46	0.5092(2)	0.2221(4)	0.20930(14)
H46	0.5566	0.2427	0.196
C13	0.45212(19)	-0.0391(3)	0.39469(13)
H13A	0.4702	-0.0157	0.3594
H13B	0.4017	-0.0717	0.3887
H13C	0.4876	-0.0918	0.4116
Cl1	0.27569(5)	0.84577(9)	0.09710(3)
Cl2	0.13102(9)	0.70195(10)	0.04351(6)
C101	0.1870(2)	0.8348(4)	0.12636(16)
H10A	0.1878	0.7717	0.1511
H10B	0.1784	0.8994	0.1488
C100	0.1234(3)	0.8232(4)	0.08424(19)
H10C	0.1226	0.8863	0.0595

H10D	0.0748	0.8219	0.1026
Cl3	0.06468(6)	-0.07109(7)	0.38149(4)
Cl4	0.08680(7)	0.16747(10)	0.51024(4)
C102	0.0432(3)	0.0291(4)	0.43118(19)
H10E	0.0175	0.0907	0.4123
H10F	0.0083	-0.0012	0.4575
C103	0.1112(3)	0.0649(5)	0.4602(2)
H10G	0.1463	0.0954	0.4341
H10H	0.1369	0.0038	0.4794

Table S16. Atomic displacement parameter of **7**.

	U11	U22	U33	U23	U13	U12
Ru1	0.01167(11)	0.01738(11)	0.01210(10)	0.00014(8)	-0.00050(8)	0.00155(8)
Ru2	0.01070(10)	0.01299(10)	0.01202(10)	0.00021(7)	-0.00019(7)	0.00036(7)
S2	0.0132(3)	0.0156(3)	0.0143(3)	0.0000(2)	0.0008(2)	0.0005(2)
P1	0.0121(3)	0.0125(3)	0.0132(3)	0.0000(2)	0.0003(2)	0.0003(2)
P2	0.0126(3)	0.0133(3)	0.0140(3)	-0.0002(2)	-0.0004(2)	0.0003(2)
S1	0.0151(3)	0.0189(3)	0.0140(3)	0.0001(2)	0.0015(2)	-0.0014(2)
C31	0.0124(13)	0.0205(13)	0.0148(12)	-0.0044(10)	0.0003(10)	0.0001(10)
C26	0.0207(14)	0.0172(13)	0.0225(14)	0.0002(11)	0.0043(11)	0.0037(11)
C10	0.0169(14)	0.0276(15)	0.0152(13)	-0.0004(11)	-0.0046(11)	0.0043(11)
C43	0.0143(13)	0.0287(15)	0.0139(12)	-0.0069(11)	0.0012(10)	-0.0026(11)
C35	0.0184(15)	0.0347(16)	0.0253(15)	-0.0077(13)	-0.0063(12)	0.0077(12)
C3	0.0163(13)	0.0232(14)	0.0171(13)	-0.0007(11)	-0.0028(10)	0.0037(11)
C19	0.0113(12)	0.0164(12)	0.0167(12)	-0.0014(10)	-0.0012(10)	0.0013(9)
C32	0.0162(14)	0.0224(14)	0.0212(14)	-0.0042(11)	0.0020(11)	-0.0002(11)
C54	0.0197(14)	0.0266(15)	0.0193(14)	0.0027(11)	0.0013(11)	-0.0019(11)
C50	0.0189(14)	0.0178(13)	0.0191(13)	-0.0004(10)	0.0012(11)	0.0003(10)
C40	0.0297(16)	0.0141(13)	0.0351(17)	0.0012(12)	-0.0137(13)	0.0012(11)
C11	0.0143(13)	0.0303(15)	0.0193(14)	0.0035(11)	-0.0052(11)	-0.0009(11)
C37	0.0187(14)	0.0134(12)	0.0218(13)	-0.0006(10)	-0.0066(11)	0.0013(10)
C20	0.0149(13)	0.0218(13)	0.0167(13)	0.0003(10)	-0.0009(10)	0.0020(10)
C2	0.0149(13)	0.0181(13)	0.0139(12)	-0.0003(10)	-0.0033(10)	-0.0013(10)
C21	0.0172(14)	0.0333(16)	0.0172(13)	-0.0024(12)	0.0018(11)	0.0046(12)
C49	0.0165(13)	0.0118(11)	0.0149(12)	-0.0007(9)	-0.0024(10)	0.0026(9)

C25	0.0182(13)	0.0129(12)	0.0161(12)	0.0018(10)	0.0028(10)	0.0051(10)
C24	0.0179(14)	0.0182(13)	0.0209(14)	-0.0001(11)	-0.0011(11)	0.0006(10)
C44	0.0183(15)	0.053(2)	0.0171(14)	0.0009(13)	0.0005(11)	0.0073(14)
C23	0.0174(14)	0.0175(13)	0.0326(16)	-0.0062(12)	-0.0028(12)	0.0016(11)
C39	0.0203(15)	0.0226(14)	0.0297(16)	0.0065(12)	-0.0067(12)	-0.0037(11)
C27	0.0280(16)	0.0158(13)	0.0303(16)	0.0027(11)	0.0130(13)	0.0034(11)
C42	0.0407(18)	0.0208(14)	0.0184(14)	-0.0009(11)	-0.0057(13)	0.0072(13)
C1	0.0152(13)	0.0211(13)	0.0148(12)	-0.0008(10)	-0.0042(10)	0.0000(10)
C48	0.0280(16)	0.0282(15)	0.0265(15)	-0.0121(12)	0.0119(13)	-0.0102(13)
C38	0.0157(13)	0.0180(13)	0.0249(14)	0.0004(11)	-0.0027(11)	-0.0002(10)
C53	0.0288(16)	0.0311(16)	0.0168(14)	0.0050(12)	0.0017(12)	-0.0005(12)
C28	0.0432(19)	0.0209(14)	0.0240(15)	0.0050(12)	0.0168(14)	0.0091(13)
C4	0.0260(15)	0.0188(14)	0.0217(14)	-0.0054(11)	-0.0078(12)	0.0033(11)
C9	0.0187(14)	0.0256(14)	0.0142(12)	0.0035(11)	-0.0021(10)	0.0066(11)
C15	0.0299(17)	0.0415(18)	0.0177(14)	0.0036(13)	0.0030(12)	0.0007(14)
C29	0.0396(18)	0.0272(15)	0.0162(14)	0.0004(11)	0.0045(13)	0.0106(13)
C5	0.0325(16)	0.0169(13)	0.0224(14)	0.0022(11)	-0.0080(12)	-0.0044(12)
C41	0.046(2)	0.0190(15)	0.0278(16)	-0.0049(12)	-0.0085(14)	0.0082(13)
C47	0.043(2)	0.048(2)	0.0271(17)	-0.0140(15)	0.0169(15)	-0.0278(17)
C30	0.0263(15)	0.0165(13)	0.0194(13)	-0.0012(10)	0.0024(11)	0.0046(11)
C36	0.0209(14)	0.0223(14)	0.0220(14)	-0.0025(11)	-0.0001(11)	0.0029(11)
C17	0.0230(16)	0.0421(19)	0.0325(17)	0.0046(14)	-0.0036(13)	-0.0092(14)
C51	0.0174(14)	0.0274(15)	0.0256(15)	0.0015(12)	-0.0023(11)	-0.0030(11)
C52	0.0243(15)	0.0300(16)	0.0197(14)	0.0007(12)	-0.0082(12)	0.0011(12)
C6	0.0230(15)	0.0239(14)	0.0168(13)	0.0026(11)	-0.0020(11)	-0.0048(11)
C22	0.0174(14)	0.0277(15)	0.0260(15)	-0.0128(12)	-0.0025(11)	0.0050(11)
C33	0.0208(15)	0.0238(14)	0.0291(15)	-0.0084(12)	0.0053(12)	-0.0062(11)
C7	0.0200(14)	0.0274(15)	0.0183(13)	-0.0016(11)	-0.0059(11)	0.0121(11)
C14	0.0334(18)	0.0271(16)	0.0325(17)	0.0058(13)	-0.0038(14)	-0.0005(13)
C8	0.0205(14)	0.0225(14)	0.0194(13)	0.0031(11)	-0.0046(11)	0.0060(11)
C16	0.0346(18)	0.0296(16)	0.0236(15)	-0.0070(12)	-0.0045(13)	0.0020(13)
C34	0.0155(14)	0.0373(17)	0.0290(16)	-0.0178(13)	-0.0015(12)	-0.0037(12)
C12	0.0133(13)	0.0419(17)	0.0153(13)	0.0010(12)	-0.0040(11)	0.0080(12)
C18	0.0192(16)	0.064(2)	0.0244(16)	-0.0031(15)	0.0056(13)	0.0025(15)
C45	0.0184(16)	0.101(3)	0.0210(16)	0.0028(19)	0.0038(13)	0.0120(19)

C46	0.0193(17)	0.102(4)	0.0228(17)	-0.0141(19)	0.0072(14)	-0.0171(19)
C13	0.0334(18)	0.0319(17)	0.0272(16)	-0.0077(13)	-0.0073(13)	0.0154(14)
Cl1	0.0370(5)	0.0769(7)	0.0270(4)	-0.0034(4)	0.0083(4)	0.0062(5)
Cl2	0.1010(10)	0.0501(6)	0.0845(9)	0.0220(6)	-0.0420(8)	-0.0232(6)
C101	0.033(2)	0.059(2)	0.045(2)	0.0020(18)	0.0080(16)	0.0068(17)
C100	0.054(3)	0.067(3)	0.053(3)	0.009(2)	-0.006(2)	0.008(2)
Cl3	0.0601(6)	0.0306(4)	0.0535(6)	-0.0004(4)	0.0182(5)	0.0037(4)
Cl4	0.0867(8)	0.0697(7)	0.0310(5)	-0.0038(5)	0.0067(5)	-0.0386(6)
C102	0.072(3)	0.075(3)	0.049(3)	0.002(2)	0.012(2)	-0.012(3)
C103	0.078(4)	0.103(4)	0.049(3)	0.010(3)	0.020(2)	-0.034(3)

(9) $[Ru_2(CO)_4(PPh_3)_2(S_2C_6H_4)]$ **9**

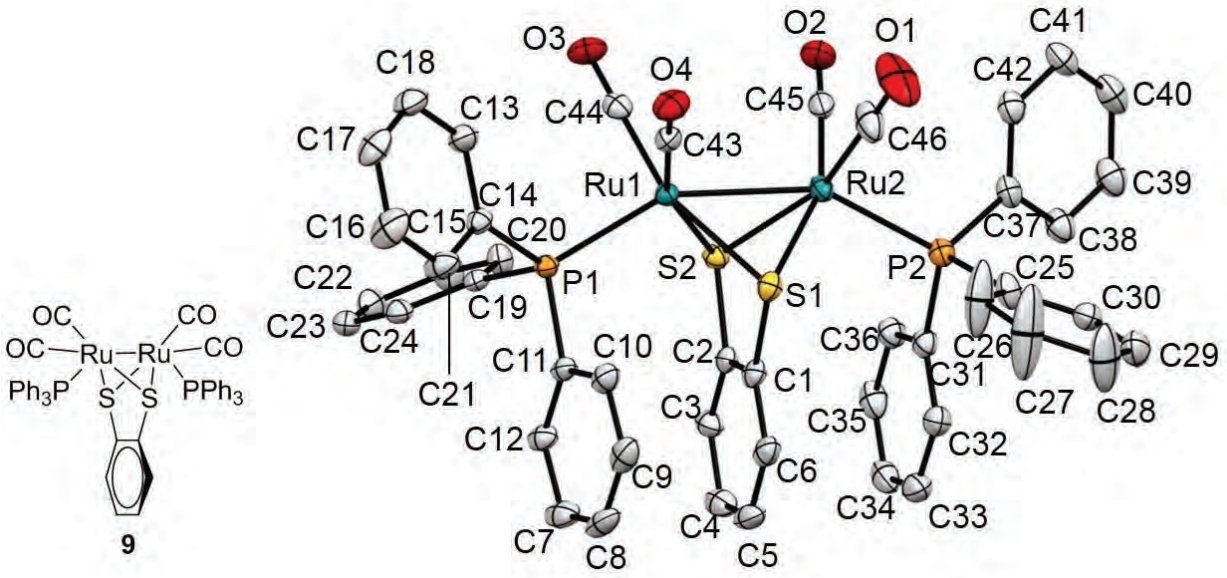

Table S17. Atomic coordination of **9**.

	x	y	z
Ru1	0.54433(3)	-0.08546(2)	0.188110(10)
Ru2	0.64683(3)	0.10544(2)	0.301223(11)
P1	0.35038(8)	-0.24453(7)	0.10546(3)
S2	0.43777(8)	-0.11226(7)	0.28747(3)
P2	0.61369(9)	0.25047(7)	0.39051(4)
S1	0.48194(9)	0.10669(7)	0.21263(3)
O3	0.6970(3)	-0.2693(2)	0.19686(11)

O2	0.8230(3)	0.0001(2)	0.37785(11)
O4	0.7446(3)	0.0495(2)	0.09747(11)
C14	0.4018(3)	-0.2825(3)	0.02476(13)
C43	0.6680(3)	-0.0036(3)	0.13125(14)
C11	0.2068(3)	-0.1880(3)	0.09010(13)
C31	0.4345(3)	0.1763(3)	0.41547(13)
C37	0.7408(4)	0.3001(3)	0.46660(14)
C45	0.7596(4)	0.0440(3)	0.34904(15)
C12	0.0656(4)	-0.2550(3)	0.10330(13)
H12	0.039	-0.3367	0.1183
C24	0.1494(3)	-0.5233(3)	0.06776(14)
H24	0.133	-0.5064	0.0261
C44	0.6374(3)	-0.2004(3)	0.19420(14)
O1	0.9193(3)	0.3205(3)	0.27075(14)
C30	0.6325(4)	0.5196(3)	0.42971(15)
H30	0.6374	0.5081	0.4732
C2	0.2866(3)	-0.0710(3)	0.27195(13)
C3	0.1536(3)	-0.1371(3)	0.29104(14)
H3	0.1381	-0.2093	0.3125
C20	0.2763(4)	-0.4448(3)	0.17845(14)
H20	0.3469	-0.3743	0.2128
C22	0.0971(4)	-0.6785(3)	0.13858(16)
H22	0.044	-0.7671	0.1457
C9	0.1422(4)	-0.0158(3)	0.06027(14)
H9	0.1682	0.0663	0.0456
C36	0.4027(4)	0.0646(3)	0.44408(14)
H36	0.4757	0.0332	0.4521
C19	0.2509(3)	-0.4173(3)	0.11814(14)
C35	0.2656(4)	-0.0002(3)	0.46074(15)
H35	0.2458	-0.0739	0.4815
C8	0.0024(4)	-0.0831(4)	0.07295(14)
H8	-0.0677	-0.0476	0.0668
C46	0.8150(4)	0.2402(3)	0.28242(16)
C6	0.1991(4)	0.0742(3)	0.22813(14)
H6	0.2149	0.147	0.2071

C32	0.3251(4)	0.2186(3)	0.40255(15)
H32	0.3449	0.2941	0.3831
C25	0.6242(4)	0.4151(3)	0.37787(15)
C23	0.0726(3)	-0.6526(3)	0.07774(15)
H23	0.0032	-0.7238	0.0432
C38	0.7019(4)	0.3287(3)	0.52866(15)
H38	0.6059	0.3217	0.5319
C21	0.1992(4)	-0.5745(3)	0.18852(15)
H21	0.2165	-0.5922	0.2299
C41	0.9822(4)	0.3488(3)	0.52111(16)
H41	1.0778	0.3541	0.5185
C10	0.2448(4)	-0.0671(3)	0.06871(13)
H10	0.3412	-0.0202	0.06
C1	0.3090(4)	0.0335(3)	0.23939(13)
C5	0.0644(4)	0.0077(3)	0.24779(14)
H5	-0.012	0.035	0.2399
C15	0.3224(4)	-0.2891(3)	-0.03324(15)
H15	0.2386	-0.2702	-0.0318
C16	0.3640(5)	-0.3227(4)	-0.09306(16)
H16	0.3084	-0.3269	-0.1322
C13	0.5241(4)	-0.3102(3)	0.02075(15)
H13	0.5808	-0.3055	0.0597
C42	0.8830(4)	0.3123(3)	0.46401(15)
H42	0.9128	0.2954	0.4227
C17	0.4841(4)	-0.3497(3)	-0.09615(16)
H17	0.5124	-0.3721	-0.1373
C34	0.1577(4)	0.0417(3)	0.44728(15)
H34	0.0631	-0.0039	0.4581
C4	0.0416(4)	-0.0972(3)	0.27864(15)
H4	-0.0507	-0.1425	0.2915
C29	0.6336(4)	0.6405(3)	0.41818(17)
H29	0.6428	0.7126	0.4539
C18	0.5641(4)	-0.3444(3)	-0.03943(16)
H18	0.6471	-0.3643	-0.0415
C7	-0.0362(4)	-0.2021(4)	0.09458(14)

H7	-0.1327	-0.2479	0.1035
C39	0.8018(4)	0.3670(3)	0.58515(16)
H39	0.7739	0.3865	0.6267
C33	0.1871(4)	0.1504(3)	0.41803(16)
H33	0.1122	0.1786	0.4085
C40	0.9417(4)	0.3772(3)	0.58143(17)
H40	1.0098	0.4036	0.6203
C26	0.6157(7)	0.4337(4)	0.31553(18)
H26	0.6107	0.3638	0.2797
C28	0.6217(6)	0.6557(4)	0.35603(19)
H28	0.6184	0.7368	0.3482
C27	0.6144(8)	0.5540(4)	0.3044(2)
H27	0.6084	0.566	0.261

Table S18. Atomic displacement parameter of **9**.

	U11	U22	U33	U23	U13	U12
Ru1	0.01539(13)	0.01876(11)	0.01585(12)	0.00293(8)	0.00350(9)	0.00644(9)
Ru2	0.01680(14)	0.02078(12)	0.01744(12)	0.00094(9)	0.00384(10)	0.00391(9)
P1	0.0156(4)	0.0199(3)	0.0168(3)	0.0040(3)	0.0034(3)	0.0085(3)
S2	0.0170(4)	0.0206(3)	0.0178(3)	0.0046(3)	0.0034(3)	0.0067(3)
P2	0.0212(4)	0.0205(3)	0.0188(4)	0.0041(3)	0.0038(3)	0.0060(3)
S1	0.0256(4)	0.0201(3)	0.0193(4)	0.0044(3)	0.0058(3)	0.0098(3)
O3	0.0309(15)	0.0414(13)	0.0377(13)	0.0160(11)	0.0087(11)	0.0241(11)
O2	0.0282(15)	0.0394(13)	0.0414(14)	0.0028(11)	-0.0029(12)	0.0173(11)
O4	0.0310(14)	0.0336(12)	0.0379(13)	0.0146(10)	0.0188(12)	0.0144(10)
C14	0.0201(17)	0.0192(13)	0.0211(14)	0.0051(11)	0.0073(13)	0.0086(11)
C43	0.0208(17)	0.0211(14)	0.0237(15)	0.0022(12)	0.0054(14)	0.0097(12)
C11	0.0206(17)	0.0283(14)	0.0130(13)	0.0019(11)	0.0017(12)	0.0150(12)
C31	0.0239(18)	0.0237(14)	0.0163(14)	0.0011(11)	0.0040(13)	0.0086(12)
C37	0.0249(18)	0.0199(13)	0.0217(15)	0.0023(11)	0.0010(13)	0.0043(12)
C45	0.0192(18)	0.0272(15)	0.0276(17)	-0.0046(13)	0.0054(14)	0.0053(13)
C12	0.0243(18)	0.0349(16)	0.0160(14)	0.0035(12)	0.0045(13)	0.0174(14)
C24	0.0181(17)	0.0292(15)	0.0223(15)	0.0031(12)	0.0045(13)	0.0114(12)
C44	0.0186(17)	0.0291(15)	0.0181(14)	0.0060(12)	0.0052(13)	0.0073(13)
O1	0.044(2)	0.0671(19)	0.0495(18)	0.0080(14)	0.0225(15)	-0.0163(15)

C30	0.0213(18)	0.0296(15)	0.0274(16)	0.0032(13)	0.0018(14)	0.0110(13)
C2	0.0203(17)	0.0242(14)	0.0152(14)	-0.0016(11)	0.0017(12)	0.0105(12)
C3	0.0179(17)	0.0311(15)	0.0197(15)	0.0014(12)	0.0029(13)	0.0082(12)
C20	0.0256(18)	0.0198(14)	0.0234(15)	0.0022(11)	0.0010(14)	0.0068(12)
C22	0.0242(19)	0.0195(14)	0.0394(19)	0.0070(13)	0.0094(15)	0.0066(12)
C9	0.046(2)	0.0363(17)	0.0165(15)	0.0026(13)	-0.0011(15)	0.0268(16)
C36	0.0251(19)	0.0254(15)	0.0226(15)	0.0046(12)	0.0040(14)	0.0087(13)
C19	0.0161(16)	0.0203(13)	0.0229(15)	0.0020(11)	0.0054(12)	0.0099(11)
C35	0.033(2)	0.0286(16)	0.0210(16)	0.0033(12)	0.0075(15)	0.0038(14)
C8	0.043(2)	0.054(2)	0.0182(15)	0.0016(14)	0.0007(15)	0.0390(19)
C46	0.036(2)	0.0376(18)	0.0230(17)	-0.0032(14)	0.0077(16)	0.0019(16)
C6	0.032(2)	0.0309(16)	0.0183(15)	-0.0011(12)	0.0002(14)	0.0187(14)
C32	0.0258(19)	0.0286(15)	0.0262(16)	0.0009(13)	0.0029(14)	0.0116(13)
C25	0.032(2)	0.0191(14)	0.0243(16)	0.0048(12)	0.0008(14)	0.0048(12)
C23	0.0180(17)	0.0238(14)	0.0323(17)	-0.0003(12)	0.0029(14)	0.0088(12)
C38	0.030(2)	0.0324(16)	0.0230(16)	0.0038(13)	0.0029(15)	0.0086(14)
C21	0.037(2)	0.0270(15)	0.0239(16)	0.0086(13)	0.0046(15)	0.0087(14)
C41	0.0233(19)	0.0292(16)	0.0360(19)	0.0047(14)	-0.0033(15)	0.0027(13)
C10	0.0301(19)	0.0303(15)	0.0172(14)	0.0035(12)	0.0023(13)	0.0177(14)
C1	0.0253(18)	0.0261(14)	0.0149(13)	-0.0005(11)	0.0041(13)	0.0131(13)
C5	0.029(2)	0.050(2)	0.0227(16)	-0.0029(14)	0.0003(15)	0.0272(16)
C15	0.034(2)	0.0480(19)	0.0211(16)	0.0059(14)	0.0060(15)	0.0275(16)
C16	0.061(3)	0.059(2)	0.0183(16)	0.0099(15)	0.0103(18)	0.039(2)
C13	0.0271(19)	0.0322(16)	0.0241(16)	0.0043(13)	0.0033(14)	0.0174(14)
C42	0.0272(19)	0.0227(14)	0.0282(16)	0.0038(12)	0.0034(14)	0.0055(13)
C17	0.048(2)	0.0399(18)	0.0256(17)	0.0086(14)	0.0187(17)	0.0251(17)
C34	0.0226(19)	0.0408(18)	0.0245(17)	-0.0053(14)	0.0071(15)	0.0031(14)
C4	0.0215(19)	0.0479(19)	0.0207(16)	-0.0008(14)	0.0045(14)	0.0126(15)
C29	0.035(2)	0.0251(16)	0.040(2)	0.0003(14)	-0.0022(17)	0.0107(14)
C18	0.030(2)	0.0373(18)	0.0388(19)	0.0065(15)	0.0138(17)	0.0201(15)
C7	0.028(2)	0.055(2)	0.0203(16)	0.0007(14)	0.0051(15)	0.0246(16)
C39	0.037(2)	0.0360(17)	0.0238(17)	0.0052(14)	0.0012(16)	0.0097(15)
C33	0.026(2)	0.0409(18)	0.0310(18)	-0.0041(14)	0.0015(15)	0.0164(15)
C40	0.033(2)	0.0289(16)	0.0327(18)	0.0085(14)	-0.0074(16)	0.0037(14)
C26	0.160(6)	0.0238(18)	0.028(2)	0.0061(15)	0.008(3)	0.028(3)

C28	0.124(5)	0.0215(18)	0.045(2)	0.0062(16)	-0.010(3)	0.022(2)
C27	0.249(8)	0.031(2)	0.030(2)	0.0107(18)	0.000(3)	0.048(3)

S2. B3LYP geometries and energies for all optimized ground-state minima

Species: 2

HF = -2628.8860894

No imaginary frequency

Zero-point correction = 0.415385 (Hartree/Particle)

Thermal correction to Energy = 0.457549

Thermal correction to Enthalpy = 0.458493

Thermal correction to Gibbs Free Energy = 0.339687

Sum of electronic and zero-point Energies = -2629.447325

Sum of electronic and thermal Energies = -2629.405161

Sum of electronic and thermal Enthalpies = -2629.404217

Sum of electronic and thermal Free Energies = -2629.523023

Coordinates: $[(\eta^6\text{-}C_6Me_6)Ru(CO)(\mu\text{-}CO)_2Fe_2(\mu\text{-}bdt)(CO)_4]$ **2**

Ru	1.85532569	0.31817590	-0.31574021
Fe	-0.64325212	-0.39774579	0.31810891
Fe	-2.88322806	-1.24638981	-0.24350501
S	-1.93868692	0.53765465	-1.41718788
S	-2.53885242	0.21535254	1.54448804
C	4.09307581	0.21720316	-1.03652998
O	0.36092640	1.98966114	1.68639606
O	0.69666185	-2.05788931	-1.73965830
O	-0.06124747	-2.44439413	2.32400136
C	0.32907156	1.07006365	0.94837183
O	-2.21752661	-3.06219039	-2.45635044
O	1.00954741	2.15495719	-2.54756538
C	0.46288296	-1.21532006	-0.94825785
C	4.02095200	1.27004852	-0.04826519
C	-0.27849726	-1.63263021	1.52624604
C	3.29659227	-0.37758298	1.63497595
C	1.27519804	1.42674347	-1.68450844
O	-3.24835487	-3.47831188	1.63148925
C	4.51840676	0.52421651	-2.45890170
C	-3.09605538	-2.60655266	0.89431284
C	3.87688484	-1.13709999	-0.64785088
O	-5.71131294	-0.72019976	-0.86120223

C	-2.70204084	1.93020429	-0.57871522
C	-2.46479971	-2.35147097	-1.58624472
C	3.11660153	-2.86782712	1.02156854
C	3.41379716	-1.42592786	0.67045194
C	-3.87868931	4.01866715	0.84676943
C	-3.60197194	4.16822342	-0.51045650
C	4.39220354	2.69702700	-0.39717207
C	-3.01138130	3.12084979	-1.23104070
C	-2.97832002	1.78161527	0.78687781
C	3.68929232	0.95408053	1.29657853
C	-3.56648215	2.82021063	1.50323299
C	3.69555096	2.02948897	2.35869799
C	-4.60599856	-0.92172146	-0.61465230
C	4.09265762	-2.26824516	-1.62794396
C	2.84146356	-0.65086067	3.05318155
H	5.61165712	0.49634300	-2.55217318
H	4.18688321	1.50957234	-2.78369609
H	4.10208028	-0.19528315	-3.16328423
H	4.05230973	-3.42389389	1.16082787
H	2.55823644	-3.35971736	0.22210727
H	2.53742294	-2.97202656	1.93504111
H	-4.33799967	4.83055132	1.40278404
H	-3.84508550	5.09728141	-1.01748758
H	3.72618601	3.41067516	0.09013285
H	4.35029061	2.89131972	-1.46673452
H	5.41601780	2.91467813	-0.06712794
H	-2.79579629	3.23097944	-2.28939089
H	-3.77859762	2.69846691	2.56101547
H	4.40013604	2.82634104	2.12006087
H	3.98067928	1.62412106	3.33087442
H	2.69844725	2.47658771	2.46226557
H	3.15545501	-2.52578437	-2.13688188
H	4.44811435	-3.16575846	-1.11909236
H	4.83410029	-2.01186971	-2.38456691
H	2.22190398	-1.54065238	3.13186920
H	2.25435025	0.18216593	3.44294554
H	3.70607475	-0.78790871	3.71533878

Species: **2'**

Zero-point correction = 0.415217 (Hartree/Particle)

Thermal correction to Energy = 0.457456

Thermal correction to Enthalpy = 0.458400

Thermal correction to Gibbs Free Energy = 0.338466

Sum of electronic and zero-point Energies = -2629.442879

Sum of electronic and thermal Energies = -2629.400640

Sum of electronic and thermal Enthalpies = -2629.399695

Sum of electronic and thermal Free Energies = -2629.519630

Coordinates: $[(\eta^6\text{-}C_6Me_6)Ru(CO)(\mu\text{-}CO)_2Fe_2(\mu\text{-}bdt)(CO)_4]$ **2**

Ru	1.92080939	-0.21861368	0.00005947
Fe	-0.70579936	0.39970455	0.00009392
Fe	-2.22232819	-1.59275050	-0.00046083
S	-2.47540700	0.16970094	1.50982411
O	0.54436863	0.04335731	2.64284749
O	1.51322204	-3.19834288	-0.00033186
C	0.41893185	0.07293912	1.47004634
C	-4.72169902	1.84377341	1.40371409
O	-1.00759748	-3.18809972	2.14440221
O	-0.61627745	3.32023066	0.00059575
C	-3.76214949	1.11963821	0.70038770
C	-1.47325372	-2.56620296	1.29292950
C	3.72129374	0.82079263	1.43037790
C	-0.61697355	2.16315673	0.00037696
C	-3.87939657	-2.27401656	-0.00074570
C	-5.68966838	2.56980346	0.69690725
C	1.61897337	-2.04337652	-0.00019260
C	4.17007536	-0.32934663	0.72277006
O	-4.93420393	-2.73535631	-0.00093611
C	3.13183626	1.90769910	0.71500728
C	2.57036632	3.06351846	1.51512310
C	4.74227686	-1.49609444	1.50199470
C	3.81691128	0.87484740	2.93815685
S	-2.47507268	0.17026517	-1.51014385
C	-4.72139290	1.84428821	-1.40390577

C	-3.76199603	1.11989421	-0.70063695
C	-5.68951613	2.57005909	-0.69704403
C	3.72135435	0.82186238	-1.42947423
C	4.17020218	-0.32876234	-0.72273045
C	3.13184484	1.90822406	-0.71331307
C	2.57044618	3.06462978	-1.51263272
C	4.74269245	-1.49476471	-1.50285662
C	3.81694256	0.87697873	-2.93721165
O	0.54459161	0.04415090	-2.64268428
C	0.41923949	0.07332780	-1.46985801
O	-1.00719678	-3.18735651	-2.14565124
C	-1.47301468	-2.56575304	-1.29405345
H	-4.71711537	1.84009645	2.48952641
H	-6.44179234	3.13256143	1.24185724
H	2.01043657	2.70225899	2.37995958
H	1.89979184	3.69351457	0.93719727
H	3.38230200	3.70058384	1.88786979
H	4.69091281	-2.43188615	0.94868049
H	4.20539230	-1.64868758	2.43848369
H	5.79765758	-1.31544704	1.74336784
H	3.94579050	1.89894590	3.29073249
H	4.66344011	0.29552176	3.30801204
H	2.90289017	0.47771556	3.39821023
H	-4.71657198	1.84100977	-2.48971845
H	-6.44152098	3.13301678	-1.24195220
H	2.01022881	2.70398712	-2.37754728
H	1.90017799	3.69448276	-0.93420188
H	3.38245285	3.70169127	-1.88522862
H	4.69249741	-2.43083849	-0.94992654
H	4.20527621	-1.64733249	-2.43905332
H	5.79775775	-1.31317493	-1.74490392
H	3.94582025	1.90131575	-3.28909094
H	4.66343968	0.29788062	-3.30749037
H	2.90290142	0.48016186	-3.39749931

Species: 1

Coordinates: [(η^6-C_6Me_6)Ru(μ-bdt)] **1**

Ru	-0.374122	0.001406	0.000052
S	1.301950	1.573987	-0.000324
S	1.291961	-1.589795	0.000139
C	4.046262	-1.414638	0.000073
C	5.253915	0.682949	-0.000259
C	-2.172473	1.452727	-0.001303
C	-2.173578	-1.421218	0.001680
C	5.248923	-0.722002	-0.000032
C	-2.081152	0.735131	-1.236684
C	-2.080976	0.737744	1.235584
C	2.823641	-0.715852	-0.000044
C	-2.120968	-0.711400	-1.237774
C	-2.248707	2.966170	-0.003104
C	-2.158606	-1.492301	-2.536302
C	-2.205754	-2.932738	0.002353
C	-2.120392	-0.708873	1.239733
C	2.829000	0.692467	-0.000252
C	-1.976528	1.492261	-2.542389
C	-2.157368	-1.486987	2.539984
C	-1.976106	1.497868	2.539540
H	4.033892	-2.501037	0.000260
H	6.196110	1.223701	-0.000334
H	6.187331	-1.269367	0.000071
H	4.050777	2.470059	-0.000528
H	-1.255758	3.430679	-0.004552
H	-2.785931	3.330149	0.874190
H	-2.787397	3.327821	-0.880488
H	-2.987607	-2.207270	-2.522184
H	-1.235162	-2.056092	-2.695356
H	-2.305712	-0.845492	-3.399478
H	-1.716566	-3.347484	0.883556
H	-1.703028	-3.348049	-0.871083
H	-3.242363	-3.294913	-0.005560

H	-2.966687	1.649357	-2.991126
H	-1.360886	0.954026	-3.263283
H	-1.511062	2.466693	-2.398982
H	-2.989352	-2.198596	2.529687
H	-2.299349	-0.837977	3.402326
H	-1.235729	-2.054105	2.697491
H	-1.510682	2.471956	2.393728
H	-1.360209	0.961436	3.261539
H	-2.966151	1.655969	2.988162

Species: **3**

Coordinates: [(η^6-C_6Me_6)Ru(CO)(μ-bdt)] **3**

Ru	0.393841	-0.094846	-0.294729
S	-1.372325	-1.597658	0.162055
S	-1.255770	1.599846	-0.340348
O	0.112974	-0.537517	-3.238598
C	2.714073	0.546815	-0.288565
C	2.037973	1.420772	0.602682
C	1.495565	0.911833	1.852254
C	1.442992	-0.467987	2.071629
C	1.929415	-1.377004	1.048258
C	2.637484	-0.876588	-0.075347
C	0.792725	-1.079197	3.286772
C	1.825246	-2.864185	1.301336
C	3.336746	-1.827952	-1.024976
C	3.542118	1.077286	-1.442259
C	2.001586	2.913724	0.352384
C	0.913399	1.912593	2.818416
C	0.220502	-0.368122	-2.096459
C	-2.861843	-0.647325	-0.045606
C	-4.107456	-1.292564	0.015801
C	-5.287974	-0.567021	-0.117437
C	-5.237411	0.814600	-0.334159
C	-4.006757	1.459930	-0.416168

C	-2.810958	0.739802	-0.263603
H	1.404703	-1.884647	3.701607
H	-0.176780	-1.509453	3.000607
H	0.612735	-0.357247	4.080103
H	2.547084	-3.175111	2.067840
H	2.025190	-3.450889	0.406896
H	0.828243	-3.133529	1.654848
H	4.219826	-2.268028	-0.545847
H	3.667315	-1.331142	-1.935086
H	2.682828	-2.647897	-1.326348
H	4.566421	0.696832	-1.368472
H	3.603000	2.163383	-1.438776
H	3.146107	0.769915	-2.414355
H	2.846552	3.419215	0.838168
H	1.081998	3.351359	0.740415
H	2.032950	3.145356	-0.711392
H	0.727812	1.488840	3.803013
H	-0.044059	2.283514	2.427412
H	1.577440	2.771429	2.946923
H	-4.139389	-2.368038	0.168443
H	-6.244639	-1.078994	-0.064380
H	-6.154448	1.385200	-0.450830
H	-3.960138	2.529960	-0.600096